Fabian Wilke
Karin Kloske
Dr. Michael Bellmann

ESRa – Evaluation of Systems for Ramming Noise Mitigation at an Offshore Test Pile

Project reference number 0325307

Final technical report

Das klingt schon besser!	That sounds better!

May 2012

Research project:	**Evaluation of Systems for Ramming Noise Mitigation at an Offshore Test Pile**
Funding recipient:	**RWE Offshore Logistics Company (OLC) GmbH**
Project reference number:	**0325307**
Duration of the project:	**01.03. 2011 – 31.12. 2011**
Project manager:	**PTJ, Forschungszentrum Jülich GmbH**

The project that forms the basis for this report was funded by the German Federal Ministry for the Environment, Nature Conservation and Reactor Safety under project reference number 0325307. The authors are responsible for the content of this publication.

Participating partners:	**Bard Engineering** **DONG Energy** **EnBW Erneuerbare Energien** **E.ON Climate Renewables** **EWE ENERGIE** **RWE Innogy/RWE OLC (project management)** **Stadtwerke München (SWM)** **Vattenfall Europe**

Sound measurement and evaluation: itap

Abstract

As part of the ESRa research project, the handling and effectiveness of **five different noise mitigation systems** for the construction of pile-driven offshore wind farms were evaluated in a round robin test conducted at the Brodten pile in Lübeck Bay (Baltic Sea). The systems were:

1. Tube with inner bubble curtain by the company IHC (IHC NMS)
2. Fire Hose System by the company Menck (Menck FHS)
3. Little Bubble Curtain (LBC) by the company Weyres
4. Noise-mitigation shells with two bubble curtains (modular design) by the company Weyres (Weyres BeKa Jacket)
5. System 5: Hydro Sound Damper by the TU Braunschweig (TUBS) and Dr. Elmer (TUBS/Elmer HSD)

All systems were used under identical environmental boundary conditions with the aim of comparing potential noise mitigation levels by way of a uniform measuring concept. ITAP GmbH has developed a specific measurement and evaluation concept for underwater noise measurements in compliance with StUK3 requirements; it also conducted and evaluated the measurements.

All noise mitigation systems tested yielded significant reduction effects. Within the 750-metre radius around the noise source that is relevant for the limit value and in the 100 – 300 Hertz frequency range where the greatest amount of energy is introduced into the water, the damping is between 0 and 10 decibel (dB) SEL. In the frequency range of up to 5,000 Hertz, which is the most sensitive audible range for marine mammals, the mitigation effect is a maximum of 25 dB.

With the test systems, the broad-band reduction of the sound exposure level (SEL) is 4.2 to 6.1 dB. Corrected by the ground effect at the test location, the test systems achieved **reductions in the broad-band SEL of approx 7 – 9 dB.**

Extended abstract

An underwater noise limit has been defined for a German wind farm project by the consenting authority BSH. It stipulates that the broad-banded sound exposure level (SEL) at a distance of 750 m from the driven pile may not exceed 160 dB (re 1 µPa).

To meet this target, **five different noise mitigation systems have been evaluated** in a round robin test within the ESRa research project. The five tested systems were

1. The Noise Mitigation Screen by IHC (IHC NMS). The system is a double-walled steel tube with air infill. A bubble curtain is generated between the tube and the driven pile.
2. The Fire Hose System by Menck (Menck FHS). The system comprises a two-layer curtain made of fire hoses that are inflated by compressed air.
3. The Little Bubble Curtain by Weyres (LBC). A system that comprises multiple, bubble-generating rings at different elevations of the water column around the driven pile.
4. A modular system comprising two composite tubes with two internal bubble curtains – Weyres (Weyres BeKa Jacket).
5. The Hydro Sound Damper by TU Braunschweig and Dr. Elmer (TUBS/Elmer HSD). It replaces air bubbles with fixed, firm bubbles of defined size and shape that are connected to a net.

All systems were to be tested under equal boundary conditions and with the same measurement concept. The “Brodten Ost” pile that had already been driven was chosen as test pile. It is situated near the coast of Brodten at a water depth of 8.50 m.

Further details can be found in the following table.

Position	N 53 59.877‘ E 10 54.489‘
Diameter	2.2 m
Height above waterline	5.5 m
Water depth	8.5 m
Embedment into soil	Approx. 65.0 m
Wall thickness	50.0 mm

Table I: Data of the test pile

ITAP GmbH has developed a measurement and evaluation concept in compliance with StUK3 requirements. The data were logged using a total of four buoys and at least two hydrophones over the water depth. Near-field

measurements were also performed and the soil vibration was measured using a geophone.

All tests were performed with a hydraulic hammer Menck MHU 270 T with a rated energy of 300 kJ.

Figure I provides an overview of the acoustic insertion loss (reduction of the SEL) over frequency. All systems worked well, but the figure shows that the achieved reductions are highly frequency-dependent:

In the frequency range 100 – 300 Hertz where the highest energy is introduced in the water, the damping is between 0 and 10 decibel (dB) SEL. In the high-frequency range up to 5,000 Hertz, which is the most sensitive range for marine mammals, the reduction reaches values of up to 25 dB.

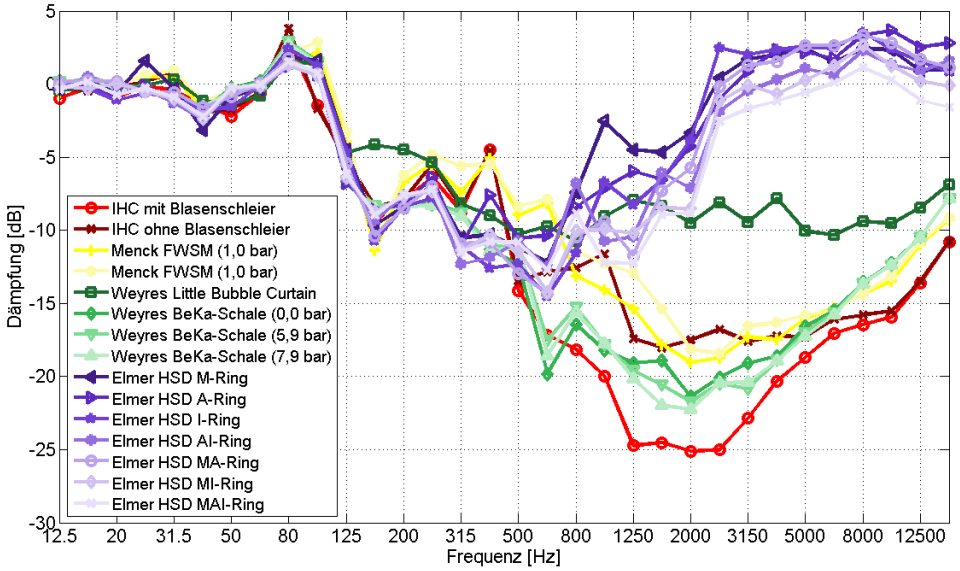

Figure I: Acoustic insertion loss (ΔSEL) in 1/3 octave bands at 750 m distance

Dämpfung [dB]	Damping [dB]
Frequenz [Hz]	Frequency [Hz]
IHC mit Blasenschleier	IHC with bubble curtain
IHC ohne Blasenschleier	IHC without bubble curtain
Menck FWSM (1,0 bar)	Menck FHS (1.0 bar)
Menck FWSM (1,0 bar)	Menck FHS (1.0 bar)
Weyres Little Bubble Curtain	Weyres Little Bubble Curtain
Weyres BeKa –Schale (0,0 bar)	Weyres BeKa-Jacket (0.0 bar)
Weyres BeKa –Schale (5,9 bar)	Weyres BeKa-Jacket (5.9 bar)
Weyres BeKa –Schale (7,9 bar)	Weyres BeKa-Jacket (7.9 bar)
Elmer HSD M-Ring	Elmer HSD M ring
Elmer HSD A -Ring	Elmer HSD O ring
Elmer HSD I -Ring	Elmer HSD I ring

Elmer HSD Al-Ring	Elmer HSD Ol ring
Elmer HSD Ma-Ring	Elmer HSD MO ring
Elmer HSD MI-Ring	Elmer HSD MI ring
Elmer HSD MAI-Ring	Elmer HSD MOI ring

The following table shows the broad-band reduction of the SEL. It is divided into near-field and far-field (750 m) measurements. As already stated, the reduction is low in the most energy-intensive frequency bands and thus the overall reduction of the SEL is below 10 dB for all systems.

However, due to the specific boundary conditions at the test location, the results have to be corrected by 2-3 dB if the systems are to be used on real-scale projects with running piles. We can therefore conclude that the tested systems have a potential **broad-band reduction of 7 – 9 dB SEL**.

No.	System	Description	ΔSEL [dB]		
			Near-field		Far-field
			Distance 6 m	Distance 13 m	Distance 375 – 750 m
1.	1	IHC NMS with bubble curtain			
2.		IHC NMS w/o bubble curtain			
3.	2	Menck FHS with 1.0 bar			
4.		Menck FHS with 2.0 bar			
5.	3	Weyres LBC			
6.	4	Weyres BeKa 0 bar			
7.		Weyres BeKa 5 bar			
8.		Weyres BeKa 7 bar			
9.	5	Elmer HSD M Ring			
10.		Elmer HSD O ring			
11.		Elmer HSD I ring			
12.		Elmer HSD MO ring			
13.		Elmer HSD MI ring			
14.		Elmer HSD OI ring			
15.		Elmer HSD MOI ring			

Table II: Achieved reduction ΔSEL

Table of contents

Abstract……..... 3
Table of contents..... 7
List of abbreviations…..... 10
Physical quantities…. 11
1. Introduction and objectives…..... 12
2. Acoustic principles……..... 15
2.1 Level variables. 16
2.1.1. (Energy) equivalent continuous sound pressure level L_{eq}..... 16
2.1.2. Single event exposure level L_E or SEL..... 17
2.1.3. Peak level L_{peak}..... 18
2.2 Sound propagation in the North Sea..... 19
2.2.1. Effect of distance……..... 19
2.2.2. Effect of water depth……..... 20
3. State of the art for underwater noise control……..... 21
4. Test site – local and technical conditions……..... 24
5. Equipment for the offshore tests.....28
5.1 Hammer 28
5.2 Offshore work platform…….....29
5.3 Air compressor…….....31
6. Noise mitigation systems.....33
6.1.1. IHC noise mitigation screen…….....34
6.1.2. „Fire hose method by the company Menck.....36
6.1.3. Little Bubble Curtain by Weyres 41
6.1.4. BeKa jacket by Weyres.....43
6.1.5. Hydro Sound Damper TU Braunschweig/Dr. Elmer.....46
6.1.6. Comparing the weights of the systems.....54
7. Executing the hydro sound and vibration measurements…….....55
7.1 Test set-up and measuring concept.....55
7.2 Drive energy measurement (PDM – pile drive monitoring)……61

7.3 Measuring process…..64
7.4 Method for evaluating the acoustic data (ITAP)……..…68
7.5 Noise prediction.....68
8. Results.....71
8.1 Driving energy…….....71
8.2 Evaluation of water properties…….....71
8.3 Influence of the different measurement positions on the sound exposure level (SEL)…….....72
8.4 Influence of impact energy on the single event exposure level (SEL).....74
8.4.1. Total level.....74
8.4.2. Noise mitigation.....76
8.5 Influence of water depth and distance to the pile on the sound exposure level (SEL)……78
8.6 Near and far-field measurements (itap) 81
8.6.1. Results of the noise mitigation system in the far field.....81
8.6.2. Results of noise mitigation in the near field.....90
8.7 Near field measurements TU BS (cf. Appendix 2)…….....98
8.7.1. Measuring equipment used and measurement positions.....98
8.7.2. Evaluation procedure for underwater noise measurements.....99
8.7.3. Results of underwater noise measurements.....101
8.8 Comparison of far-field and near-field measurements.....105
8.9 Measuring uncertainties and tolerances.....107
9. Discussion of the results.....108
9.1 Comparison between the Brodten pile (location for ESRa) and other project locations.....108
9.1.1. Boundary conditions Brodten pile.....108
9.1.2. Ground coupling (“preblow”).....110
9.1.3. Comparison of an ESRa noise mitigation system at different locations…….....117
9.1.4. Influence of the water depth.....119
9.1.5. Interim result…. 120

9.2 State of the science in the sector of noise mitigation concepts and noise mitigation systems…….....120
9.2.1. Noise mitigation systems in overview…….....120
9.3 How can the noise mitigation systems tested from ESRa be improved?.....124
9.4 Outcome.....126
10. Summary and Outlook…….....129
11. Literature, Guidelines, and Aids Used…….....132
12. Schedule of Figures.....135
13. Schedule of Tables.....142
14. APPENDIX 1: Itap Noise Prognosis.....143
15. APPENDIX 2: TUBS Close Proximity Measurements.....156

List of abbreviations

O-ring	Outer ring of the Elmer HSD
OI-Ring	Outer and inner ring of the Elmer HSD
BSH	*Bundesamt für Seeschifffahrt und Hydrographie* (Federal Maritime and Hydrographic Agency)
dB	Decibel
Elmer HSD	Hydro Sound Damper of the TU Braunschweig and Dr. Elmer
ESRa	Evaluation of Systems for Ramming Noise Mitigation at an Offshore Test Pile
I-ring	Inner ring of the Elmer HSD
IHC NMS	Noise mitigation screen (tube with inner bubble curtain by the company IHC)
M-ring	Middle ring of the Elmer HSD
MI-ring	Middle + inner ring of the Elmer HSD
MO-ring	Middle + outer ring of the Elmer HSD
MOI-ring	Middle + outer + inner ring of the Elmer HSD
Menck FHS	Fire hose system by the company Menck
MP	Measuring position
NMS	Noise mitigation system
OWF	Offshore wind farm
PDM	Pile driving monitoring
StUK 3	Standard “Investigation of the Impacts of Offshore Wind Turbines on the Marine Environment”
TUBS	Braunschweig University of Technology
Weyres BeKa Jacket	Noise-mitigation shells in lightweight construction with two bubble curtains (modular design) by the company Weyres
Weyres LBC	Little bubble curtain (Weyres)

Physical quantities

Variable	Description	Unit
SEL	Sound exposure level, identical to the single event exposure level L_E	[dB]
Z	Characteristic impedance	Rayl [10Ns/m3]
p	Sound pressure	[Pa]
ρ	Density of the medium	[Kg/m3]
L_{eq}	(Energy) equivalent continuous sound pressure level	[dB]
L_E	Single event exposure level (identical to the sound exposure level – SEL)	[dB]
L_{peak}	Peak sound pressure level	[dB]
p(t)	Time-dependent sound level	[Pa]
p_0	Reference sound pressure (when underwater noise 1 µPa)	[Pa]
T	Average time	[s]
T_0	Reference value 1 second	[s]
n	Number of piles	dimensionless
L_{hg}	Noise or background level between the individual piles	[dB]
$\lvert p_{peak} \rvert$	Maximum sound pressure measured (positive or negative)	[Pa]
TL	Transmission loss	[dB]
k	Constant (for the North Sea k = 15)	dimensionless
λ	Wavelength of sound wave	[m]
R	Distance from pile	[m]
f_S	Sampling frequency	[Hz]
ΔSEL	Difference in the SEL between the application without (reference) and with noise mitigation concept	[dB]
ΔL_{peak}	Difference in the peak level between the application without (reference) and with noise mitigation concept	[dB]
f_g	Frequency limit for sound transmission with continuous excitation	[Hz]
h	Water depth	[m]
c_{Water}	Speed of sound in water	[m/s]
$c_{Sediment}$	Speed of sound in sediment	[m/s]
f	Sound frequency	[Hz]

Table 1: Overview of the main physical quantities and parameters and their units of measurement.

1. Introduction and objectives

Almost 30 offshore wind park projects in German coastal waters and in the German EEZ have currently been approved for the generation of renewable energy and many more have been planned for the future. These wind parks are to be built in both the Baltic Sea and the North Sea.

Offshore wind parks are generally built using pile-driven foundation structures. In offshore applications, these building measures mainly take place below the surface of the water. From a conservation point of view, authorities regard the noise emissions that occur when the conventional foundations are driven into the seabed as problematic for marine mammals in particular. In an incidental provision to the existing authorisations, the responsible approving authority (BSH) in the exclusive economic zone (EEZ) has instructed that, when building and installing the parks, state-of-the-art methods are to be used in order to mitigate as far as possible the acoustic impact in accordance with the specific site conditions. An emission limit value was used as reference and is particularly important when driving the piles; this value is 160 dB (SEL) at a distance of 750 m from the emission source. Depending on the date of the authorisation, in the justification of the relevant incidental provision, this value is given as “desirable”. In more recent authorisations, it is, in part, given as “compulsory” in the authorisation constraints.

Discussions with marine biologists and approving authorities reveal that, when installing the foundations for future offshore wind farms (OWF), it will be essential to use practicable noise mitigation measures when driving piles. At the same time, there is currently no “state of the art” ensuring that noise is maintained at the required level in the marine area when driving piles. Innovative noise reduction techniques that would theoretically be possible are frequently still at the concept stage, are often not yet sufficiently advanced for large-scale technical implementation and are thus not available on the market.

In view of the expected size and number of these foundation structures in both the North Sea and Baltic Sea, the selection, testing, effectiveness and manageability of noise mitigation methods are of crucial importance in order to realise effective and efficient mitigation measures at a justifiable cost on the high seas.

To this end, prior testing and optimisation of suitable noise reduction measures have to be performed on a full scale; initially, this will preferably be carried out in a coastal area for greater convenience. For this reason, under the aegis of RWE OLC GmbH, a total of eight builders and operators of German offshore wind parks (Bard Engineering, DONG Energy, EnBW Erneuerbare Energien, E.ON Climate Renewables, EWE ENERGIE, RWE Innogy, Stadtwerke München, Vattenfall Europe) have joined forces in an industry-wide cooperation in order to use the ESRa project to create a large multiplier for the knowledge obtained.

The aim of the ESRa project is to identify, test and evaluate innovative design and operating concepts for safe, practical and cost-effective noise control when building pile-driven offshore wind farms.

Noise mitigation systems by various manufacturers and at different stages of development are to be evaluated on a large-scale test pile. For the first time, as part of the planned project, a larger number of systems (approx. 4-5) are to be used under identical boundary conditions and a comparison made of their potential noise reduction levels by means of a uniform measuring concept. ITAP (Institute for Technical and Applied Physics) GmbH was commissioned both to develop the measuring concept and to conduct the measurements. The measurements and the evaluations of the underwater noise emissions are to be conducted on the basis of the existing standard investigation concept (StUK 3 [1]) of the Federal Maritime and Hydrographic Agency (BSH). In addition to the underwater noise measurements, vibration measurements are also to be conducted in the sediment close to the driven pile.

Based on the results of the measurements and experience applying the various noise control concepts, as far as is possible on the basis of the data obtained, recommendations are to be derived for systems that offer reliable compliance with the limit values currently under discussion and, at the same time, that enable large-scale implementation and integration in installation logistics. The findings thus obtained can form the basis for further full-scale trials and help wind park operators when defining potentially suitable noise mitigation systems.

2. Acoustic principles

Sound is a rapid, frequently periodic fluctuation in air pressure superimposed on the atmospheric pressure (in water, on the hydrostatic pressure). The water particles move “to and fro” and this movement is generally described in terms of its speed, the so-called particle velocity. The particle velocity refers to the speed with which the particle is displaced from its original position in a medium. The particle velocity should not be confused with the speed of sound c_{Water}, namely the propagation velocity of sound in a medium that, in the case of water, is generally in the range of c_{Water} = 1500 m/s^2. As a rule, the particle velocity v is much smaller than the speed of sound c.

Sound pressure p and particle velocity v are related via the acoustic characteristic impedance Z, which characterises the wave resistance of the medium, as follows:

$$Z = \frac{p}{v} \qquad \text{Equation 2.1}$$

In the far-field, i.e. at some distance (depending on frequency) from the sound source, the impedance is given by:

$$Z = \rho c \qquad \text{Equation 2.2}$$

where
ρ – density of the medium.

For a sound pressure amplitude of, for example, 1 Pa (with a sinusoidal signal, this corresponds to a sound pressure level of 117 dB re 1 µPa or a peak level of 120 dB re 1µPa, see Section 2.1), this gives us a particle velocity in water of approx. 0.7 µm/s.

2.1 Level variables

In acoustics, the intensity of noise is not generally described directly by the sound pressure (or particle velocity), but rather, as is familiar from telecommunications, by the level in dB (decibel). However, there are different sound level parameters. In the context of this study in relation to the StUK3 [1], the following variables are important:

- (Energy) equivalent continuous sound pressure level L_{eq}
- Single event exposure level LE (identical to the sound exposure level – SEL)
- Peak level L_{peak}

The L_{eq} and the L_E or SEL can both be given independently of frequency, i.e. as broad-band single-number values, as well as frequency-specific, e.g. in the third octave band spectrum. The guide value of 160 dB at a distance of 750 m as specified by the BSH for pile-driving refers to the broad-band single event exposure level L_E or SEL (single-number value).

The above-mentioned level variables are described in brief below.

2.1.1. (Energy) equivalent continuous sound pressure level L_{eq}

The L_{eq} is the most common parameter in acoustics and is defined as

$$L_{eq} = 10 \log \left(\frac{1}{T} \int_0^T \frac{p(t)^2}{p_0^2} dt \right) \quad \text{[dB]} \quad \text{Equation 2.3}$$

where
p(t) - time-dependent sound pressure
p_0 - the reference sound pressure (with underwater sound, 1 µPa)
T - the average time

In words, equation 2.3 means: square the observed variations of the time dependent pressure *p(t)*, take the average value over time *T* and divide by the square of the reference sound pressure p_0^2 (energetic average). The logarithm of this value when multiplied by 10 is the energy equivalent continuous sound pressure level L_{eq} expressed in dB.

2.1.2. Single event exposure level L_E or SEL

The L_{eq} alone is insufficient to characterise pile-driving noise as it is not only a function of the strength of the blows driving the piles but also of the average time and of the intervals between the blows. The single event exposure level L_E or the sound exposure level (SEL) is more suitable (in German-speaking areas, the single event exposure level L_E is mainly used) and is defined as follows:

$$\mathrm{SEL} = 10 \log \left(\frac{1}{T0} \int_{T_1}^{T_2} \frac{p(t)^2}{p_0^2} dt \right) \quad \text{[dB]} \quad \text{Equation 2.4}$$

where

T_1 and T_2 - Start and end time of the average values (these are to be selected such that the sound event lies between T_1 and T_2, approx. 0.05 – 0.40 s in Figure 1)
T_0 - Reference value 1 second

The single event exposure level of an acoustic pulse (pile-driving blow) is thus the level (L_{eq}) of a continuous sound of duration 1 s and with the same sound energy as the pulse.

It is more difficult to measure the SEL or L_E directly than it is to measure the L_{eq}, however, both variables can be easily converted from one to the other:

$$\mathrm{SEL} = 10\log(10^{L_{eq/10}}) - 10\log\frac{nT_0}{T} \quad \text{[dB]} \quad \text{Equation 2.5}$$

n - Number of noise events, namely pile-driving blows, within a time T
T_0 - 1 s
L_{hg} - Noise or background level between the individual pile-driving blows

From an L_{eq} measurement, equation 2.5 thus gives the average sound exposure level SEL or L_E of n noise events (pile-driving strokes). In the event that the background level between the strokes is significantly lower than the pile-driving noise (e.g. > 10 dB), the following calculation can be made with sufficient accuracy using a simplification of equation 2.5:

$$\mathrm{SEL} \approx L_{eq} - 10\log\frac{nT_0}{T} \quad \text{[dB]} \quad \text{Equation 2.6}$$

2.1.3. Peak level L_{peak}

This variable is a measure of peak sound pressure levels. Unlike L_{eq} and L_E or SEL, there is no average:

$$\mathrm{L_{peak}} = 20\log\left(\frac{|P_{peak}|}{P_0}\right) \quad \text{[dB]} \quad \text{Equation 2.7}$$

where
p_{peak} - maximum measured positive or negative sound pressure

An example is shown in Figure 1. The peak level L_{peak} is always greater than the single event exposure level. As a rule, when driving piles, the difference between the L_{peak} and the SEL is 20 dB to 25 dB [2]. Some authors prefer the peak-to-peak value rather than the L_{peak}. Figure 1 shows a definition of this variable.

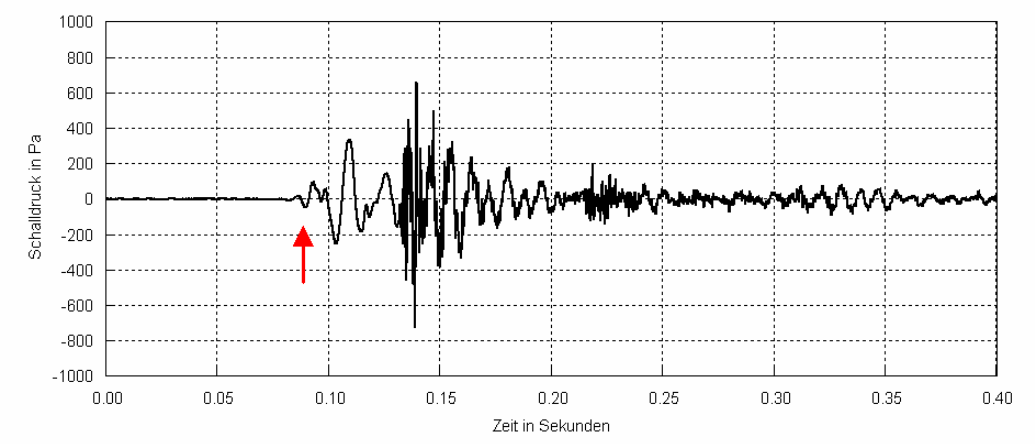

Figure 1: Signature time signal of underwater sound with a pile-driving blow as measured at a distance of approx. 100 metres.

Schalldruck in Pa	Sound pressure in Pa
Zeit in Sekunden	Time in seconds

2.2 Sound propagation in the North Sea

2.2.1. Effect of distance

For approximate calculations, we can assume that sound pressure decreases with distance according to a simple power law. The level in dB then falls off as:

$$\mathrm{TL} = \mathrm{k} \cdot \log\left(\frac{r_2}{r_1}\right) \quad [\mathrm{dB}] \qquad \text{Equation 2.8}$$

where

r_1 and r_2 - Distance to the source of the sound increases from r_1 to r_2

TL - Transmission loss

K - Constant (for the North Sea, $k = 15$ can be assumed; for the Baltic Sea, $k = 15$ is also assumed for approximate estimates)

The transmission loss or TL is often given for a distance $r_1 = 1$ m (fictitious distance to an imagined point source). The sound power of a pile-driving blow as calculated at a distance of 1 m is often also known as the source level. Equation 2.8 is then simplified to *TL = k log (r/metre)*. However, this simple calculation does not take into account the fact that the fall in sound pressure with distance is also frequency-dependent. Furthermore, the above formula is only applicable to the “far-field” of an acoustic signal, i.e. at some distance (frequency-dependent) from the source.

Note: In air, depending on frequency, the boundary between near- and far-field is approx. *2λ* (*λ* – wavelength; frequency-dependent; [3]). There are no detailed studies of near- and far-field for underwater sound generated when driving piles for wind farms. The boundary between near- and far-field is expected to be in the range of 2λ to 10λ.

In addition, at distances of a few kilometres, the absorption of the water plays a role and reduces sound pressure further. Furthermore, at such great distances, weather also affects the sound pressure in water; with a strong wind and swell, the sound pressure level is reduced. This is due to the surface roughness of the sea and, above all, to the greater volume of air that is carried into the upper layer of the sea by the motion of the waves.

Von Thiele and Schellenstede [4] have published approximate formulae to calculate sound propagation for various regions in the North Sea, as well as for “calm” and “rough” seas (from [6]):

$$\mathrm{TL} = (16.07 + 0.185\mathrm{F})(\log(\mathrm{R}) + 3) + (0.174 + 0.046F + 0.005F^2)R \quad \text{[dB]} \qquad \text{Equation 2.9}$$

where
F = *10 log(f/[kHz])*
R – Distance

Strictly speaking, the correlations according to Equation 2.9 apply only for wintry conditions with a good mixing of the water without a pronounced sound velocity profile in the North Sea (German Bight). There are no formulae or dependencies to calculate the attenuation as a function of distance for the Baltic Sea. However, it can be assumed that the water is mixed completely and that there is not a pronounced sound velocity profile in the area under investigation (here the Baltic Sea, *Lübeck Bay*). For this reason, the formula of Thiele and Schellenstede [4] (Equation 2.9) will be used here for the location in question, as well as for the approximate calculations in Section 8.

2.2.2. Effect of water depth

Sound propagation in the sea is also affected by the depth of the water. Below a certain limiting frequency, continuous sound propagation is not possible; the calmer the water, the higher this frequency. Depending on the sediment type, in water that is 10 m deep, the limiting frequency f_g is in the range of 100 Hz [6]. Sound near the limiting frequency is attenuated or damped more as the distance from the sound source increases, as is calculated using Equation 2.9.

3. State of the art for underwater noise control

Piles, particularly when driven by hydraulic hammers, create high-frequency sound at a very high level [7]. This kind of impulse sound is usually described by two sound levels. The first is the peak level of the maximum momentary positive or negative sound pressure described in the previous section. The second variable used to describe underwater sound is the single event sound pressure level SEL.

Various measurements taken during offshore pile-driving for research platforms and foundation structures for wind farms in the North Sea and Baltic Sea have revealed underwater sound levels SEL that regularly exceed the currently required limit value of 160 dB by more than 10 dB. There are basically two different approaches for reducing sound emission: reducing the source strength and reducing the sound propagation. In the case of the first of the two approaches (e.g. reducing the impulse duration), tight technological restrictions apply for the pile-driving energies required for the relevant foundation dimensions. Consequently, the approaches for reducing sound propagation currently documented also include absorber systems. Their operating principle is based on the introduction of a layer into the path of the sound that creates an acoustic impedance mismatch and partially absorbs the sound energy, namely converts it into heat.

In the past, the only field-tested method for mitigating the noise of hydraulic engineering measures (coastal bridges and maritime construction sites) was the bubble curtain. This had a damping effect that cannot simply be applied to offshore wind farms. In tidal waters, there is also the problem of holding the bubbles securely in the path of the sound. In recent years, both the big bubble curtain and the little bubble curtain have been tested during the course of various research projects for the wind energy industry, as listed below. The maximum noise mitigation of the bubble curtain was about 12 dB, however, due to technical problems, the latter method was not implemented in full. In terms of underwater noise, investigations of other noise mitigation systems, such as covering the driven pile with insulating material or lengthening the impact blow, had a much lower damping effect than the bubble curtain.

From the previous application of these sound mitigation systems, we can conclude that, as a rule, it is highly likely that a reduction in underwater noise of approx. 10 dB can be achieved. On this basis, we can conclude that, based on the technology currently available, there is currently no noise-mitigation system that complies with the limit value as specified by the BSH.

The results of the research projects listed below provided the basis for the focus of the current project:

- Investigations as part of the installation of the FINO 1 research platform ([8] Standardverfahren zur Ermittlung und Bewertung der Belastung der Meeresumwelt durch die Schallimmission von Offshore-Windenergieanlagen, 2004)

- Experience gained when applying various sound mitigation systems at a test pile in the Baltic Sea ([9] Minderung des Unterwasserschalls bei Rammarbeiten für Offshore-WEA – Praktische Erprobung verschiedener Verfahren unter Offshore-Bedingungen, 2006)

- Noise measurements at the Amrumbank West met mast and at a maritime construction site. ([7] Standardverfahren zur Ermittlung und Bewertung der Belastung der Meeresumwelt durch die Schallimmission von Offshore-Windenergieanlagen, Projekt “Schall 2”, 2007)

- Investigation of noise mitigation measures at the FINO 2 measuring platform ([10] Abschlussbericht zum Forschungsvorhaben 0329947b, 2007)

- Investigations into the design, testing, realisation and verification of low-noise construction methods and noise-reducing techniques during the construction of offshore wind farms ([11] “Schall 3“ project, 2010)

- Use of the big bubble curtain at the FINO 3 research platform. ([12] Abschlussbericht zum BMU-Projekt "Erforschung und Anwendung von Schallminimierungsmaßnahmen beim Rammen des FINO3-Monopiles – Schall FINO3", 2010)

- Research into the little bubble curtain sound-mitigation measure in the alpha ventus test field ([13] Verbundprojekt im Rahmen von alpha ventus, 2010).

4. Test site – local and technical conditions

The “Brodten Ost” test pile is located in Lübeck Bay near Travemünde, about 2.4 km northeast of the “Brodtener Ufer” (Figure 2 and Figure 3). It has the coordinates 53°59.9’N 010°54.6’E.

The pile was erected by Menck GmbH in the 1980s for test purposes. The water depth at the location is about 8.5 m with a variation of ± 0.50 m. Figure 4 shows the water depth in the area around the pile. The pile is a steel pipe with a diameter of 2.139 m and a wall thickness of 50 mm. According to Menck [14], it is embedded more than 65.0 m into the seabed. The remaining pile length above the seabed is 13.30 m, which means that, with a water depth of 8.20 m measured prior to testing, the height above the waterline is 5.10 m. It is not expected that the pile will be driven further into the ground by additional blows of the hammer.

Figure 2: The test pile near Travemünde.

The white cap improves visibility for shipping and is removed for pile-driving tests (photos from [9]).

Figure 3: Geographic position of the test pile in Lübeck Bay (source: [14]).

Brodtener Pfahl	Brodten pile

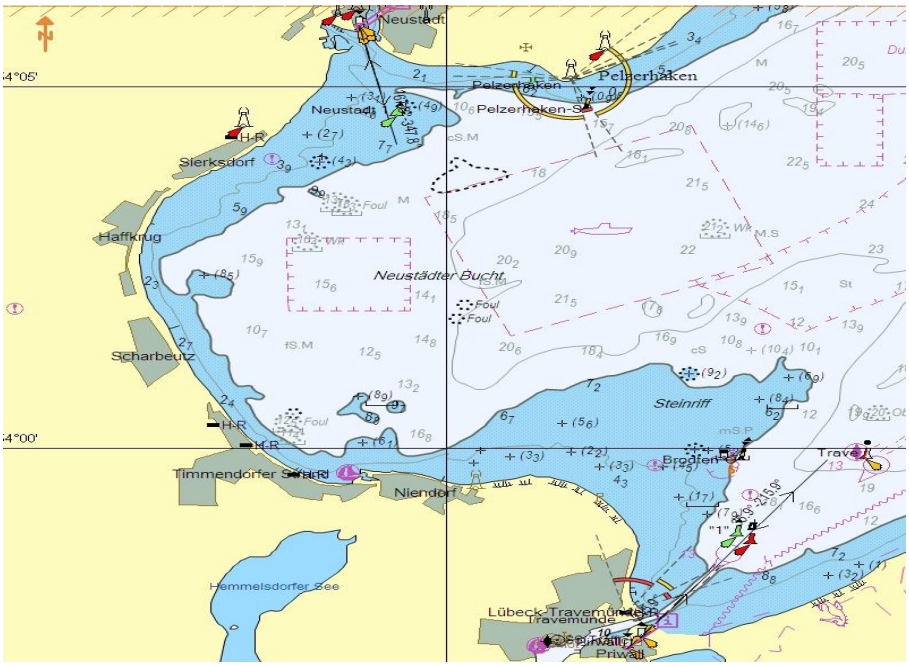

Figure 4: Map section of Lübeck Bay [15] indicating the test pile near the Brodten-Ost cardinal buoy

It was also particularly important to safeguard the measuring instruments to be set up near the test pile against direct background noise (noise from passing motor vessels) and unauthorised removal, as well as to keep any curious onlookers away from the test area. To this end, an application was submitted to the WSA Lübeck to make this an exclusion zone; the application was approved.

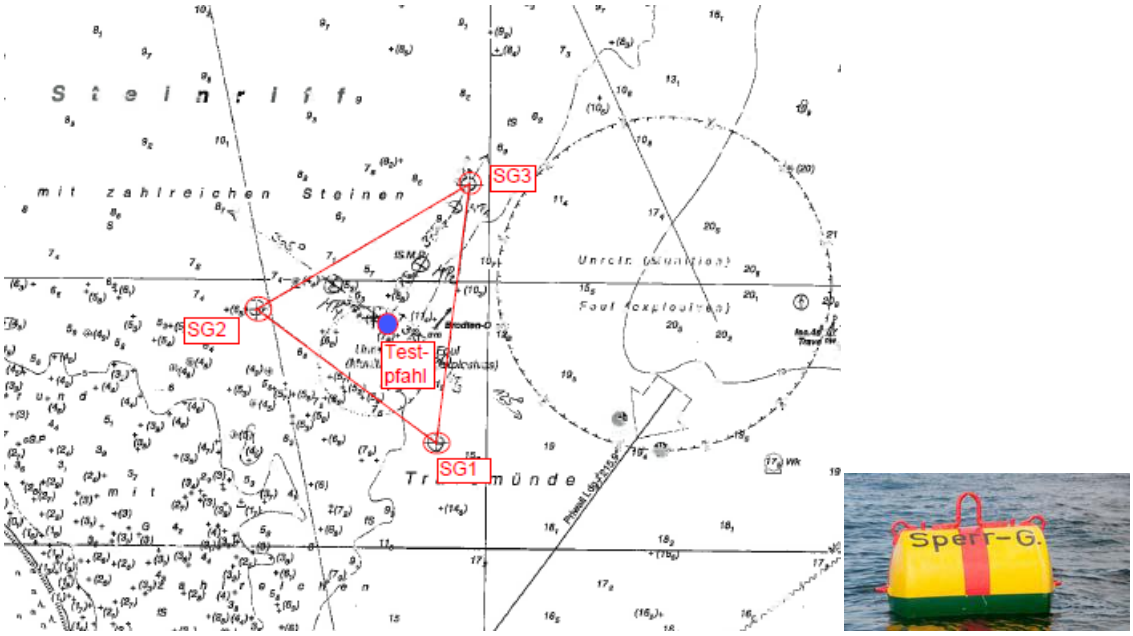

Figure 5: Position of the exclusion around the test pile

SG1	EZ1
SG2	EZ 2
SG3	EZ 3
Testpfahl	Test pile
Steinriff mit zahlreichen Steinen	Stone reef with numerous rocks
Sperr-G	Exclusion Z

Menck provided an approximate ground stratigraphy from 1985 (Table 2). This is not based on local ground surveys but was compiled using technical publications and ground surveys conducted nearby. Accurate information regarding the layer thicknesses of the individual types of soil is not available. The possible inclusion of interglacial clays (basin clay) in the boulder clay shown in Table 2 is significant for the ESRa field tests. These inclusions will presumably be lenticular, however, the dimensions are not yet known. From an acoustic perspective, a slightly firm, slow basin clay layer will prevent sound radiation from the fast (much firmer) boulder clay layer. In this case, it can be assumed that reflections return a large part of the sound energy introduced into the basin clay to the water.

Depth in relation to sea level		Geological layer	Soil layer	Volume change modulus
From	To			
-Sea level [m]	- Sea level [m]	-	-	MN/m²
-8.5	10.5	Holocene	Sand and gravel	-
-10.5	-63.5	Pleistocene	Boulder clay	50 – 300
			Basin clay	5 – 50
			Pleistocene sand and gravel	80 – 100
-63.5	-300	Tertiary	Tarras clay	2 – 4
			Mica clay	4 – 10
			Medium and fine sands	-

Table 2: Soil conditions at the Brodten Ost test pile.

5. Equipment for the offshore tests

5.1 Hammer

In order to carry out the tests, both a work platform and a suitable pile-driving hammer were required. The hammer had to be capable of transferring sufficient energy to the pile in order to generate a noise level comparable with that generated when driving offshore foundation structures. The hammer chosen was the MHU-270 T by MENCK. It had to be adapted to the 2.139 m pile diameter by means of a pile-driving helmet adapter and a pile-driving helmet. The underwater weight was not taken into account as the test pile still protruded from the water. However, it was important to ensure that the pile-driving helmet was not too long as it would otherwise have got in the way of the test equipment that was to reach as far as the surface of the water. The total weight of the pile hammer, pile-driving helmet and pile-driving helmet adapter was 63 tons. It is important to note that, despite its misleading name, when operated above the water level, the hammer has a maximum impact energy of 300 kJ (compare Figure 6).

MHU deepwater series

	Unit	270T	400T	500T	750T
Minimum energy	kJ	30	40	50	75
Maximum energy - surface	kJ	300	440	550	820
Maximum energy – 1000 m depth	kJ	270	400	500	750
Oil flow	l/min	600	1000	1150	1600
Blow rate at max energy	bl/min	40	38	38	38
Ram weight	t	16.2	24.3	30.2	45.4
Total hammer weight	t	30.8	49.1	59.8	79.6
Standard Configuration					
Pile sleeve		1.6m	60”	2.2m	84”
Total weight dry w/MHP DWS	t	66	85.8	113.7	147.8
Total weight under water	t	52.5	75.5	90	118.3
Hammer length w/pile sleeve	m	12.7	14.5	16	17.6

Figure 6: Hammer specification MHU 270 T (source: www.menck.com)

Figure 7: Hammer placed on the pile (photo: Patrice Kunte)

5.2 Offshore work platform

A range of equipment was required in order to carry out the tests. In addition to the pile hammer with its various accessories, a crawler crane, air compressor, office container and at least one test device had to be kept on-site. For this reason, a stable work platform was essential in order to transport both the pile-driving hammer and the test equipment and to subsequently stabilise and operate them near the test pile. Alternatively, an installation ship, with or without engine, such as is used to install foundation structures for offshore wind parks, could also be used. Due to the seasonal conditions at the test location with just a low wave height and moderate water depth, a stilt-mounted pontoon without engine was used to perform the work. Unlike installation ships with hydraulically operated jack-ups, a stilt-mounted pontoon has 2-4 lowerable legs that stabilise its position in the swell but do not suppress the movement completely.

In addition to holding the equipment listed above, the RHR 1 work pontoon shown in Figure 8 and provided by the ‘logistics’ joint venture (TAGU/HOCHTIEF) was large enough to hold two work boats, two diesel tanks, a total of five containers and a second test device. Neustadt was chosen as the base port for mobilising and loading the test equipment (Figure 9).

Figure 8: Stilt-mounted pontoon RHR 1 with equipment (photo: Patrice Kunte)

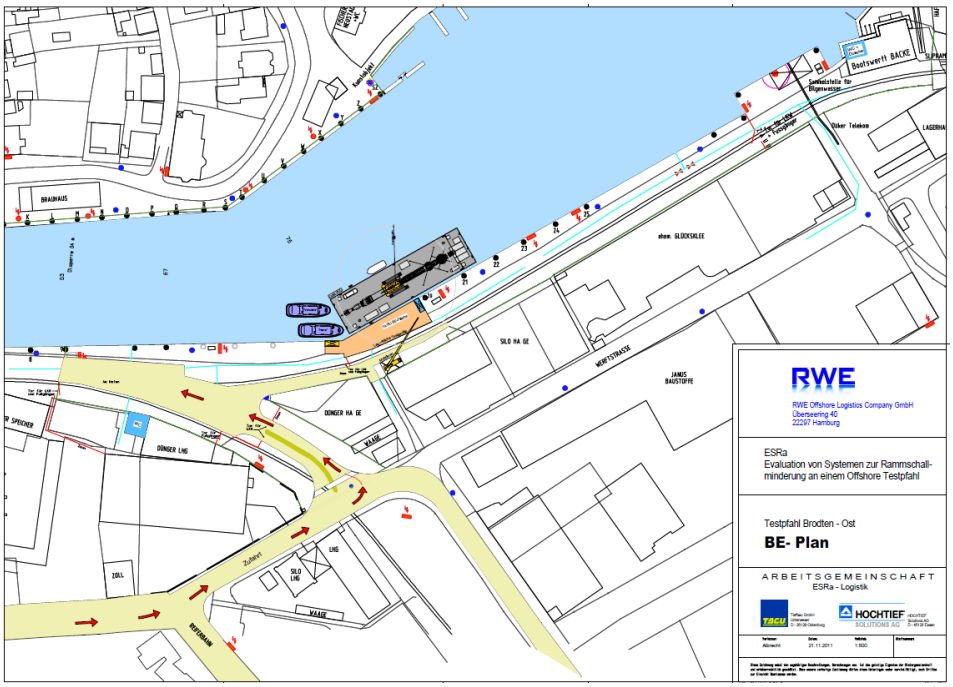

ESRa	ESRa
Evaluation von Systemen zur Rammschallminderung an einem Offshore Testpfahl	Evaluation of Systems for Ramming Noise Mitigation at an Offshore Test Pile
Testpfahl Brodten-Ost	Brodten-Ost test pile
Arbeitsgemeinschaft	Joint venture

Figure 9: Mooring of the stilt-mounted pontoon in the port of Neustadt, construction site plan [16]

5.3 Air compressor

A controllable, oil-free air compressor type CompAir C210TS-12 was installed onboard the work platform in order to supply the individual test systems. At a maximum operating pressure of 12 bar, this has an output free air delivery of 21 m³/min (see also Figure 10). For operation with the Menck noise mitigation system (cf. Section 6.1.2), the compressor was fitted with a controller in order to reduce the pressure to the level required for the fire hoses.

Model	C210TS-12 (new DLT2701 electronic controller)
Hz	50
Series	C Series
Description	Portable compressors (C Series Turboscrew – 16 to 27 m^3/min)
Gas compressed	Air
Output free air delivery at rated pressure (m3/min)	21
Minimum operating pressure (bar g)	5
Max or rated operating pressure (bar g)	12
Maximum operating pressure (bar g)	12
Motor output (kW)	180
Noise level	100 (LWA) 71 (LPA)
Length (mm)	5195
Width (mm)	1960
Height (mm)	2350
Compressed air outlets (inches)	3 x 3/4” + 1 x 2”
Off load speed (rpm)	1000
Full load speed (rpm)	2400
Oil capacity (l)	65
Weight: adjustable towbar, braked (kg)	3310
Fuel tank capacity (l)	370
Wheel track (mm)	1720
Ground clearance (mm)	220
Tyre size (mm)	205 R 14 C
Canopy length (mm)	3750
Engine type	Cummins QSB6,7
Cooling system	Water cooled
At rated operating pressure **12 bar g,** output free air delivery = **21 m^3/min**	

Figure 10: Air compressor used (source: www.compair.de)

6. Noise mitigation systems

Based on the investigations and research reports available at the time, prior to submitting the application, the “Sound” working group of the offshore foundation operator forum compiled a selection matrix in order to evaluate the available noise mitigation methods with respect to noise mitigation potential and installation. This provided the basis for selecting the systems tested as part of ESRa. As some of the systems under consideration were still at the concept phase, their noise mitigation potential was evaluated on the basis of theoretical calculations or the results of small-scale tests.

As a rule, when comparing measurements taken at different locations, boundary conditions such as water depth, ground parameters and pile driver have to be taken into account. Numerical methods for transferring the measurement results to alternative locations or the standardisation of different methods are hardly possible at present. In order to still enable comparability with previous and future projects, a so-called ‘reference system’ has to be tested in parallel. The decision was taken to use a bubble curtain system with a known principle of operation and/or damping potential that had already been tested on a large scale. The “Sound” working group selected the following system:

- Little bubble curtain/LBC; by the company Weyres

The large bubble curtain was not used. In retrospect, due to the distance from the driving location, a large bubble curtain would have absorbed a larger part of the sound reintroduced via the seabed, simplifying the evaluation of the site conditions at the Brodten pile.

As part of the ESRa project, the following **five** different noise mitigation systems (NMS) by four different manufacturers were used:

1. Tube with inner bubble curtain by the company IHC (IHC NMS)
2. Fire hose system by the company Menck (Menck FHS)
3. Little bubble curtain (LBC) by the company Weyres (Weyres LBC)
4. Noise-mitigation shells with two bubble curtains (modular design) by the company Weyres (Weyres BeKa Jacket)
5. System 5: hydro sound damper by the TU Braunschweig (TUBS) and Dr. Elmer (TUBS/Elmer HSD)

The noise mitigation methods used are described in detail below. The descriptions are largely the work of the companies IHC, Menck, Weyres and TUBS [17], [18], [19], [20], [21].

6.1.1. IHC noise mitigation screen

The noise mitigation screen by IHC Hydrohammer B.V. is a double-wall steel tube with a protected bubble curtain between the tube and driving pile. The system is placed over the pile and is effective along the entire length of the water column at the pile.

With an outer diameter of 3.65 m, the ICH tube weighs 30 t at a water depth of 8.20 m at the test pile and has a total length of 9 m. The air-filled, two-shell system has an inner diameter of 3.10 m, which means that the impedance layer is 275 m thick. The two 20 and 15 mm thick steel sheets of the tube are welded at the ends. In more recent IHC systems, these steel bridges are no longer necessary as plastic parts are fitted.

Inner guide rolls (see Figure 11) enable easy handling when placing over the pile and keep the system at a uniform distance to the pile (Figure 12).

Pressure hoses are then used to fill the gap (compare Figure 13) with air at a pressure of approx. 6 bar and a rate of 3 m^3/h. The nozzle system creates air bubbles at several levels. The nozzle system reduces compressor output and size compared with conventional bubble curtains.

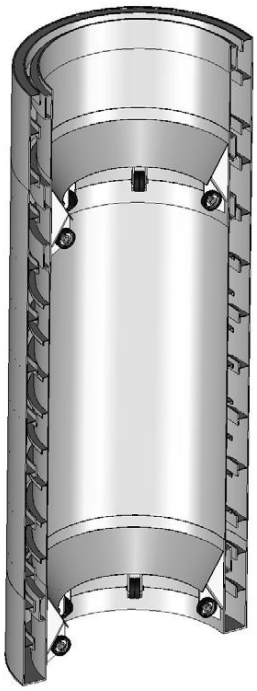

Figure 11: Noise mitigation screen by the company IHC, schematic structure

Figure 12: IHC NMS during installation (photo: Patrice Kunte)

Figure 13: View of the gap between the pile/NMS during operation of the bubble curtain (photo: Patrice Kunte)

6.1.2. Fire hose method by the company Menck

As part of the ESRa research project, the company MENCK designed a fire hose system in order to investigate the fundamental effectiveness and handling of such systems in practical application. As lightweight fire hoses are used, relatively small and compact noise mitigation systems can be developed and this is a major factor in the economic construction of wind farms.

Figure 14: Menck fire hose system being lifted off the deck of the work platform (left) and during installation at the pile (right) (photo: Patrice Kunte)

The test system consists of 222 staggered fire hoses that are attached with hose clamps to the air distribution ring (top) and ballast ring (bottom) (Figure 15). Four buoyancy bodies are attached to the air distribution ring and keep the fire hoses taut. Compressed air is supplied to the hoses via the hollow air distribution ring. The relative pressure of the air in the hoses is set at 1 bar in order to prevent the hoses from collapsing under the hydrostatic water pressure. The fire hoses are arranged staggered to increase the effective thickness of the noise mitigating air wall and to prevent larger gaps. For design reasons, a small gap remains between the hoses as they are fastened to the nozzles with hose clamps. The outer row of hoses was designed for easy dismantling in order to be able to investigate the effect of single and double hose layers (due to the limited amount of time offshore, the single-row test was not performed as part of ESRa).

Figure 15: Close-up of the lower end of the NMS with the fire hose connections (photo: Patrice Kunte)

The entire system consists of two halves, which can be easily transported by truck. The dimensions are such that both halves also fit inside a 40” open-top container. A base plate is mounted below the ballast ring for better handling of the folded hoses. During operation, the base plate remains on deck.

The sea fastening of the fire hose noise mitigation system is put in place by bracing the lifting lugs of the upper ring and fixing the lower ring to the base plate. The lower ring is attached to the base plate by clamping elements on both the inside and the outside. The base plate is welded on deck. The upper ring is also screwed securely to the lower ring of the fire hose noise mitigation system.

Figure 16: Sea fastening of the fire hose system (photo: Patrice Kunte)

Handling for operation of the fire hose noise control system is simple: the screws between the upper and lower part are undone and the clamping elements between the lower ring and the base plate, as well as the lashing straps, are removed in preparation for use. The system can then be pulled apart vertically for installation and operation and lifted off the base plate for installation at the pile. With the test system used, before installation, the air-filled hoses were held together by ropes arranged in a spiral pattern to prevent the hose sleeve from separating due to the tidal flow and waves. Before being lifted, a low air pressure was applied to the hoses in order to stabilise the tension in the ropes.

After use, before returning the system to the deck, the natural ambient pressure of water is used to expel the air from the hoses. The simple evacuation of air from the hoses reduces the volume of the hoses to a minimum so that, similarly to the situation before use, little storage space is required inside the system. When storing the fire hose noise mitigation system, the hoses are pulled together with a loop in order to ensure that they are folded to optimum effect.

The main dimensions (length x width x height) are approx.:

- Hoses, folded: 4.9 m x 4.9 m x 2.0 m
- Hoses, opened out: 4.9 m x 4.9 m x 8.9 m

The total weight is approx. 20 t. For further details, see the following figure.

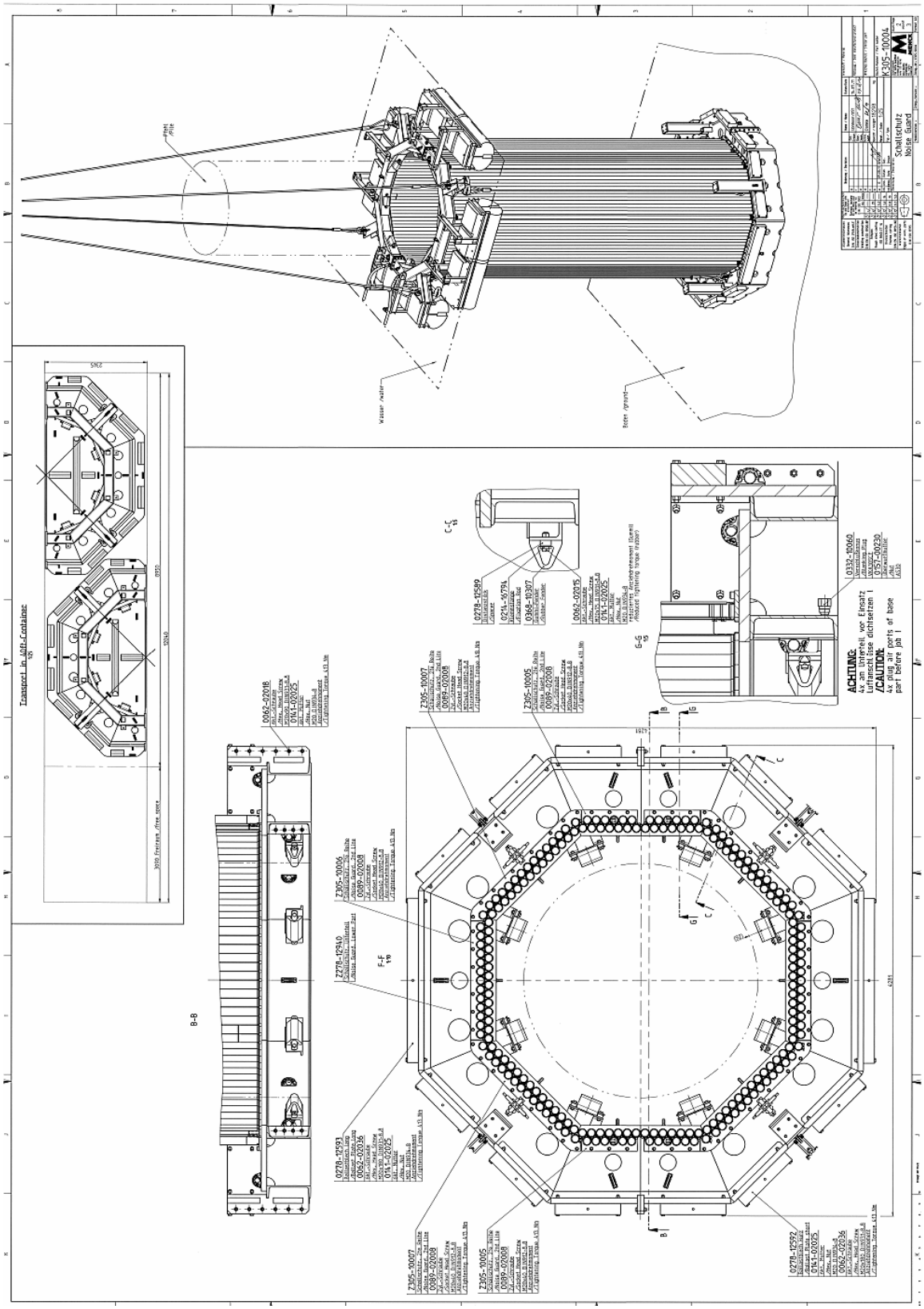

Figure 17: Schematic representation showing the components of the fire hose system

6.1.3. Little bubble curtain by Weyres

The little bubble curtain (LBC) by the company Weyres is a layered and guided bubble curtain, i.e. at different water depths, air bubbles are released into the water and baffle plates are installed around the entire system to prevent the air bubbles from being carried away by the tidal current. The system has an octagonal footprint and the diameter at its widest point is 5.25 m.

The entire system is designed so that the individual layers can be stacked telescopically in order to ensure that the design is as compact as possible for transport purposes (Figure 18). The system is centred on the pile via an opening in the base unit and the appropriate rising centring unit (Figure 18 right). The upper two layers of bubbles with their baffle plates are designed to float so that, after lowering the base unit, the system automatically adjusts to the respective water depth.

Figure 18: Retracted and telescopically extended LBC system (photo left: Patrice Kunte, photo right: Weyres)

In addition to the ring circuits with outlets shown in the following figure, there are five further ring circuits near the two floating outlet levels with baffle plates (Figure 18 right).

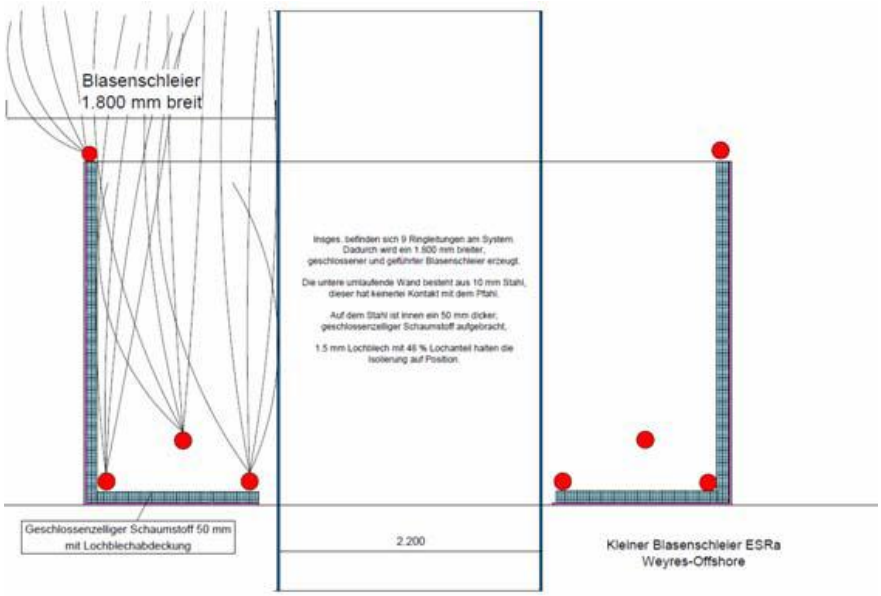

Blasenschleier	Bubble curtain
1.800 mm breit	1,800 mm wide
Geschlossenzelliger Schaumstoff 50 mm mit Lochblechabdeckung	Closed-cell foam 50 mm with perforated plate cover
Kleinen Blasenschleier ESRa Weyres-Offshore	Little bubble curtain ESRa Weyres-Offshore

Figure 19: Ring circuits that generate the bubble curtain near the base unit, which is lined with 50 mm foam (source: Weyres)

The following figure shows the installed system in operation.

Figure 20: Weyres little bubble curtain in operation (photo: Patrice Kunte)

6.1.4. BeKa jacket by Weyres

The BeKa jackets by the company Weyres are multi-layer sound-insulation shells (Figure 21) that are braced and held by an outer frame construction. They have a footprint of 4.0 x 4.0 m and a length of 9 m. The total weight of this comprehensively tested system is 39.8 tons.

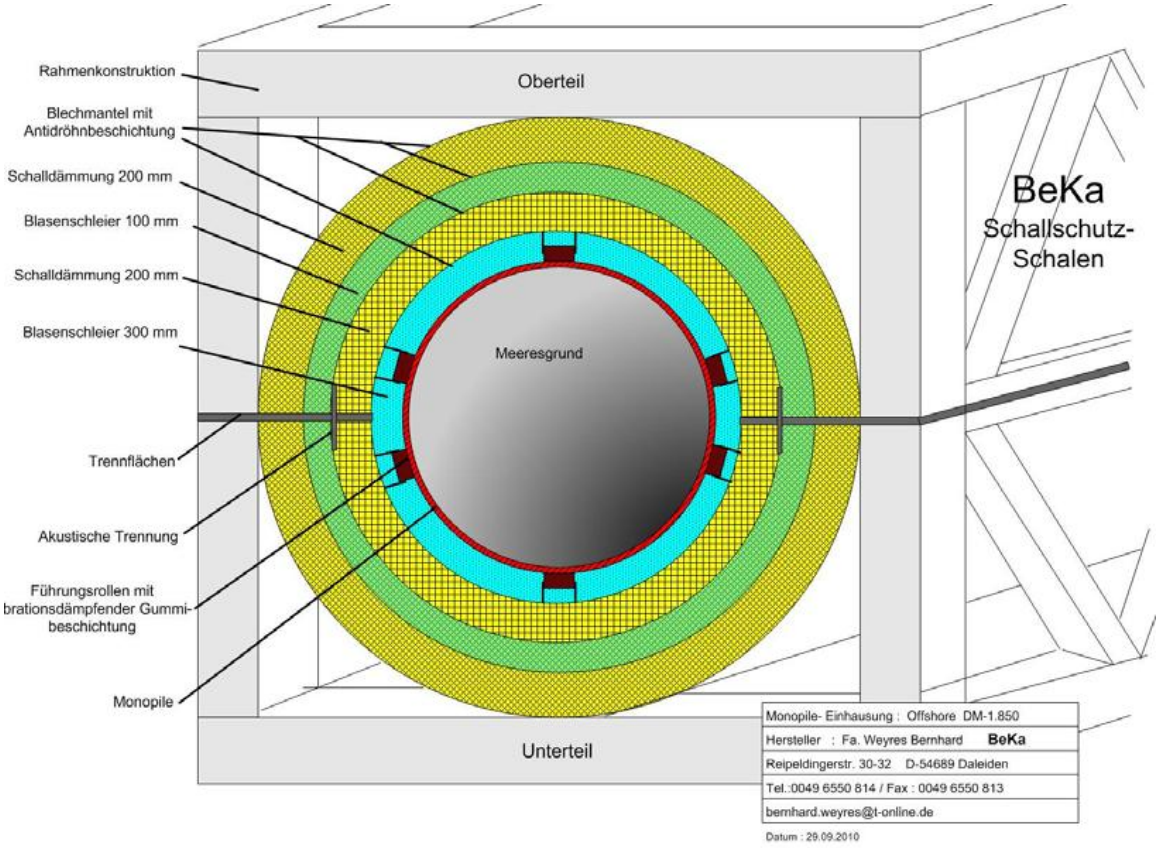

BeKa Schallschutz-Schalen	BeKa sound-insulation shells
Oberteil	Upper part
Meeresgrund	Seabed
Rahmenkonstruktion	Frame construction
Blechmantel mit Antidroehnbeschichtung	Metal jacket with anti-drumming coating
Schalldaemmung 200 mm	Sound insulation 200 m
Blasenschleier 100 mm	Air bubble curtain 100 mm
Schalldaemmung 200 mm	Sound insulation 200 m
Blasenschleier 300 mm	Air bubble curtain 300 m
Trennflaechen	Interfaces
Akustische Trennung	Acoustic decoupling
Fuehrungsrollen mit brationsdaempfender Gummibeschichtung	Guide rolls with vibration damping rubber coating
Monopile	Monopile

Unterteil	Lower part
Monopile Einhausung: Offshore DM-1.850	Monopile casing: offshore DM 1,850
Hersteller: Fa Weyres Bernhard BeKa	Manufacturer: Weyres Bernhard BeKa
Reipeldingerstr. 30-32 D-54689 Daleiden	Reipeldingerstr. 30-32 D-54689 Daleiden
Tel: 0049 6550 814 / Fax: 0049 6550 813	Tel: 0049 6550 814 / Fax: 0049 6550 813
Bernhard.weyres@t-online.de	Bernhard.weyres@t-online.de
Datum: 29.09.2010	Date: 29.09.2010

Figure 21: BeKa jacket by the company Weyres, design drawing

The structure shown consists of five layers:

- Layer 1 300 mm bubble curtain directly at the MP
- Layer 2 20 mm full-surface lining made of low-reflection rubber
- Layer 3 200 mm double steel jacket with sound insulation filling (spec. weight approx. 400-600 kg/m³)
- Layer 4 150 mm bubble curtain with acoustic decoupling between layer 3 and layer 5 by means of industrial vibration dampers
- Layer 5 200 mm double steel jacket with sound insulation filling (spec. weight approx. 600-800 kg/m³)

The first independent bubble curtain (layer 1) around the pile is approx. 300 mm wide and is separated from the tidal flow. The bubbles are generated by low-noise injection nozzles arranged at various levels. At the base, the pile is enclosed by a close-fitting rubber sleeve to prevent sludge from entering, suctioned by the Venturi principle. The shock sound waves created by the hammer blows are reduced by the bubble curtain (item 1) and then hit the full-surface 20 mm thick rubber coating (item 2). The reduced sound waves then hit the first 200 mm thick noise control construction (layer 3). This contains a specially blended material that, in trials, produced an optimum measured result. The specific weight is approx. 400-600 kg/m³. As a next measure, a second bubble curtain is installed (layer 4). Here, too, the air is injected via low-noise nozzles arranged at different levels. Only one compressor is required to generate the compressed air. The fifth noise mitigation measure consists of a second noise control construction (similar to the structure at layer 3). The two noise control constructions (layers 3 and 5) are acoustically completely isolated from one another by an industrial vibration damper. No vibrations can be transferred outside of the system. In addition, in the base area, there is a noise control measure that, depending on the quality of the soil, can be embedded in the seabed. If necessary, this can also be replaced. The BeKa system is offered as a modular system. In this way, it is possible to compensate for water depths of 5 – 45 m. With a monopole 6,500 mm in diameter and a water depth of approx. 30m, the total weight should be max. 180 tons.

The BeKa system consists of two half-shells. On the one hand, this facilitates transport. On the other hand, with sufficient crane capacity, a pile can be inserted in the lower shell. After “closing” the system over the upper half shell, the entire system comprising the pile and the BeKa shell can be lifted into position. The BeKa jacket is fixed to the pile using cleats or similar devices and the entire system is fixed to the installation ship prior to pile driving.

Figure 22: Two-part structure of the Weyres BeKa jacket (photo: Patrice Kunte)

Figure 23: BeKa jacket during installation (photo: Patrice Kunte)

6.1.5. Hydro Sound Damper TU Braunschweig/Dr. Elmer

The principle of the hydro sound damper

Air, rather than steel, is the ideal medium for insulating and reducing hydro sound. The innovative, patented method of the hydro sound damper (HSD) only uses air-cooled, small HSD balloons and HSD foam elements for the effective mitigation of hydro sound in offshore pile-driving operations. The HSD elements are fixed to a close-meshed net that can be installed flexibly around the sound source in the water. As shown in Figure 24, steel is only used for the weights on the seabed and for substructures above the water level.

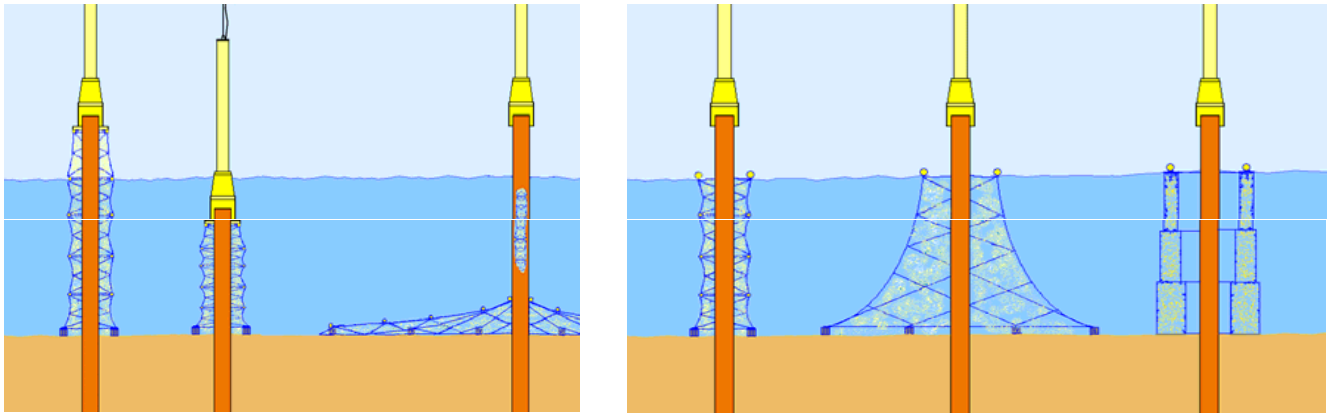

Figure 24: Application examples and different nets with hydro sound dampers (source: TU Braunschweig/Dr. Elmer)

The method offers an optimum, cost-effective and highly-efficient use of material. It is lightweight, flexible in its application and straightforward to manufacture, transport and deploy in practical operation.

Figure 24 shows different variants for the use of HSD nets. The nets are lowered by winches and, independently of the pile, can be fixed to buoyancy bodies or to the pile driver or pile driving guide for simple coverage of large areas of the seabed in order to also reduce the indirect sound re-entry via the ground. HSD nets can also be stretched over rigid framework structures or used a large distance away independently of the driving pile.

The principle of hydro sound dampers is a specific technical development and an application optimisation of the air bubbles that occur naturally in water.

Air bubbles in water mitigate noise by scattering and absorbing hydro sound waves. The noise mitigating effect of the bubbles is exceptionally high, particularly in the range of their resonant frequency, but the bubbles have to be

controlled and their resonant frequency adjusted. However, this is not the case with natural air bubbles.

In the case of natural air bubbles in water, there is a non-controllable, largely constant, inversely proportionate relationship between the diameter and the resonant frequency of an air bubble. The resonant frequency of HSD balloons can be adjusted by means of the inner pressure, stiffness and thickness of the enveloping membrane, independently of size. HSD elements can be adjusted to the frequency range of hydro sound waves by means of the size alone and, due to the interaction with the surrounding water, achieve very high noise mitigating effects.

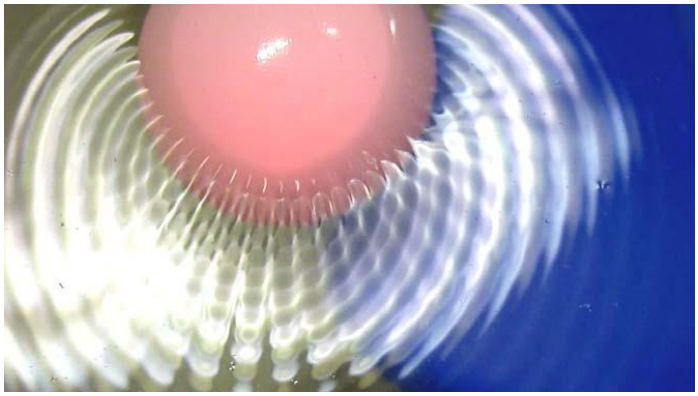

Figure 25: Interaction of an HSD balloon to scatter and radiate sound waves (source: TU Braunschweig/Dr. Elmer)

Robust HSD foam elements are another possibility. They are specified via their size and material. All key properties of the HSD elements that have an impact on noise mitigation, such as resonant frequency, form, size, position, number, distances and damping, can be exactly adjusted to the properties and spectrum of a sound source. The required concentration of HSD elements is approx. 0.1% to 1% in volume locally, but also higher in deeper layers. With low concentrations, the vertical lifting force of the HSD elements, as well as horizontal forces from tidal flows, are still low and can be easily absorbed as the HSD nets are permeable to tidal flows.

A major advantage for offshore use is that hydro sound dampers do not need a compressed air supply.

The HSD test system for the ESRa investigations

Numerical simulations and measurement investigations have shown that, even at small concentrations, noise reductions of approx. 20-30 dB have been achieved in the range from the HSD elements' resonant frequency to up to three or five times the frequency. In practice, 5-7 different element sizes can be used to cover the entire frequency range from 50 to 10,000 Hz.

Consequently, for the offshore tests conducted as part of the ESRa research project, it was particularly interesting to obtain more detailed information and results about the effective frequency range of HSD elements of the same size or same resonant frequency when driving piles offshore.

For this reason, for the ESRa tests, all HSD elements used were designed to have the same resonant frequency of approx. 100 to 500 Hz. As a result, effective noise mitigation was mainly expected in the frequency range of approx. 100 to 500 Hz. This frequency range represents the main frequency range in the radiated hydro sound during offshore pile driving events. According to the results of theoretical and measurement investigations, only slight noise mitigation can be expected below 100 Hz, whilst noise mitigation slowly decreases above approx. 500 Hz.

Figure 26 shows the structure and mode of operation of an HSD test system. The entire HSD net, including the required weights, is housed in a floating, ring-shaped construction and lowered by winches.

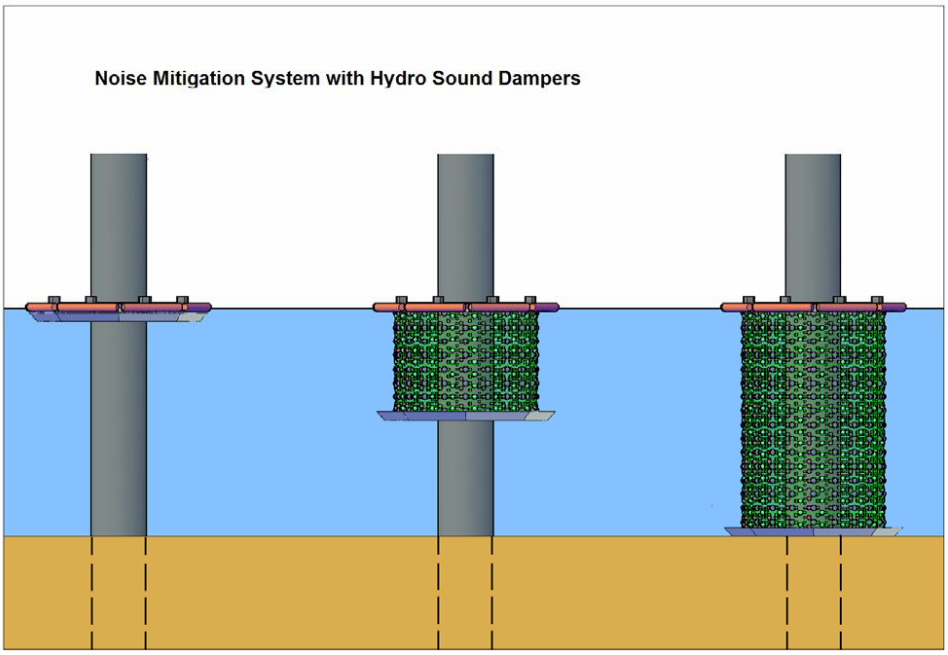

Figure 26: HSD test system with a net (retracted, half lowered and fully lowered) (source: TU Braunschweig/Dr. Elmer)

In order to investigate different HSD nets as part of the ESRa measurements, a special test construction was developed to enable the simultaneous investigation of three different HSD nets.

Structure and use of the ESRa HSD construction

To test the HSD system of the ESRa project, the HSD team planned, built and monitored the construction during testing. The following points were important:

- Cost-effectiveness
- One-off application, related to the events at the Brodten pile
- Possibility of testing three different HSD nets and combinations thereof

The aim of the tests conducted as part of this project was to check the effectiveness of three nets equipped with different HSD elements. All three nets had a mesh width of 2.0 x 2.0 cm and a thread thickness of 1.2 mm. All HSD elements were attached 20 x 20 cm apart. To lower these three nets, a floating construction was built that could safely hold the winches for lowering the nets. It was important that the construction could float because, after being positioned by the mobile crane, the latter had to be used to place the hammer. During this time, the construction (platform) has to safely hold the dead weight, as well as the heavy weights hanging on the lower edges of the nets. This was ensured by constructing buoyancy bodies of adequate dimensions. Figure 3 shows the design drawing of the platform built. Four manually operated cable winches were installed on the platform for each of the three nets. Operating as double cable winches, via deflection pulleys, these then held the heavyweight rings via eight uniformly distributed steel ropes. This meant that each net could be lowered and raised either individually or in combination to the seabed. This method has only been implemented for this research project. For future offshore applications, automatic, hydraulic cable winches will be used that only lower a single net.

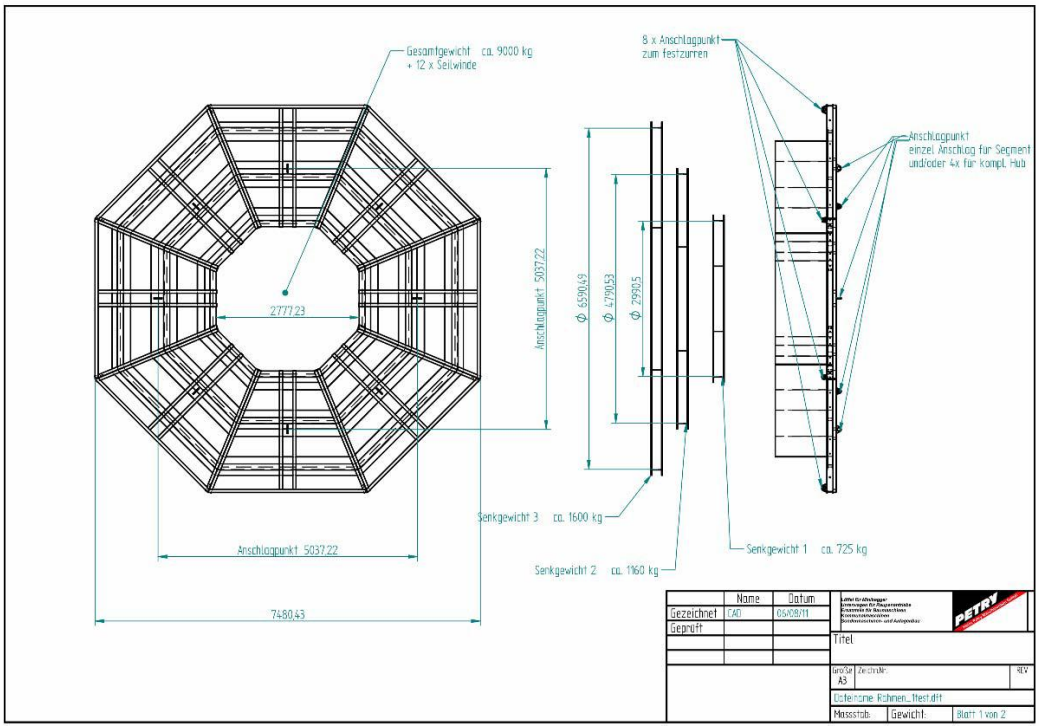

Figure 27: Design drawing of the ESRa HSD platform (source: TU Braunschweig/Dr. Elmer)

The three nets and their components can be described as follows:

– Net 1 (inner net)

The inner net (diameter 2.90 m) was fitted with double-layer air-filled HSD balloons.

Figure 28: Constructing the inner net with double-layer air-filled HSD balloons (source: TU Braunschweig/Dr. Elmer)

– Net 2 (middle net)

The middle net (diameter 4.80 m) was fitted with robust HSD foam elements.

Figure 29: Constructing the middle net with HSD foam elements (source: TU Braunschweig/Dr. Elmer)

– Net 3 (outer net)

The outer net (diameter 6.60 m) was fitted with single-layer air-filled HSD balloons.

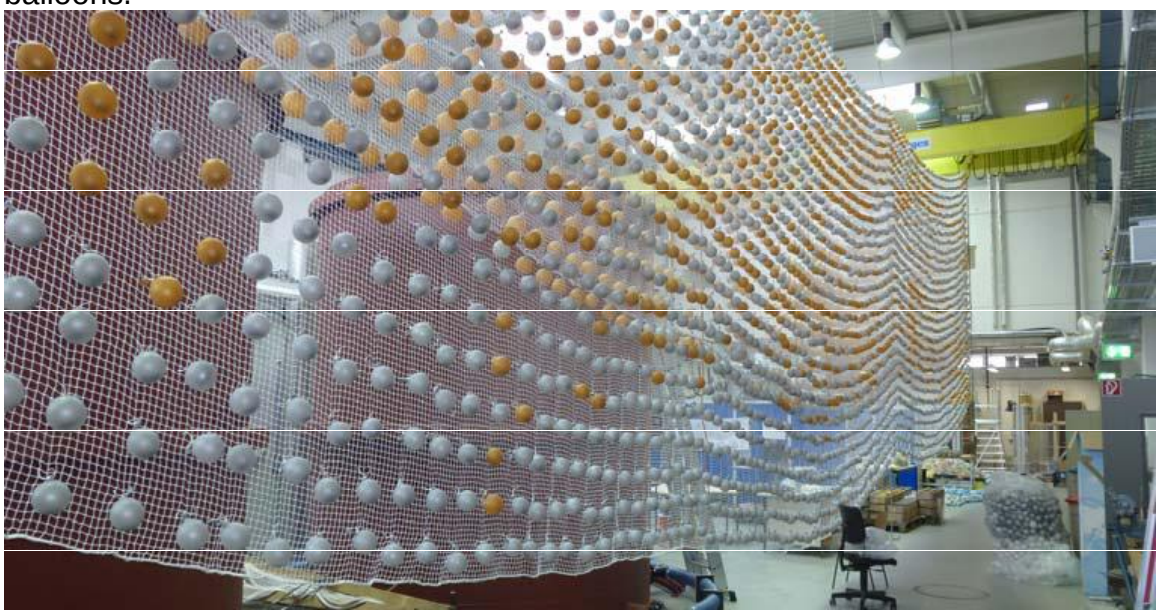

Figure 30: Constructing the outer net with single-layer HSD balloons (source: TU Braunschweig/Dr. Elmer)

Figure 31: The entire HSD platform above the test pile (photo: Patrice Kunte)

Figure 32: Scientific muscle strength lowers the inner net (photo: Patrice Kunte)

6.1.6. Comparing the weights of the systems

Due to the special boundary and environmental conditions at the Brodten pile, it is difficult to provide detailed information about integrating the systems into the logistics of an offshore wind farm in deeper water. However, looking at the system weight provides an initial indication. Table 3 shows a summary of the weight of the ESRa test systems. Column 4 also compares the respective weight with a 9-m long section of the driven pile (on average, this corresponds to the length of the test equipment). For systems with buoyancy bodies 2, 3, 5, a large part of their weight is carried by the ballast ring and the buoyancy bodies. This means that, when scaling the systems for deeper water, the system weight will only increase to a disproportionately low degree. Against this background, the LBC and HSD in particular stand out on the strength of their low weight and associated ease of handling.

However, the weight of the ‘tube-like’ systems 1+4 is clearly greater than the weight of the section of pile to be enclosed. When scaled up to a real wind farm, this results in system dimensions and weights that, with a monopile structure, for example, could match that of the driving pile. Such systems can only be used effectively if installation equipment is available with adequate room on deck and a sufficient payload.

No.	System	Weight [to]	% of the pile weight (in relation to a length of 9 m)
1	IHC NMS	29.4	127
2	Menck	20	86
3	Weyres LBC	7.4	32
4	Weyres BeKa	39.8	172
5	TU BS HSD	10	43

Table 3: Weights of the test systems and comparison with a 9 m section of the test pile

7. Executing the hydro sound and vibration measurements

7.1 Test set-up and measuring concept

A test pile by Menck GmbH was used as driving pile (see Section 4). The pile data are again summarised in Table 4. A prior inspection revealed that there was no significant accumulation of seaweed or mussels on the test pile.

The principal test set-up is shown in Figure 33. Various noise mitigation systems are placed over the driving pile. The hammer had a maximum impact energy of approx. 300 kJ. The hammer, the respective noise mitigation systems and the necessary crane and accessories (e.g. compressor for compressed air) were located onboard a stilt-mounted pontoon, as shown in Figure 33. Every day, apart from 22 August 2011, two tugs brought these to a defined position in front of the pontoon. As the tugs travelled to and from the pontoon each day, there were slight deviations in the exact position of the work pontoon.

The underwater sound measurements were conducted at five different measurement positions around the test pile, see Figure 36 and Table 6. Autonomous measurement systems were mainly used, being dropped in four of the measurement positions (Figure 34). In addition, an array consisting of four hydrophones and a geophone were used, Figure 35.

Position	N 53 59.877' E 10 54.489'
Diameter	2.2 m
Height above water level	5.5 m
Water depth	8.5 m
Length in seabed	approx. 65.0 m
Wall thickness	50.0 mm

Table 4: Test pile data

The dropped measurement systems each had two hydrophones (underwater microphones), each of which was positioned with a buoyancy body at a height of about 1.8 m and 3.6 m above the seabed (sediment). The measurement electronics were located in a steel casing that also served as anchor weight. In addition, a rope, including anchor chain and anchor, was used for securing to the seabed. A rope with marker buoy was used to mark the measurement position, Figure 33. This measurement system was located at a distance of 375 m to 750 m from the test pile.

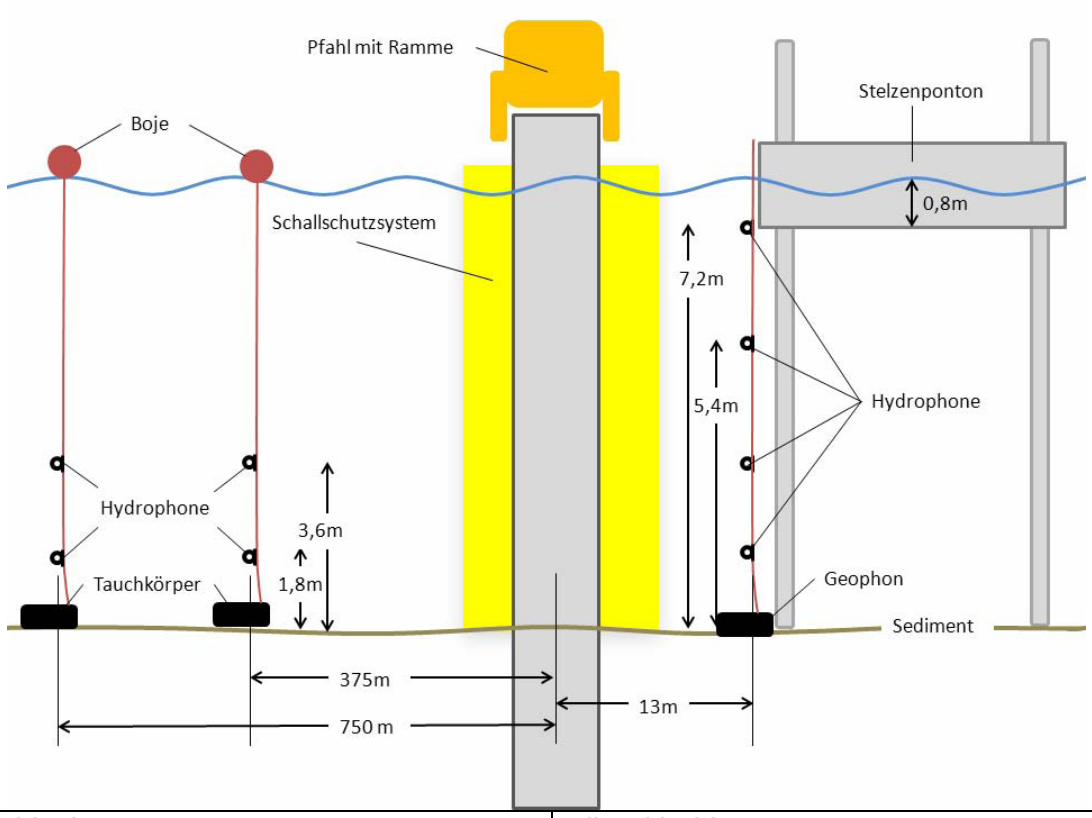

Pfahl mit Ramme	Pile with driver
Stelzenponton	Stilt-mounted pontoon
Boje	Buoy
Schallshutzsystem	Noise control system
Hydrophone	Hydrophones
Tauchkoerper	Immersed body
Hydrophone	Hydrophones
Geophon	Geophone
Sediment	Sediment

Figure 33: Test set-up (not to scale)

In addition, a hydrophone array, incl. a geophone, was installed on the work pontoon in the near field. This system consisted of a steel casing containing an axial geophone (vertical alignment). This casing also served as weight anchor. Using a rope filled with lead, four hydrophones were attached at different distances from the seabed. The measuring electronics were located onboard the work pontoon, Figure 35.

All measurement systems recorded the time signals (“tape recordings”) of the underwater sounds (hydro sound or velocity of the vibration), which were later evaluated on land.

In addition to the underwater sound measurements, the sound speed, water temperature and salinity were measured each day from the work pontoon using a CTD sensor.

Table 5 summarises the measurement systems used. Figure 36 shows the geographical positions of the five measurement positions used. Table 6 summarises the corresponding geographical coordinates of the measurement positions.

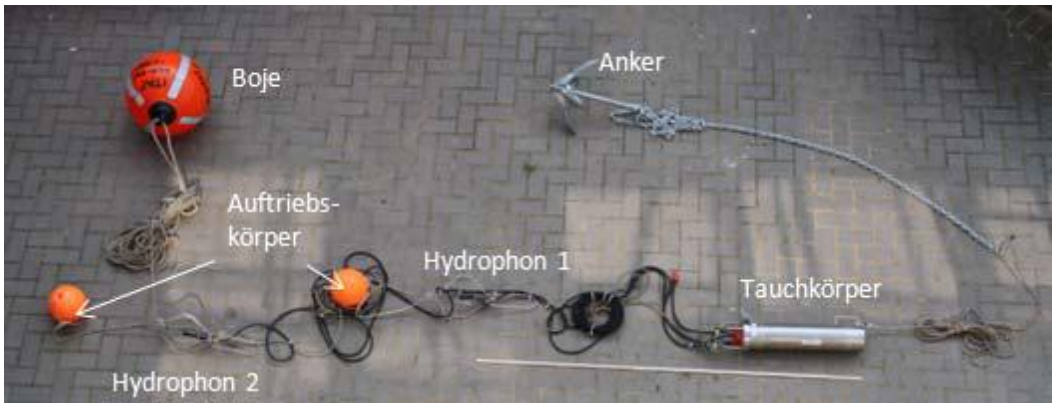

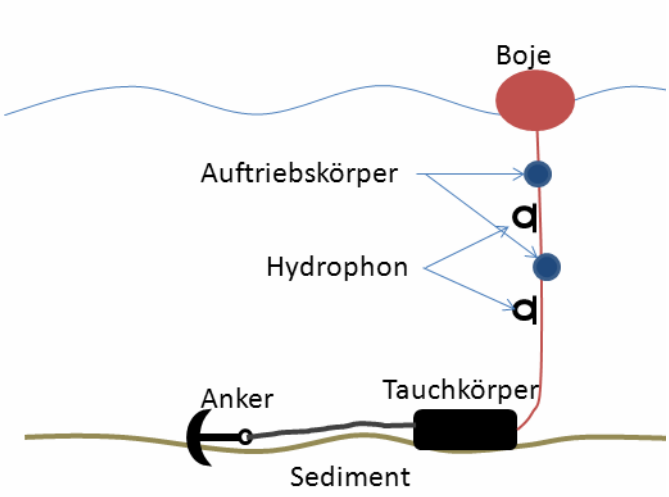

Boje	Buoy
Anker	Anchor
Auftriebskoerper	Buoyancy body
Hydrophon 1	Hydrophone 1
Hydrophon 2	Hydrophone 2
Tauchkoerper	Immersed body

Figure 34: Autonomous measurement systems of ITAP GmbH for measuring underwater sound at measurement positions MP1 to MP4. Top: photo; bottom: schematic diagram

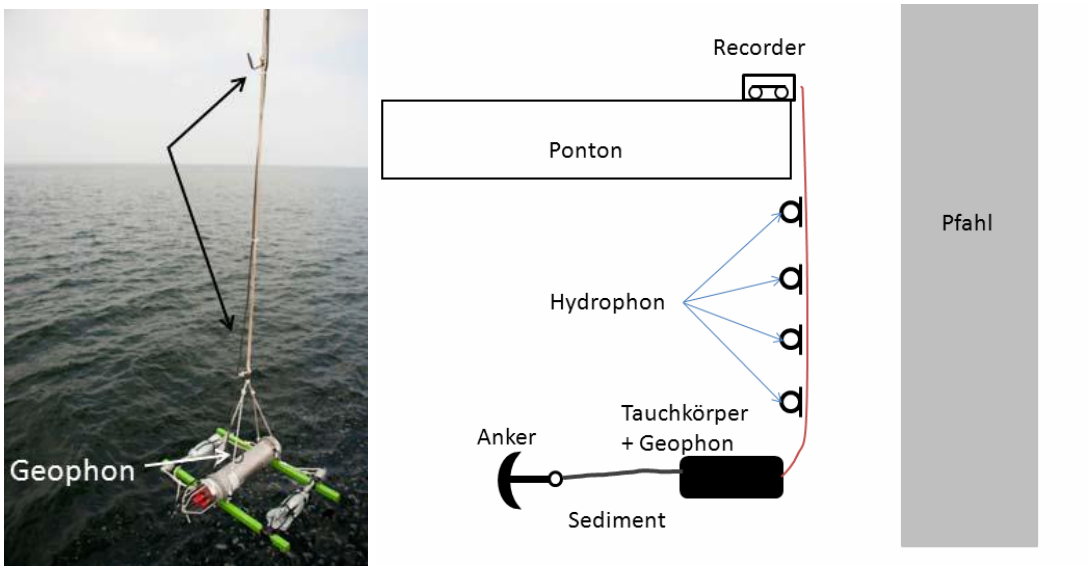

Hydrophone	Hydrophones
Geophon	Geophone
Recorder	Recorder
Ponton	Pontoon
Hydrophon	Hydrophone
Tauchkoerper + Geophon	Immersed body + geophone
Anker	Anchor
Sediment	Sediment
Pfahl	Pile

Figure 35: Measuring system ("array") consisting of one geophone and four hydrophones (MP5). Left: photo; right; schematic diagram

Device	Manufacturer	Important technical data / number	Comment / measurement location
Autonomous under water sound measurement system (Figure 4.3)	itap	Frequency range: 10 Hz- 20 kHz Recording capacity: approx. 50 h Number: 4 pcs.	Measuring systems MP1 to MP4
Hydrophone TC 4033	RESON	Sensitivity: approx. 0.5 pC/Pa Number: 6 pcs.	
Hydrophone P200	STN Atlas	Sensitivity: approx. 1.4 pC/Pa Number: 2 pcs.	
Geophone SM 6B	SENOR	Frequency range: 0.1	Measuring

(Figure 4.4)		Hz – 10 kHz Number: 1 pcs.	system MP5 Array from the pontoon
Hydrophone TC 4013	RESON	Sensitivity: approx. 0.12 pC/Pa Number: 6 pcs.	
Laptop VAIO	Sony		
External soundcard Fireface UC	RME	Connection via USB 2.0	
Power amplifier	itap	0.1 mV/pC	In combination with all hydrophones
Calibration source with charge signal	itap	Sinus signal 1 kHz, 10 – 100-1000 mV_{rms} and charge 100 pC_{rms}	Measuring systems with hydrophones P200 and TC 4033
Pressure chamber	itap	80 to 160 Hz, 140 – 155 dB re 1µPa adjustable	Calibration of hydrophones and measurement systems in the laboratory
Microphone calibrator 4231	Bruel & Kjær		
Microphone 4189 and preamplifier 2671 as reference in the pressure chamber	Bruel & Kjær		
Signal analyser 35670a	Hewlett-Packard		
GPS tracker	Garmin		

Table 5: Equipment used

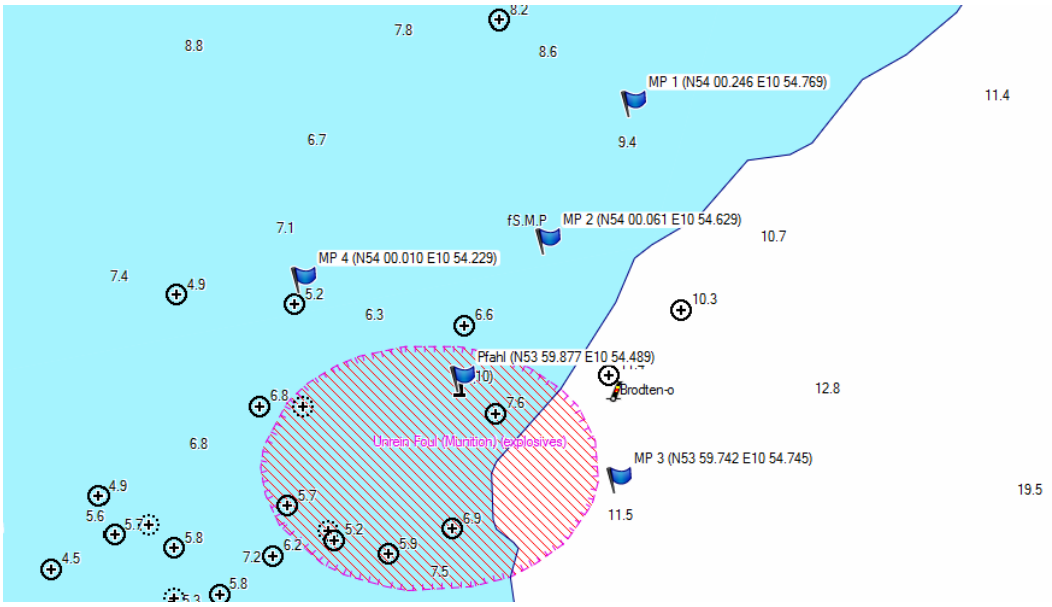

Figure 36: Measurement positions used

No.	Measurement position	Coordinates	Distance from pile [m]	Water depth [m]	Sensor	Height above seabed [m]
1	MP1.1	54°00.246‘ 10°54.769‘	750	approx. 9.0	Hydrophone	1.8
2	MP1.2				Hydrophone	3.6
3	MP2.1	54° 00.061‘ 10°54.629‘	375	approx. 7.7	Hydrophone	1.8
4	MP2.2				Hydrophone	3.6
5	MP3.1	53°59.742‘ 10°54.745‘	375	approx. 11.5	Hydrophone	1.8
6	MP3.2				Hydrophone	3.6
7	MP4.1	54°00.010‘ 10°54.229‘	375	approx. 6.0	Hydrophone	1.8
8	MP4.2				Hydrophone	3.6
9	MP5.1	53°59.877‘ 10°54.489‘	13	approx. 8.5	Hydrophone	1.8
10	MP5.2				Hydrophone	3.6
11	MP5.3				Hydrophone	5.4
12	MP5.4				Hydrophone	7.2
13	MP5.5				Geophone	0.0

Table 6: Geographic location of the measurement positions used and their identification

7.2 Drive energy measurement (PDM – pile drive monitoring)

As part of the ESRa project, during testing, the TU Braunschweig conducted dynamic load tests to determine the amount of energy transferred to the pile. The measurements serve to prove the comparability of the tests.

A dynamic load test measures the expansions and accelerations created by the hammer blow below the pile head. These two variables can be used to determine the energy introduced at sensor level. Figure 37 shows an impression of the sensors applied at the Brodten pile.

Figure 37: Measurement position of acceleration sensor (right) and expansion sensor (left) at the Brodten pile

The measurement equipment consisted of pairs of sensors offset by 180° on the pile. Each pair consisted of one expansion sensor and one acceleration sensor connected to the measuring computer via cables. The measurement equipment was screwed to the pile below the pile helmet (Figure 38).

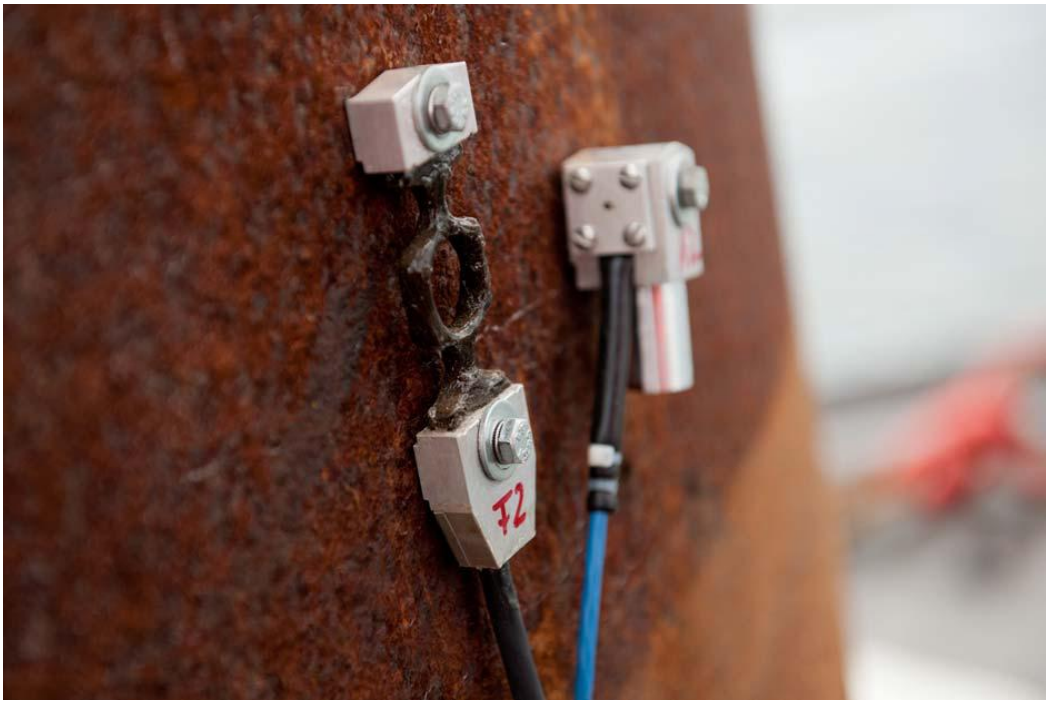

Figure 38: Details of sensor for measuring the pile energy (photo: Patrice Kunte)

The tests at Brodten pile each provided for three series of blows with impact energies of 100, 200 and 300 kNm. Each series of blows consisted of 20 individual blows. Each noise control system and one reference measurement without noise control system was investigated according to this method. Table 7 lists the energy at the pile head [24] calculated on the basis of the measured expansion and acceleration. The diagram in Section 15, Appendix 2 shows the energy generated by the blows.

Gegenüberstellung Nominalwert Rammenergie zu gemessenem Energieeintrag Pfahl:

Nominal Rammenergie in kJ	NMS von IHC mit 7,0 bar	NMS von IHC ohne Druckluft	Feuerwehrschläuche von MENCK mit 1,0 bar	Feuerwehrschläuche von MENCK mit 2,0 bar	Kleiner Blasenschleier von Weyres mit 7,9 bar	BEKA-Schalen von Weyres mit 7,9 bar	BEKA-Schalen von Weyres mit 5,0 bar	BEKA-Schalen von Weyres ohne Druckluft	HSD von TU BS mit mittl. Netz	HSD von TU BS mit mittl. + äußerem Netz	HSD von TU BS mit mittl. äußerem + innerem Netz	HSD von TU BS mit äußerem + innerem Netz	HSD von TU BS mit äußerem Netz	HSD von TU BS mit innerem Netz	HSD von TU BS mit innerem + mittlerem Netz
	gemessene Energie auf Höhe der Messaufnehmer in kJ														
100,0	77,9	79,9	79,3	81,3	87,8	86,7	84,7	85,6	84,4	87,6	86,9	86,0	86,1	84,3	82,8
100,0	88,0	89,3	90,4	90,5	94,2	96,7	94,2	96,7	95,1	98,3	96,5	96,1	95,8	93,0	92,2
100,0	97,5	99,1	98,5	100,2	116,2	104,2	103,1	104,7	105,0	106,3	105,3	104,1	103,9	102,5	102,3
100,0	106,3	108,7	109,0	110,7	118,0	116,0	111,3	112,8	116,6	116,1	114,8	114,6	113,5	112,6	111,9
100,0	114,4	118,6	117,7	121,3	123,8	126,7	121,9	123,5	127,5	125,7	124,6	124,9	122,9	121,2	121,1
100,0	118,1	122,3	122,6	126,8	127,5	124,6	123,3	125,0	132,2	126,3	125,8	127,9	122,5	121,1	121,5
100,0	117,9	123,1	122,4	126,9	127,2	124,6	121,7	119,3	131,9	122,0	122,4	121,2	118,5	119,0	126,5
100,0	113,4	118,4	118,8	121,8	120,2	120,2	121,4	118,8	127,5	116,7	116,7	116,3	113,9	116,5	119,3
100,0	109,4	114,4	114,2	111,8	114,7	115,9	118,4	112,3	118,1	111,4	112,3	112,0	109,9	111,2	111,6
100,0	104,6	109,8	104,2	102,1	105,7	105,0	108,1	102,9	109,4	107,1	103,2	103,1	101,3	102,4	101,7
100,0	100,6	104,8	95,8	92,6	92,5	95,4	97,2	98,4	98,6	102,6	97,2	92,8	94,9	92,9	91,8
100,0	95,7	99,3	91,2	88,9	90,0	91,7	88,4	94,5	94,3	97,1	92,7	88,7	89,9	86,9	86,3
100,0	91,5	95,2	86,8	84,9	86,5	86,4	86,7	93,3	90,0	92,2	93,3	88,4	90,3	86,9	82,1
100,0	92,1	95,0	86,5	84,2	88,4	86,5	86,4	92,9	90,0	92,8	92,7	88,6	90,1	86,4	81,7
100,0	91,5	94,5	86,7	84,4	87,7	87,1	94,2	93,1	90,3	92,4	93,1	88,5	90,1	86,3	81,6
100,0	91,6	94,9	87,1	84,2	83,4	86,5	86,7	94,3	89,5	92,5	92,5	88,2	90,1	86,5	81,0
100,0	92,4	94,5	87,4	84,7	83,0	85,9	87,2	93,7	89,9	92,6	92,7	88,4	91,1	86,6	85,7
100,0	92,3	95,0	87,7	84,4	92,6	86,6	86,8	93,4	89,9	92,2	93,2	87,8	90,5	86,5	91,6
100,0	91,6	95,7	87,9	88,6	91,5	87,0	88,1	94,1	90,2	92,3	92,4	88,7	90,3	86,7	96,2
100,0	91,1	94,7	87,3		80,1	88,5	96,1	87,2	90,1	92,4	92,0	90,4		65,8	72,2
200,0	151,1	159,2	159,0	162,8	166,1	168,2	172,2	172,9	177,6	172,0	173,8	173,6	171,9	169,4	169,9
200,0	158,7	167,6	166,6	170,1	180,5	180,1	176,2	181,2	190,0	179,7	182,5	181,8	180,3	176,5	176,0
200,0	168,2	176,7	176,4	181,9	192,0	188,3	188,2	192,1	197,8	187,1	190,3	188,7	187,2	184,2	185,7
200,0	177,0	185,4	184,2	190,6	193,2	196,5	197,6	195,1	205,0	196,0	197,9	196,9	197,1	194,0	193,9
200,0	186,2	194,0	194,7	199,6	209,7	205,3	208,8	203,8	215,3	204,2	205,7	205,5	204,5	202,5	201,8
200,0	195,1	200,8	203,5	206,9	216,2	212,9	221,7	213,2	223,0	216,7	215,0	212,5	212,2	212,1	209,0
200,0	200,8	201,0	204,2	210,7	215,1	216,7	219,7	213,1	223,4	216,0	214,6	214,0	213,0	209,1	209,6
200,0	200,2	201,7	203,6	211,0	219,6	219,2	209,2	216,0	221,0	216,5	213,3	209,1	207,1	207,7	206,5
200,0	199,7	200,8	202,1	211,2	214,1	215,0	207,7	219,4	220,3	211,5	214,0	204,9	205,3	201,4	201,2
200,0	201,2	201,0	198,4	208,0	213,7	211,5	204,7	212,7	211,6	207,7	209,1	201,1	201,2	198,6	197,3
200,0	195,6	196,7	194,3	203,2	208,5	204,2	196,2	207,3	203,3	199,9	200,8	196,3	195,8	195,4	194,2
200,0	191,5	194,3	190,1	199,7	208,3	194,7	194,6	197,5	196,8	191,9	193,9	192,0	190,5	191,7	188,8
200,0	186,6	188,3	185,3	195,9	200,0	191,7	192,0	193,2	190,7	187,2	191,2	188,6	186,6	185,4	184,8
200,0	187,6	184,4	180,5	191,3	195,7	186,6	189,5	190,1	183,3	183,0	186,5	184,9	182,6	184,1	181,7
200,0	187,0	184,2	181,1	187,3	196,4	183,7	185,9	190,7	181,5	182,6	178,7	185,1	183,1	182,2	181,5
200,0	186,6	184,2	180,9	188,7	191,3	185,6	190,9	186,4	182,1	182,5	178,4	184,6	183,5	183,3	181,8
200,0	187,2	184,7	179,6	187,6	203,6	182,5	188,9	184,3	181,4	183,5	177,8	184,1	183,4	183,0	182,1
200,0	189,0	185,4	179,8	188,6	201,6	183,2	189,4	183,9	182,1	183,7	178,3	184,8	183,4	182,5	180,2
200,0	189,7	184,2	180,0	188,2	203,1	183,5	189,0	183,7	182,0	183,2	178,9	184,5	182,6	181,5	181,5
200,0	190,4	185,9	179,6	187,5	201,0	177,6	158,7	186,3	187,4	184,9	153,1	176,4	185,5	180,1	178,6
300,0	230,5	274,0	279,2	277,4	308,5	279,7	287,6	281,1	301,1	288,2	281,4	284,3	279,4	282,6	275,1
300,0	241,8	279,4	279,9	274,2	288,3	275,9	285,0	280,4	296,9	291,6	284,7	285,8	285,3	286,9	280,5
300,0	241,9	281,7	282,7	280,4	274,5	277,9	282,9	286,2	293,1	290,5	284,8	284,1	287,2	287,1	281,0
300,0	242,4	283,7	274,6	275,2	313,4	279,9	283,3	287,3	293,0	296,9	283,3	287,5	288,3	286,7	280,6
300,0	242,8	285,5	282,2	277,5	291,4	280,5	282,8	284,4	293,6	290,8	285,6	286,4	288,1	286,5	281,0
300,0	242,1	284,4	282,7	277,4	303,3	278,0	286,1	284,3	295,2	290,1	284,4	285,6	287,7	290,9	281,7
300,0	242,7	280,9	284,0	278,5	297,9	277,1	287,1	289,1	290,5	285,4	285,4	280,4	285,4	285,0	280,9
300,0	249,3	284,4	283,0	276,9	299,2	279,6	283,9	295,9	285,5	281,3	283,9	274,0	279,9	279,6	283,5
300,0	261,0	284,8	284,6	278,6	293,3	282,9	286,3	291,1	286,9	278,4	284,8	271,8	276,2	277,0	283,1
300,0	263,3	289,4	282,7	276,7	294,6	286,8	283,2	287,3	286,7	279,7	285,3	274,0	270,8	270,0	281,4
300,0	264,1	284,2	282,8	279,0	294,2	283,0	280,2	284,2	289,7	284,2	285,4	274,4	268,6	265,2	281,6
300,0	263,7	283,4	286,3	276,5	300,7	279,9	287,2	289,3	286,5	279,0	282,9	271,5	271,6	266,9	283,0
300,0	267,2	282,6	282,1	277,2	295,1	281,1	284,0	285,2	287,7	278,9	283,4	273,9	268,0	265,4	277,6
300,0	292,5	286,0	283,8	282,7	289,6	281,7	284,2	285,6	287,2	279,7	281,3	272,8	268,5	264,6	273,7
300,0	281,3	289,8	285,8	277,7	294,1	280,6	284,4	289,0	287,4	279,7	282,7	274,2	271,2	264,3	273,4
300,0	281,4	288,3	284,1	283,2	286,3	278,4	288,3	284,3	287,0	279,8	282,9	273,1	267,0	264,1	271,9
300,0	282,6	283,8	284,0	282,4	306,0	282,3	283,0	286,9	288,2	277,9	283,7	270,4	266,4	264,4	275,0
300,0	282,2	287,4	283,3	280,1	301,8	278,2	283,7	291,4	289,1	279,5	285,5	272,7	271,3	266,0	274,5
300,0	282,0	290,1	283,9	278,6	295,5	284,7	284,6	283,4	290,2	278,1	285,2	270,3	269,9	265,8	272,9
300,0	282,4	284,7	287,1	281,6	288,6	248,0	274,0	288,5	286,2	254,5	280,7	261,3	254,8	264,8	272,5

Gegenueberstellung Nominalwert Rammenergie zu gemessenem Energieeintrag Pfahl:	Comparison between nominal value of drive energy and the measured energy transferred to the pile:
Nominal Rammenergie in kJ	Nominal drive energy in kJ
NMS von IHC mit 7,0 bar	NMS by IHC with 7.0 bar
NMS von IHC ohne Druckluft	NMS by IHC without compressed air
Feuerwehrschlaeuche von MENCK mit 1,0 bar	Fire hoses by MENCK with 1.0 bar
Feuerwehrschlaeuche von MENCK mit 2,0 bar	Fire hoses by MENCK with 2.0 bar
Kleiner Blasenschleier von Weyres mit 7,9 bar	Little bubble curtain by Weyres with 7.9 bar
BEKA-Schalen von Weyres mit 7,9 bar	BEKA jackets by Weyres with 7.9 bar
BEKA-Schalen von Weyres mit 5,0 bar	BEKA jackets by Weyres with 5.0 bar
BEKA-Schalen von Weyres ohne Druckluft	BEKA jackets by Weyres without compressed air
HSD von TU BS mit mittl. Netz	HSD by TUBS with middle net
HSD von TU BS mit mittl. + auesserem Netz	HSD by TUBS with middle and outer net
HSD von TU BS mit mittl. auesserem + innerem Netz	HSD by TUBS with middle, outer + inner net
HSD von TU BS mit auesserem + innerem Netz	HSD by TUBS with outer + inner net
HSD von TU BS mit auesserem Netz	HSD by TUBS with outer net
HSD von TU BS mit innerem Netz	HSD by TUBS with inner net
HSD von TU BS mit innerem + mittlerem Netz	HSD by TUBS with inner + middle net
Gemessene Energie auf Hoehe der Messaufnehmer in kJ	Energy measured at sensor level in kJ

Table 7: Results of the drive energy measurement for all NMS [24]

7.3 Measuring process

All measurements were taken in the period from 21 to 24 August 2011. Table 8 shows the sequence of the noise control systems investigated, including variations. A total of 19 different noise control system configurations, including four reference configurations without noise control system, were investigated.

Two tugs positioned the work pontoon in front of the test pile on 21, 23 and 24 August. The work pontoon has stilts to keep it in position. As the tugs moved the pontoon to the pile several times, it was not possible to replicate exactly measurement position MP5 each day.

Figure 39 shows the daily schedule for conducting the measurements.

On each day of testing, the respective noise mitigation system (NMS) was first installed. During this time, a crew boat was used to take the four autonomous measurement systems to the measurement positions MP1 to MP4. In addition, the on-board crane placed the hydrophone array with geophone in the water (MP5) on 21, 23 and 24 August 2011.

No.	Date	NMS	Property / variation	Pressure [bar]	Driving energy [kJ]
1	21.08.2011	IHC NMS	With bubble curtain between pile and IHC tube	7.0	100, 200, 300
2			Without bubble curtain between pile and IHC tube	0.0	
3		Reference (no noise mitigation system / NMS)			
4	22.08.2011	Menck fire hose method with two rows of hoses	Different constant pressure within the hoses	1.0	100, 200, 300
5				2.0	
6		Reference (no noise mitigation system / NMS)			300
7	23.08.2011	Weyres little bubble curtain	Layered and guided	7.9	100, 200, 300
8		Weyres BeKa jacket	With bubble curtain	7.9	
				5.0	
9			Without bubble curtain	0.0	
10					
11		Reference (no noise mitigation system / NMS)			300
12	24.08.2011	Elmer hydro sound damper	Middle ring		100, 200, 300
13			Middle + outer ring		
14			All rings		
15			Inner + outer ring		
16			outer ring		
17			Inner ring		
18			Inner + middle ring		
19		Reference (no noise mitigation system / NMS)			300

Table 8: Sequence of noise mitigation systems used with the respective variations

After installing the respective noise mitigation system (NMS), TU Braunschweig (TUBS) attached the relevant measurement sensors to the pile in order to determine the amount of driving energy introduced (pile drive monitoring, cf. Section 7.2). The pile was then driven with the installed noise mitigation system.

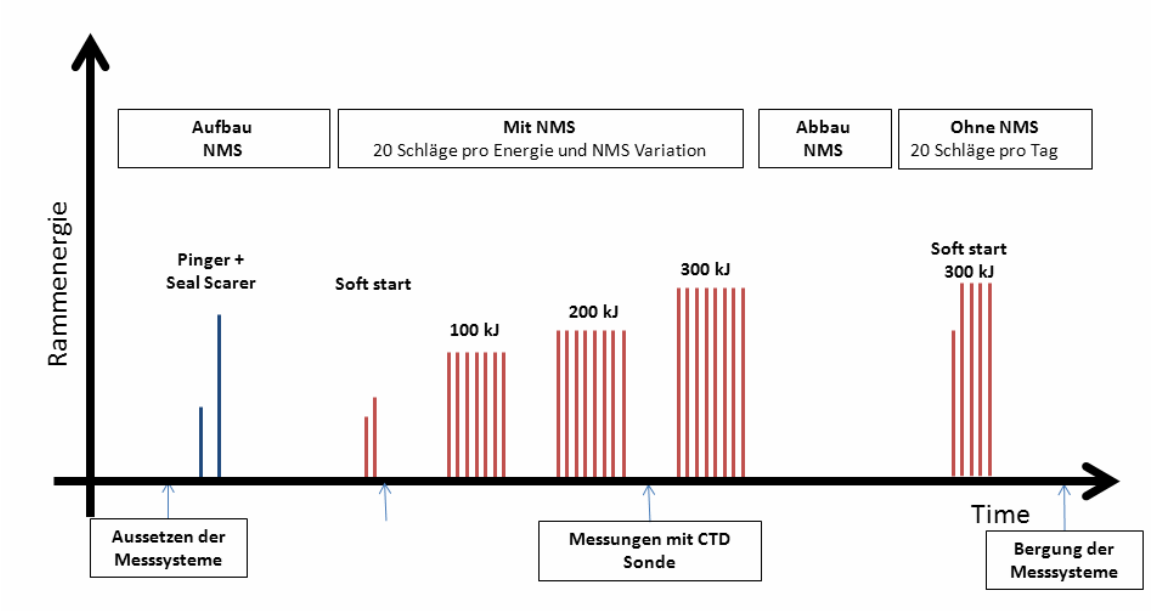

Rammenergie	Driving energy
Aufbau NMS	NMS setup
Mit NMS	With NMS
20 Schlaege prop Energie und NMS Variation	20 blows per energy and NMS variation
Abbau NMS	NMS dismantling
Ohne NMS	Without NMS
20 Schlaege pro Tag	20 blows per day
Pinger + Seal Scarer	Pinger + seal scarer
Soft start	Soft start
Aussetzen der Messsysteme	Measurement lead time
Messungen mit CTD Sonde	Measurements with CTD sensor
Bergung der Messsysteme	Retrieval of the measurement systems

Figure 39: Schematic time diagram of the testing procedure on each day of measurement

The respective NMS was then dismantled and the pile driven without noise mitigation system. In the following, these pile driving events are referred to as the reference measurement.

The reference measurements were performed on the first day of testing (21 August 2011). Each reference measurement consisted of six blows with a driving energy of 100, 200 and 300 kJ. On all other days, 20 blows à 300 kJ driving energy were performed.

On each day of measuring, the water temperature, sound speed and salinity were measured several times from the pontoon using a CTD sensor.

All measuring sensors by itap GmbH were retrieved each day after completing the reference measurements (with the exception of the hydrophone array (MP5) on 21 August 2011). The measurement data were then backed up each day.

On 21 August 2011, the measurement system at measurement position MP4 suffered a technical failure and, as a result, there are no measurement data for this day and this measuring point. Table 9 lists the measurements taken.

In total, 52 different driving variations (6 reference measurements without noise mitigation system, 46 measurements with noise mitigation system) were measured (time signals) using a total of 13 sensors and stored in a database.

No.	System	MP 1 (750m)	MP 2 (375m)	MP 3 (375m)	MP 4 (375m)	MP 5 (Array)
1	IHC tube with bubble curtain	☺	☺	☺	-	☺
2	IHC tube without bubble curtain	☺	☺	☺	-	☺
3	Menck with 1bar pressure	☺	☺	☺	☺	☺
4	Menck with 2bar pressure	☺	☺	☺	☺	☺
5	Weyres little bubble curtain	☺	☺	☺	☺	☺
6	Weyres BEKA 0 bar	☺	☺	☺	☺	☺
7	Weyres BEKA 5 bar	☺	☺	☺	☺	☺
8	Weyres BEKA 7 bar	☺	☺	☺	☺	☺
9	HSD M ring	☺	☺	☺	☺	☺
10	HSD O ring	☺	☺	☺	☺	☺
11	HSD I ring	☺	☺	☺	☺	☺
12	HSD MO ring	☺	☺	☺	☺	☺
13	HSD MI ring	☺	☺	☺	☺	☺
14	HSD OI ring	☺	☺	☺	☺	☺
15	HSD MOI ring	☺	☺	☺	☺	☺
16	IHC reference	☺	☺	☺	-	☺
17	Menck reference	☺	☺	☺	☺	☺
18	Weyres reference	☺	☺	☺	☺	☺
19	HSD reference	☺	☺	☺	☺	☺

Table 9: List of the measurements taken (☺ = correct; - = measurement not taken).

7.4 Method for evaluating the acoustic data (ITAP)

All hydrophone and geophone signals are available as WAV files. The sampling frequency of the autonomous measurement systems dropped at positions MP1 to MP4 was f_S = 44.1 kHz. The signals are available as standard stereo WAV files. The hydrophone array and geophone (MP5) had a sampling frequency of f_S = 96 kHz. The recording of the four hydrophones and the geophone was time-synchronised and each recording saved as mono-WAV file.

As a rule, pile driving with driving energy and a variation in the selected noise mitigation system did not take longer than 60 s. Using a high-pass filter (frequency limit 20 Hz, Butterworth filter degree 6), the low-frequency signal parts of the hydrophone signals that are typically generated by wind and possibly by the wash of the waves were weakened.

By determining the energy equivalent continuous sound pressure level L_{eq} over 60 s and additionally counting the pile driving events performed during this period, it was possible to calculate the average single event exposure level L_E or SEL according to the FFT method. This method can be used, as the noise between the individual pile driving events was at least 30 dB quieter than the pile driving pulses. First, an FFT of length 2^{22} or 2^{23} was calculated and subsequently converted into standardised third-octave spectra. Due to the high frequency resolution, this conversion is also sufficiently accurate at low frequencies. In order to present the results, the third-octave spectra are limited to the frequency range of 12.5 to 16 kHz. All mathematical operations were carried out using a program developed at ITAP for Matlab by Mathworks. The program was verified using a spectrum analyser (HP35670a dynamic signal analyser).

7.5 Noise prediction

In spring 2011, during the ESRa project planning phase, it emerged that the “Brodten Ost” test pile is situated in an FFH region (Figure 40). In order to still be able to carry out the research project, an FFH preliminary test [22] was carried out in order to evaluate the effects of the noise emitted during testing on the marine environment. This preliminary test included a noise prediction, which was carried out by itap GmbH. For the complete noise prediction, please refer to Section 14: Appendix 1.

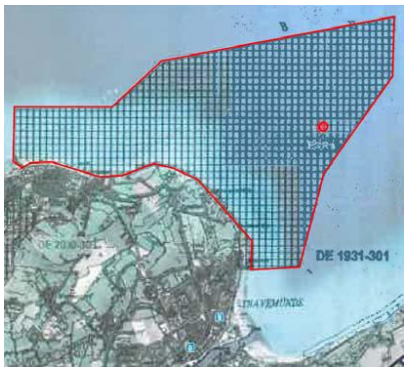

Figure 40: FFH region: "1931-301 Baltic Coast at Brodtner Ufer"

Figure 41 shows the results of the propagation calculation according to the PE model for paths 1 (to Brodtener Ufer) and 2 (to the shipping channel). The sound exposure level (SEL) of a pile driving blow at a receiver at a depth of 2 m is shown. The sound level decreases continuously in the westerly direction (path 1); 700 m from the coastline near Brodten, the SEL falls to below 150 dB re 1 µPa. Closer towards the beach, it falls further to approx. 130 dB re 1 µPa. In the southeasterly direction (135°), the sound level initially falls dramatically over the first 1000 metres from the driving pile, then remains at 150 to 155 dB re 1 µPa up to 3500 m away, and only drops to below 150 dB re 1 µPa at 200 to 300 m from the coastline.

The above-named levels decrease towards the surface of the water, namely when the receiver depth is less than 2 m. With increasing depth, the level increases slightly and, at a depth of 8 m, by about 3 dB compared with the value at a depth of 2 m.

Towards the open sea (path 3, Figure 42), the sound level decreases as the distance from the driving pile increases. According to the calculation, the value fell short of the precautionary value of 160 dB re 1 µPa at approx. 1.6 km established by the German Federal Environment Agency (Umweltbundesamt).

By way of comparison, Figure 41 and Figure 42 show the result of the simple calculation using Thiele's formula. As this does not take account of any water depth profiles, it is not possible to obtain any realistic values for the stretches towards the coast. However, for direction 3, it offers a usable approximation for up to about 2 km.

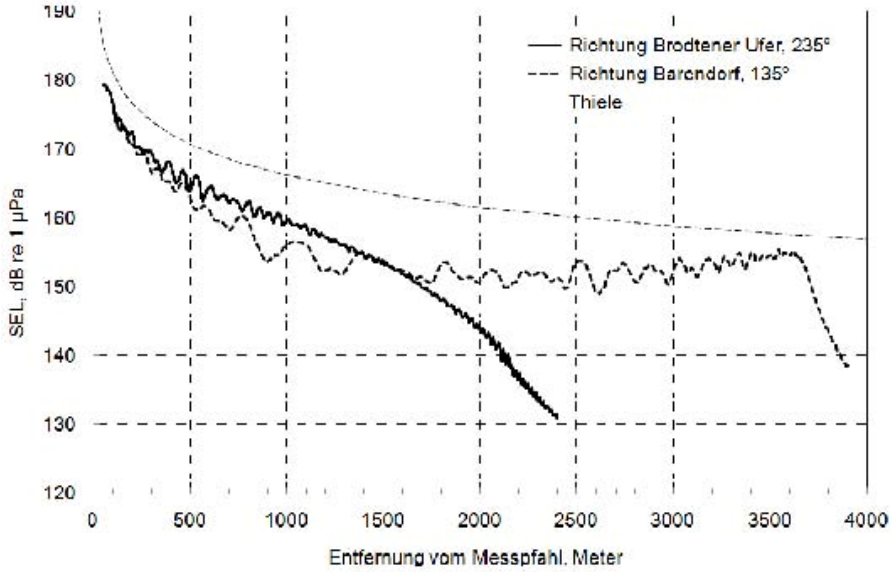

Richtung Brodtener Ufer, 235°	Direction Brodtener Ufer, 235°
Richtung Barendorf, 135°	Direction Barendorf, 135°
Entfernung vom Messpfahl, Meter	Distance in metres from measuring pile

Figure 41: Predicted single event exposure level at a depth of 2 m along the stretches 1 and 2

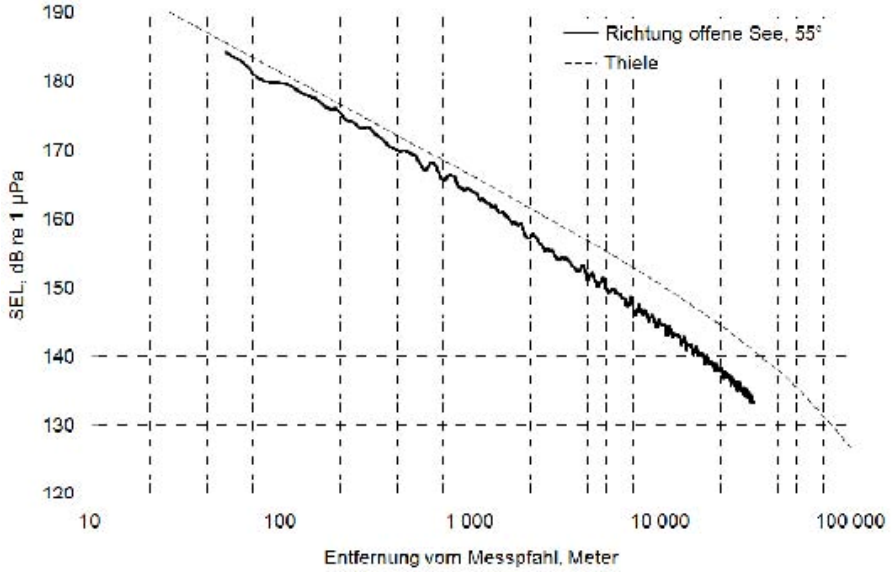

Richtung offene See, 55°	Direction open sea, 55°
Entfernung vom Messpfahl, Meter	Distance in metres from measuring pile

Figure 42: *Predicted single event exposure level at a depth of 8 m northeast of the pile*

8. Results

The analyses of the underwater sound measurements are presented below. Section 8.1 looks at the driving energy introduced during the tests. Section 8.2 shows the prevailing water conditions (speed of sound, etc.) when taking the measurements. The influence of the different measurement positions (Section 8.3), the driving energy (Section 0), the water depth and the distance (Section 8.5) on the single event exposure level L_E or SEL are then presented. This evaluation is generally based on the reference condition, i.e. without the influence of a noise mitigation system. Section 8.6 presents and compares the potential noise mitigation of the five noise mitigation systems tested. Section 8.7 contains near-field measurements of the TUBS. The complete report about the near-field measurements of the TUBS is available in Section 15, Appendix 2. This section also contains numerical calculations for sound propagation at the Brodten pile.

8.1 Driving energy

The measurement report of the TU Braunschweig regarding the driving energy introduced at the test pile clearly shows that the target driving energies of 100, 200 and 300 kJ were generated approximately during each driving cycle. There are slight deviations (approx. 10%) in the driving energy generated by the individual noise mitigation systems, including their variations, however, these do not have any major influence on the level values. For this reason, in the following, there is no further analysis of the measurement data with respect to the energy actually generated.

8.2 Evaluation of water properties

The water properties temperature, salinity and sound speed did not change significantly over the four measurement data sets. Figure 43 shows the water properties temperature, salinity and sound speed as a function of the water depth of a representative measurement. The water conditions are measured at intervals of 0.5 m water depth when lowering and recovering the CTD sensor.

Figure 43 shows that both the temperature and the sound speed hardly change over a water depth of 8.5 m. The sound speed falls slightly by 5 m/s to 1481 m/s on the seabed. The temperature drops from 17.6°C at the water surface to a minimum of 15.7°C at the sediment. The salinity remains relatively constant over the water depth.

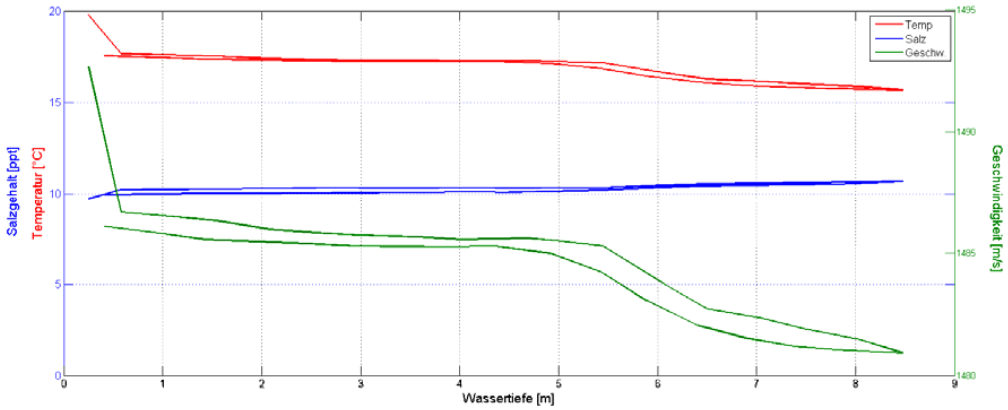

Figure 43: Water properties (temperature – red line; salinity – green; speed of sound – blue) during a representative measurement.

The measurement results show that the Baltic Sea was well mixed when the measurements were taken and that there was no noticeable water stratification.

8.3 Influence of the different measurement positions on the sound exposure level (SEL)

Figure 44 shows the respective third-octave spectra of the reference measurements (without sound mitigation system) for the four test days at measurement position MP1.1 (750 m distance, 1.8 m hydrophone height – StUK 3-compliant measurement position). The third-octave spectra do not differ substantially. Smaller differences in the individual third-octave spectra are the result of measurement uncertainties and possibly also the fact that the measurement systems were not positioned down to the last metre every day. Based on the results shown in Figure 44, the reference measurements taken on the respective day are used to calculate the difference third-octave spectra of each noise mitigation system.

Figure 45 compares the third-octave spectra at measurement positions MP1.1, MP2.1, MP3.1, MP4.1 and MP5.1 (each with a hydrophone height of 1.8 m above the sediment) of a representative reference measurement (21.08.2011). At measurement positions MP2.1 to MP4.1, despite being the same distance from the test pile, differences of up to ± 5 dB were recorded in the third-octave level value. On the one hand, the differences in the third-octave spectra could, in part, be explained by the different water depths at defined frequencies. On the other hand, repetitive measurements of the underwater sound generally also reveal differences of the same magnitude when taken at the same measurement position and with comparable excitation.

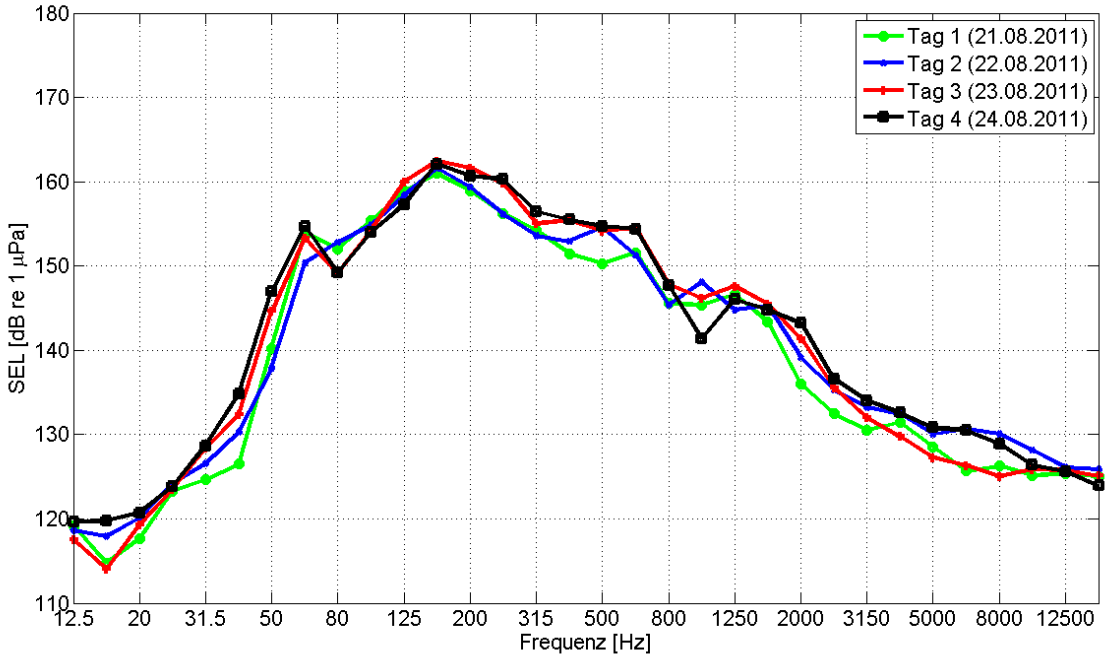

Frequenz [Hz]	Frequency [Hz]
Tag 1 (21.08.2011)	Day 1 (21.08.2011)
Tag 2 (22.08.2011)	Day 2 (22.08.2011)
Tag 3 (23.08.2011)	Day 3 (23.08.2011)
Tag 4 (24.08.2011)	Day 4 (24.08.2011)

Figure 44: Third-octave spectra of the reference measurements (no noise mitigation system) at measurement position MP1.1 (750 m distance, 1.8 m hydrophone height) with a driving energy of 300 kJ on the four different measurement days.

For this reason, in the following sections, not only the individual results of the respective measurement positions is given but also the median value from the measurement positions MP2.1, MP3.1 and MP4.1 for the third-octave spectra and the median value from MP1.1, MP2.1, MP3.1 and MP4.1 for the damping (difference between the third-octave spectra with and without noise mitigation systems, corresponds to the TL).

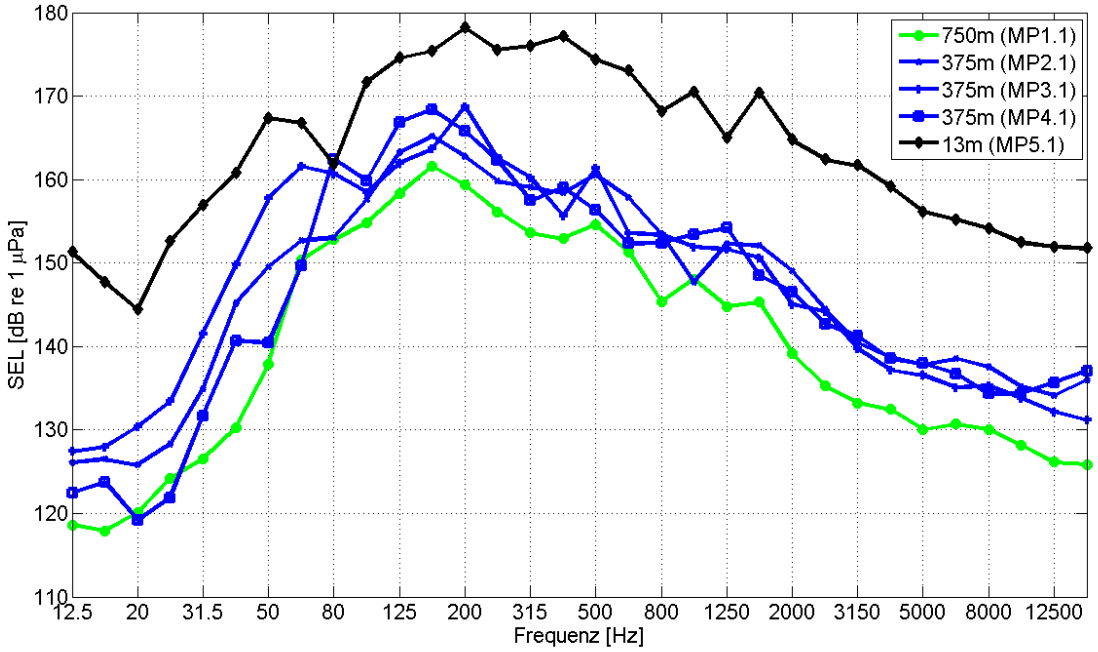

Frequenz [Hz]	Frequency [Hz]

Figure 45: Third-octave spectra of a reference measurement (no noise mitigation system) at measurement positions MP1.1, MP2.1, MP3.1, MP4.1 and MP5.1 (hydrophone height 1.8 m above sediment) with a driving energy of 300 kJ.

8.4 Influence of impact energy on the single event exposure level (SEL)

8.4.1. Total level

Figure 46 shows the single event exposure level (median of the total level) for the reference measurements as a function of impact energy and distance.

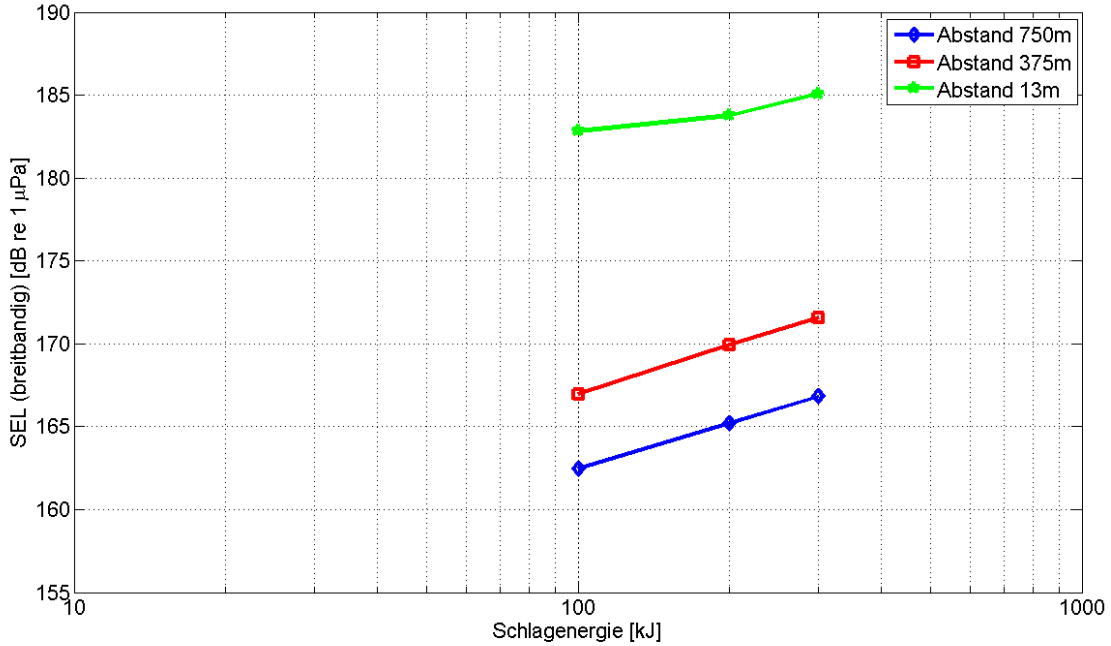

SEL (breitbrandig) [dB re 1µPa]	SEL (broad-band) [dB re 1µPa]
Abstand 750m	Distance 750m
Abstand 375m	Distance 375m
Abstand 13m	Distance 13m

Figure 46: Single event exposure level L_E or SEL (total level) as a function of the impact energy and distance

Comparable studies indicate that a level increase of $\Delta L \approx k \log_{10}(E2/E1)$ dB where k = 10 … 15 is to be expected when increasing impact energy from E1 to E2. This corresponds to an approx. 3.0 to 4.5 dB increase in SEL each time the driving energy is doubled. For the available results, in the far-field (distance 375 m or 750 m), an increase of approx. 3 dB can also be measured each time the driving energy is doubled. In the near-field at a distance of approx. 13 m from the pile, there is a much lower constant K.

The factor K is generally frequency-dependent. With lower frequencies (f< 1 kHz), it is in the range of 10 to 12 and, at higher frequencies, k increases to values of >20. As the greatest amount of energy is in the range between 80 and 500 Hz for one pile driving blow, this frequency range generally also dominates the level (see Figure 44 and Figure 45).

8.4.2. Noise mitigation

Figure 47 and Figure 48 show the influence of impact energy on noise mitigation (damping or difference between third-octave spectra with and without noise mitigation measure) using the noise mitigation system (system 1: IHC NMS) by way of example.

Figure 47 shows the frequency-resolved median values with and without noise mitigation system (NMS) at measurement positions MP2.1 to MP4.1 (distance 375 m, hydrophone height 1.8 m above sediment) for impact energies of 100, 200 and 300 kJ.

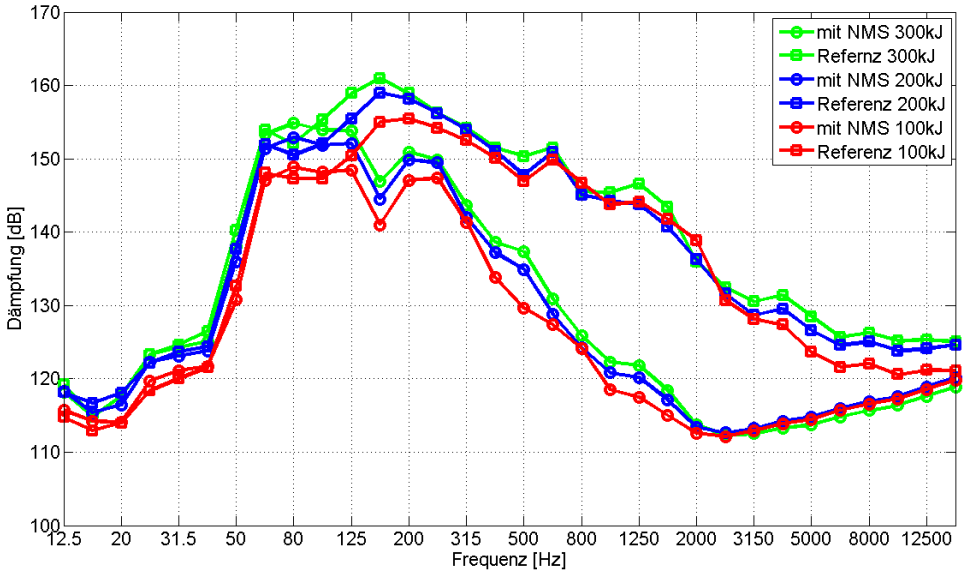

Daempfung [dB]	Damping [dB]
Frequenz [Hz]	Frequency [Hz]
Mit NMS 300 kJ	With NMS 300 kJ
Refernz 300 kJ	Reference 300 kJ
Mit NMS 200kJ	With NMS 200kJ
Referenz 200kJ	Reference 200kJ
Mit NMS 100 kJ	With NMS 100 kJ
Referenz 100kJ	Reference 100kJ

Figure 47: The median values of the third-octave spectra measured at the measurement positions MP2.1, MP3.1 and MP4.1 (hydrophone height 1.8 m, distance to pile 375 m) with and without noise mitigation system as a function of the selected impact energy

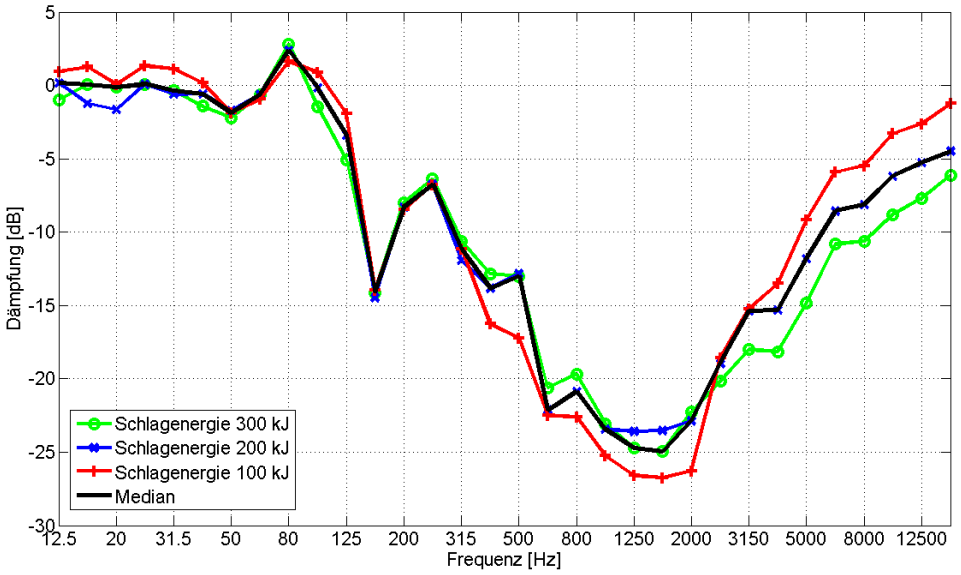

Daempfung [dB]	Damping [dB]
Frequenz [Hz]	Frequency [Hz]
Schlagenergie 300 kJ	Impact energy 300 kJ
Schlagenergie 200 kJ	Impact energy 200 kJ
Schlagenergie 100 kJ	Impact energy 100 kJ
Median	Median

Figure 48: Associated difference spectrum of the respective measuring condition (respective median over measurement positions MP1.1, MP2.1, MP3.1 and MP4.1).

With a reduced impact energy, the individual third-octave values, particularly between 100 and 400 Hz, are reduced by 2 to 4 dB.

Figure 48 shows the respective frequency-resolved median values of the noise mitigation above measurement positions MP1.1 to MP4.1 (distance 375 m and 750 m, hydrophone height 1.8 m above sediment) per impact energy. In addition, the median value of noise mitigation is shown for all impact energies used.

It is clear that, up to approx. 100 Hz, there is no noise mitigation. As frequency increases, a greater noise reduction of up to 25 dB at 1,250 Hz is achieved. Above 1,600 Hz, the noise mitigation decreases slightly.

There are no major deviations between the impact energies used. For this reason, only the results for 300 kJ impact energy will be shown in the following.

8.5 Influence of water depth and distance to the pile on the sound exposure level (SEL)

Figure 49 shows the single event exposure level (total level) as a function of the distance to the pile, the hydrophone height and the measurement day. All single event exposure levels (total level) shown were obtained using an average impact energy of 300 kJ and without installing a noise mitigation system.

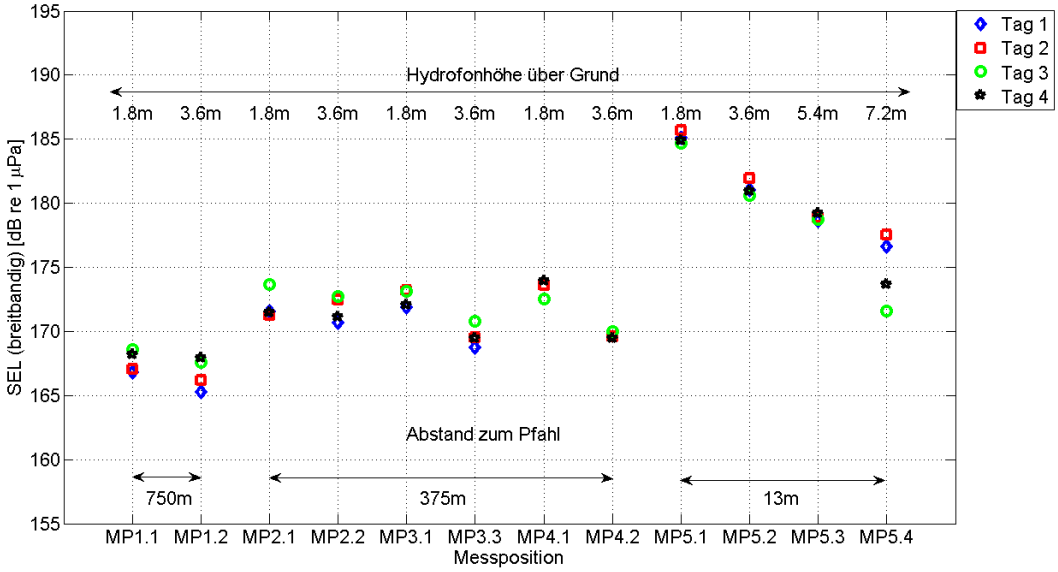

Hydrofonhoehe ueber Grund	Hydrophone height above ground
SEL (breitbrandig) [dB re 1µPa]	SEL (broad-band) [dB re 1µPa]
Messposition	Measurement position
MP1.1	MP1.1
MP1.2	MP1.2
Abstand zum Pfahl	Distance to pile
Tag 1	Day 1
Tag 2	Day 2
Tag 3	Day 3
Tag 4	Day 4

Figure 49: Single event exposure level L_E or SEL (total level) as a function of the hydrophone height above ground and the distance to the test pile when pile driving without noise mitigation system (impact energy 300 kJ).

Apart from measurement position MP5.1, there are hardly any deviations between days 1 to 4 at the same hydrophone height (1.8 m). Smaller deviations can be explained by the slight deviations in water conditions, the distance to the pile and/or measurement repetition (measurement uncertainty).

Compared with measurement positions MP1.1, MP2.1, MP3.1, MP4.1 and MP5.1, the single event exposure level decreases markedly with the distance to the pile.

The single event exposure level is reduced by up to 3.5 dB (MP4.2) as the hydrophone height above ground increases. This reduction in level can be

expected on the basis of the theory of sound propagation in water (multiple reflections).

In the case of measurement position MP5, the level decreases towards the surface of the water by up to 13 dB. The clear differences between days 1 and 2 and days 3 and 4 can be explained by the different positions of the work pontoon in front of the pile and the associated water depths. On day 3, the measurement position MP5.4 was just below the surface of the water so that, due to the expected impedance discontinuity between water and air (anechoic termination), the sound pressure level must be about zero.

Figure 50 shows the single event exposure level (total level) from Figure 49 of the hydrophone 1.8 m above ground (MP1.1 to MP5.1) as a function of the distance to the pile. Due to the slight differences, no distinction is made between the individual measuring days. In addition, based on measurement position MP1.1 (StUK-compliant measurement position), the SEL is shown as a function of distance using the formula by Thiele & Schellenstede (equation 2.9). There is a good correlation between the calculated SEL value (red line) at 375 m and the measurement data (blue rhombuses). For the measurement data at approx. 13 m from the pile (MP5.1), there is a difference of approx. 10 dB compared with the calculated values. The calculation formula of Thiele & Schellenstede [4] is expressly only defined for parts of the North Sea and a complete mixing of the water column. However, for the “far field” (375 m to 750 m), there is still a good correlation between measurement data and the calculation. In the literature, there are comparisons between the calculated and measured SEL at differences of up to several kilometres [23] that confirm a good correlation between the calculation and the measurement in the far field. However, for the acoustic “near field”, there are considerable differences between the values of the calculation formula of Thiele & Schellenstede and the measurement data.

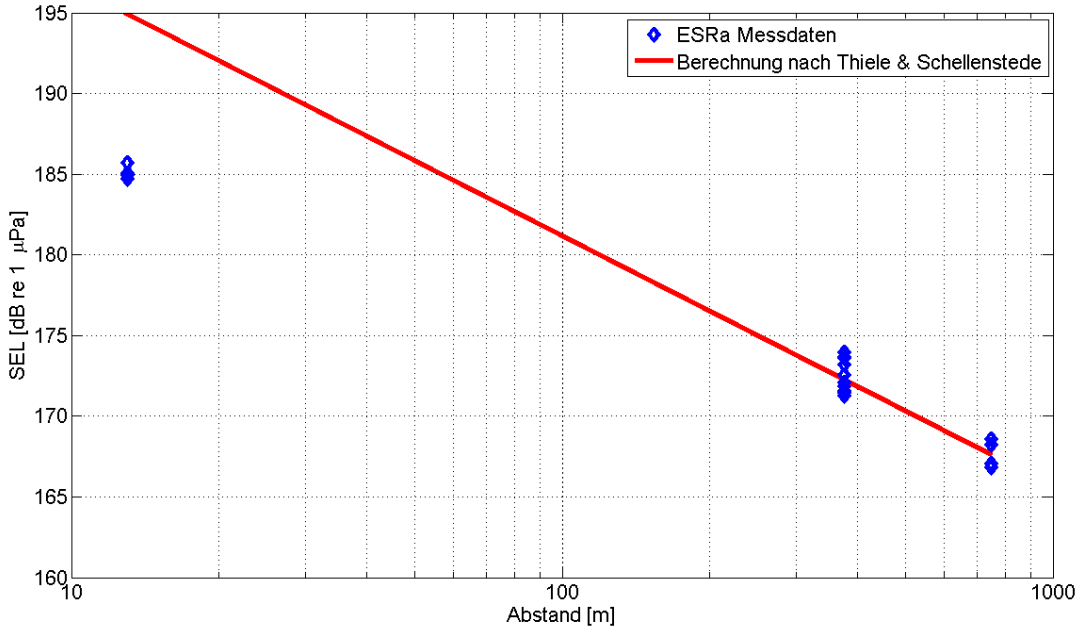

Abstand [m]	Distance [m]
ESRa Messdaten	ESRa measurement data
Berechnung nach Thiele & Schellenstede	Calculation according to Thiele & Schellenstede

Figure 50: Single event exposure level L_E or SEL (total level) as a function of the distance to the test pile when pile driving without noise mitigation measures (impact energy 300 kJ). In addition, the expected (calculated) single event exposure level according to Thiele & Schellenstede [4] is shown as a function of distance.

8.6 Near and far-field measurements (itap)

8.6.1. Results of the noise mitigation system in the far field

In order to illustrate the transmission loss TL of the individual noise mitigation measures, not only the individual third-octave spectra are shown in the following but also the difference third-octave spectra both without (reference) and with noise mitigation system. When illustrating the third-octave spectra, the frequency-resolved median values over measurement positions MP2.1 to MP4.1 (distance 375 m to the pile) are used. In order to illustrate the noise mitigation of the individual systems (sound transmission suppression), the median values of measurement positions MP1.1 to MP4.1 are used (distance 375 m and 750 m to the pile).

a) System 1: IHC NMS

The IHC NMS system was tested once with a bubble curtain between the test pile and ICH NMS system and once without bubble curtain. The bubble curtain was generated at the compressor with an air pressure of 7.0 bar. Figure 51

and Figure 52 show the third-octave spectra with and without noise mitigation system or the difference spectrum with / without noise mitigation system for the IHC NMS system (damping).

Due to a failure in the autonomous measurement system at measurement position MP4.1, no data are available for this position.

b) System 2: Menck fire hose

In the noise mitigation system by Menck (fire hose method), the compressor was set up to provide two different constant air pressures of 1.0 and 2.0 bar within the two closed fire hose rings. Figure 53 and Figure 54 show the third-octave spectra with and without noise mitigation system or the difference spectrum with / without noise mitigation system.

c) System 3: Weyres little bubble curtain

The LBC was only tested with one air pressure (compressor side 7.9 bar). Figure 55 and Figure 56 and 5.14 show the third-octave spectra with and without noise mitigation system or the difference spectrum with / without noise mitigation system.

d) System 4: BeKa jacket

The BeKa jacket was tested in three variations: i) + ii) with inner bubble curtain with an air pressure of 2.9 and 7.0 bar at the compressor and iii) without bubble curtain. A fourth variation that involved pumping out the water between the BeKa jacket and the test pile was not carried out for safety reasons. Figure 57 and Figure 58 show the third-octave spectra with and without noise mitigation system or the difference spectrum with / without noise mitigation system.

e) System 5: Elmer hydro sound damper

The Elmer hydro sound damper has three different rings (I – inner ring; M – middle ring; O – outer ring) that are lowered and tested in all permutations. There were a total of seven possible variations. Figure 59 and Figure 60 show the third-octave spectra with and without noise mitigation system or the difference spectrum with / without noise mitigation system.

f) Comparison of all noise mitigation systems

In practice, the monitoring method based on StUK 3 is used to determine the single event exposure level (SEL, broad-band or total level) and compared with the precautionary value of 160 dB at a distance of 750 m. For this reason, in Table 10, the respective SEL values (row 3) and the L_{peak} values (row 4) are summarised for each measurement at the StUK3-compliant measurement position MP1.1 (750 m distance, lower third of the water). In addition, in Table 10, row 5 and 6, the potential noise reduction (differences with and without

noise mitigation systems) for the SEL and the L_{peak} as median value are summarised across measurement positions MP1.1 to MP4.1.

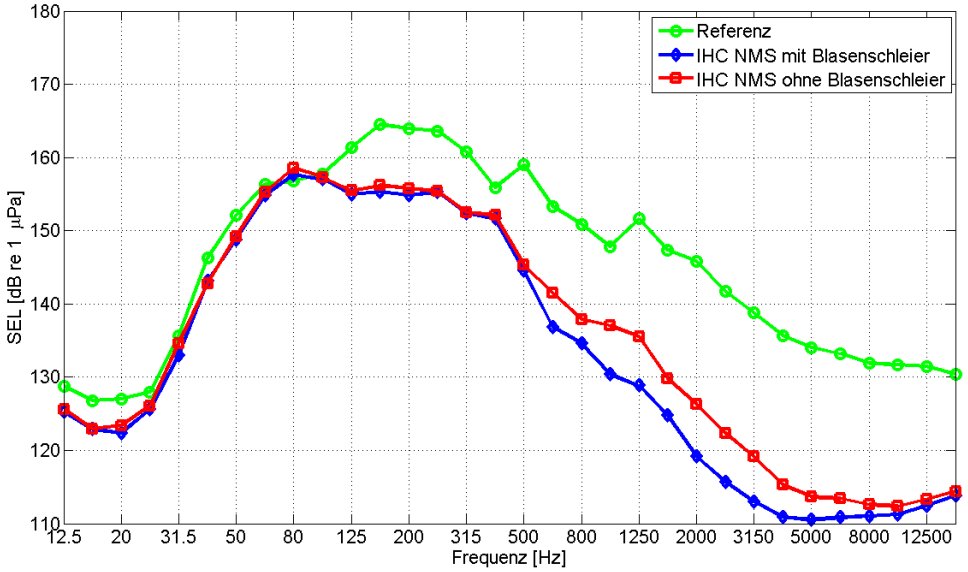

Frequenz [Hz]	Frequency [Hz]
Referenz	Reference
IHC NMS mit Blasenschleier	IHC NMS with bubble curtain
IHC NMS ohne Blasenschleier	IHC NMS without bubble curtain

Figure 51: The median values of the third-octave spectra measured at measurement positions MP2.1 and MP3.1 (hydrophone height 1.8 m, distance to pile 375 m) with and without noise mitigation system for the IHC NMS system, with and without inner bubble curtain

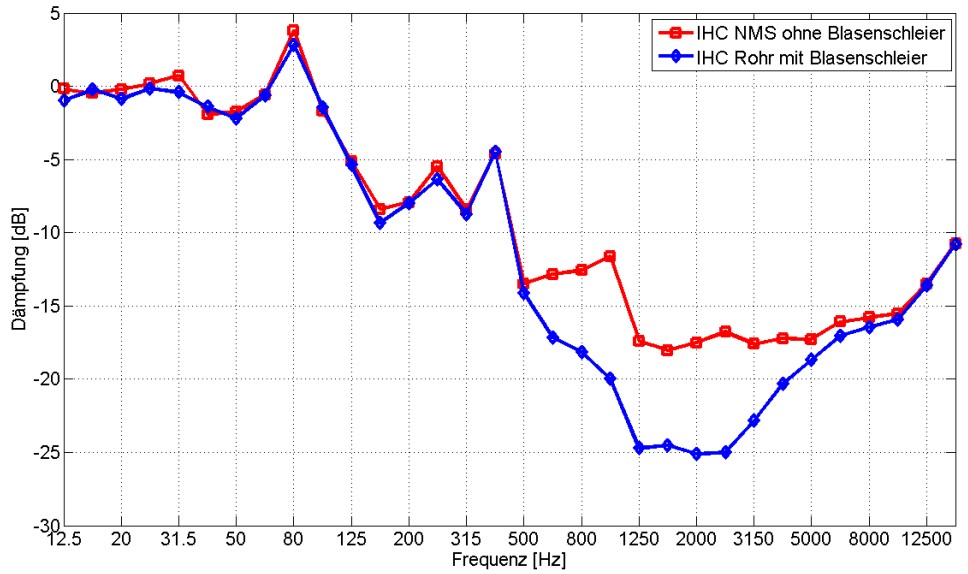

Daempfung [dB]	Damping [dB]
Frequenz [Hz]	Frequency [Hz]
IHC NMS ohne Blasenschleier	IHC NMS without bubble curtain
IHC Rohr mit Blasenschleier	IHC NMS with bubble curtain

Figure 52: Corresponding difference spectrum (sound transmission suppression) of the respective measurement condition

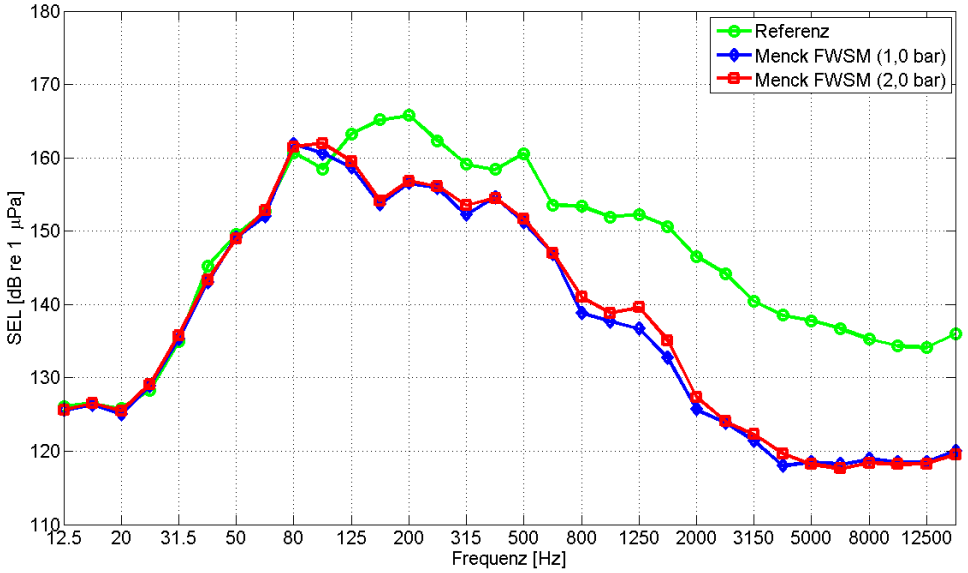

Frequenz [Hz]	Frequency [Hz]
Referenz	Reference
Menck FWSM (1,0 bar)	Menck FHSM (1.0 bar)
Menck FWSM (2,0 bar)	Menck FHSM (2.0 bar)

Figure 53: The median values of the third-octave spectra measured at measurement positions MP2.1, MP3.1 and MP4.1 (hydrophone height 1.8 m, distance to pile 375 m) with and without noise mitigation system for the Menck fire hose method with two different air pressures.

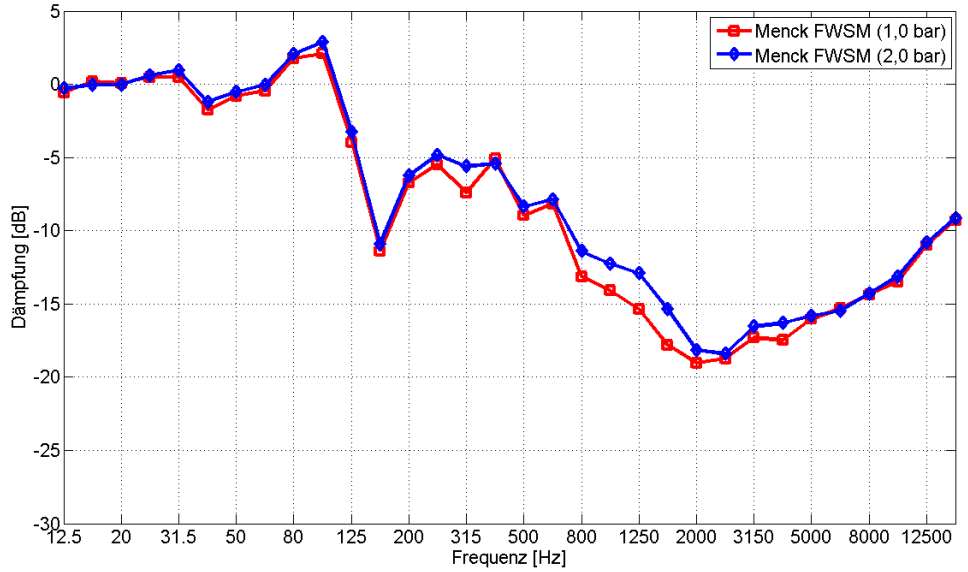

Daempfung [dB]	Damping [dB]
Frequenz [Hz]	Frequency [Hz]
Menck FWSM (1,0 bar)	Menck FHSM (1.0 bar)

Menck FWSM (2,0 bar)	Menck FHSM (2.0 bar)

Figure 54: Corresponding difference spectrum (sound transmission suppression) of the respective measurement condition.

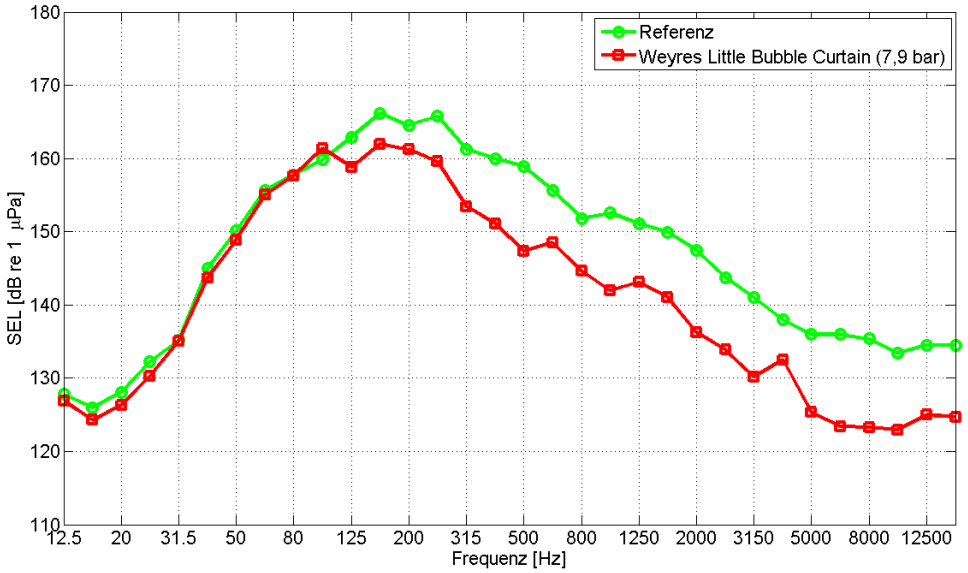

Frequenz [Hz]	Frequency [Hz]
Referenz	Reference

Figure 55: The median values of the third-octave spectra measured at measurement positions MP2.1, MP3.1 and MP4.1 (hydrophone height 1.8 m, distance to pile 375 m) with and without noise mitigation system for the Weyres little bubble curtain

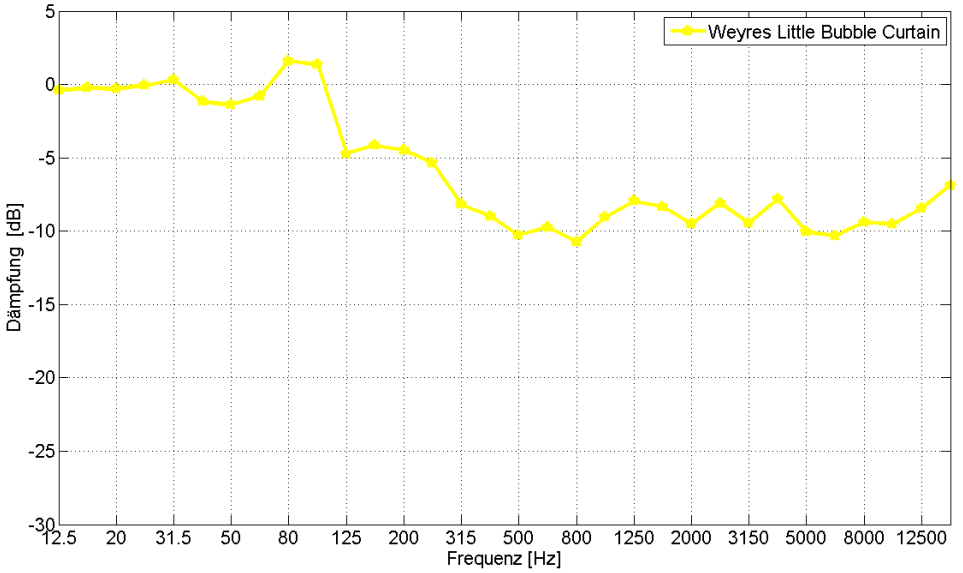

Daempfung [dB]	Damping [dB]
Frequenz [Hz]	Frequency [Hz]

Figure 56: Corresponding difference spectrum (sound transmission suppression) of the respective measurement condition (respective median of measurement positions MP1.1, MP2.1, MP3.1 and MP4.1).

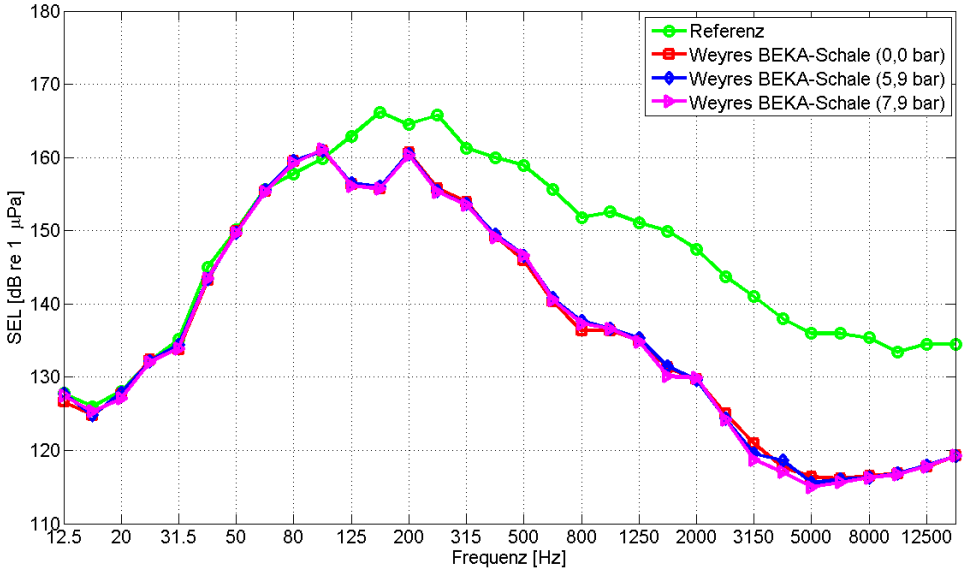

Frequenz [Hz]	Frequency [Hz]
Referenz	Reference
Weyres BEKA-Schale (0,0 bar)	Weyres BEKA jacket (0.0 bar)
Weyres BEKA-Schale (5,9 bar)	Weyres BEKA jacket (5.9 bar)
Weyres BEKA-Schale (7,9 bar)	Weyres BEKA jacket (7.9 bar)

Figure 57: The median values of the third-octave spectra measured at measurement positions MP2.1, MP3.1 and MP4.1 (hydrophone height 1.8 m, distance to pile 375 m) with and without noise mitigation system for the BeKa jacket, with and without Weyres inner bubble curtain

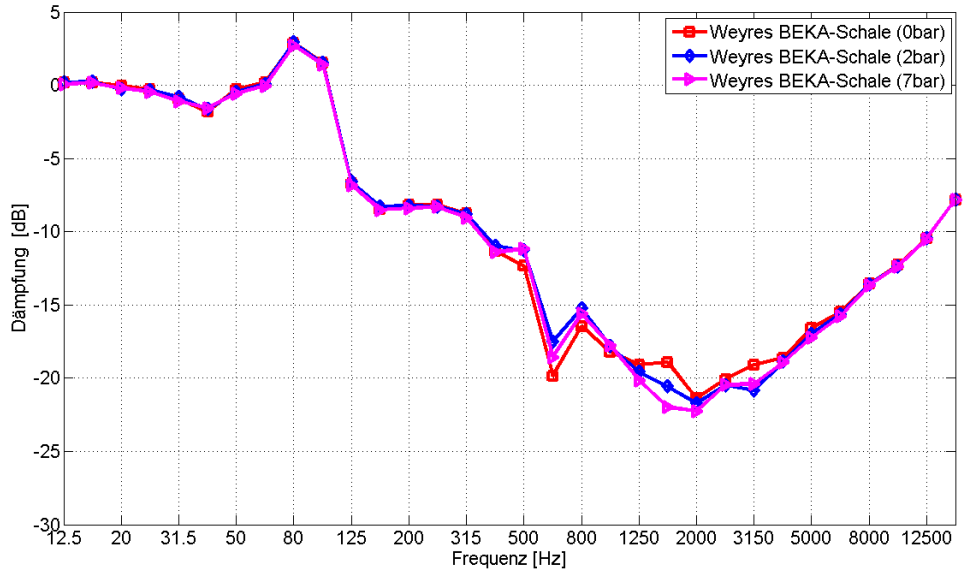

Daempfung [dB]	Damping [dB]
Frequenz [Hz]	Frequency [Hz]

Weyres BEKA-Schale (0bar)	Weyres BEKA jacket (0bar)
Weyres BEKA-Schale (2bar)	Weyres BEKA jacket (2bar)
Weyres BEKA-Schale (7bar)	Weyres BEKA jacket (7bar)

Figure 58: Corresponding difference spectrum (sound transmission suppression) of the respective measurement condition (respective median of measurement positions MP1.1, MP2.1, MP3.1 and MP4.1).

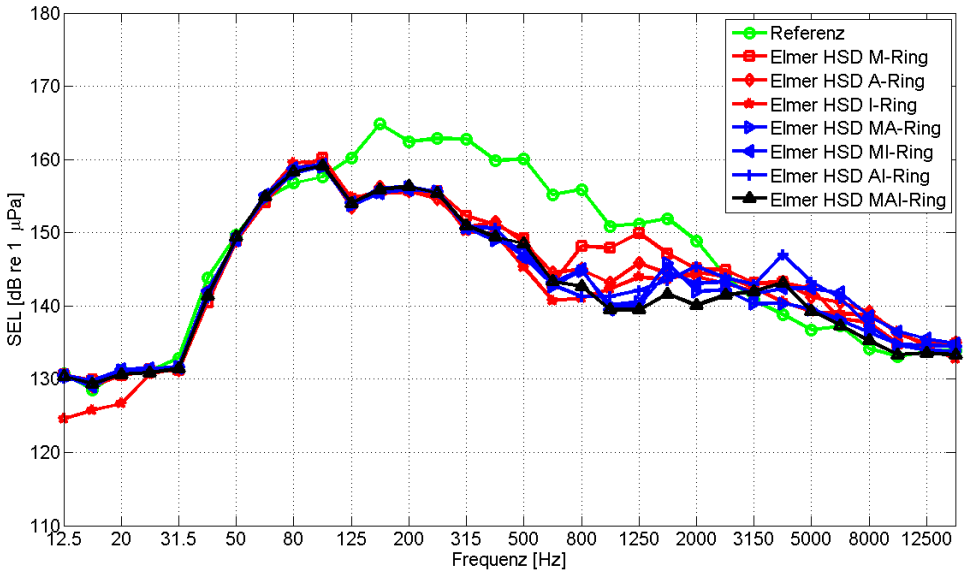

Frequenz [Hz]	Frequency [Hz]
Referenz	Reference
Elmer HSD M-Ring	Elmer HSD M ring
Elmer HSD A-Ring	Elmer HSD O ring
Elmer HSD I-Ring	Elmer HSD I ring
Elmer HSD MA-Ring	Elmer HSD MO ring
Elmer HSD MI-Ring	Elmer HSD MI ring
Elmer HSD AI-Ring	Elmer HSD OI ring
Elmer HSD MAI-Ring	Elmer HSD MOI ring

Figure 59: The median values of the third-octave spectra measured at measurement positions MP2.1, MP3.1 and MP4.1 (hydrophone height 1.8 m, distance to pile 375 m) with and without noise mitigation system of the Elmer hydro sound damper. The three rings (I – inner ring; M – middle ring; O – Outer ring) offer seven different possibilities

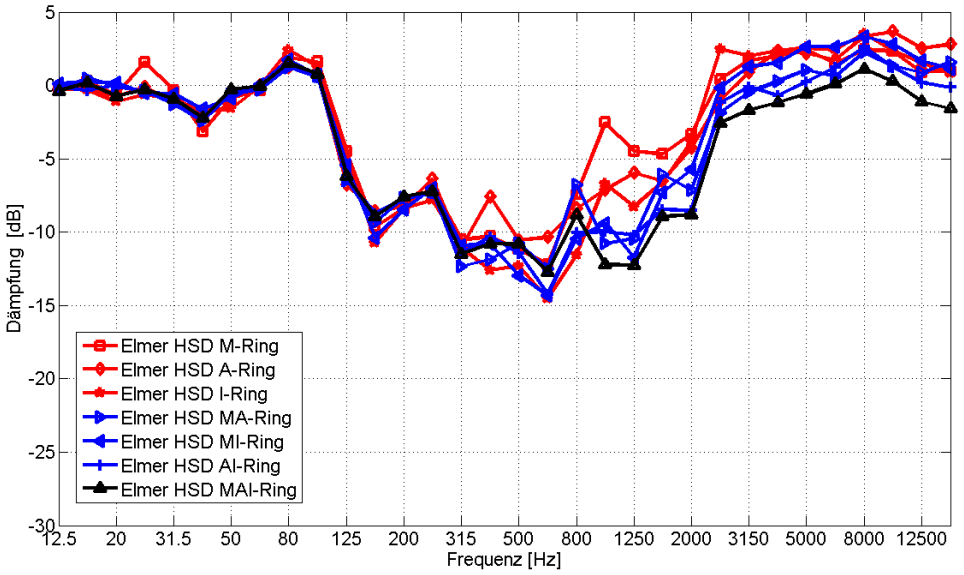

Daempfung [dB]	Damping [dB]
Frequenz [Hz]	Frequency [Hz]
Elmer HSD M-Ring	Elmer HSD M ring
Elmer HSD A-Ring	Elmer HSD O ring
Elmer HSD I-Ring	Elmer HSD I ring
Elmer HSD MA-Ring	Elmer HSD MO ring
Elmer HSD MI-Ring	Elmer HSD MI ring
Elmer HSD AI-Ring	Elmer HSD OI ring
Elmer HSD MAI-Ring	Elmer HSD MOI ring

Figure 60: Corresponding difference spectrum (sound transmission suppression) of the respective measurement condition (respective median of measurement positions MP1.1, MP2.1, MP3.1 and MP4.1).

In the median, there are (broad-band) noise reductions from 4.4 dB (Menck fire hose method with a pressure of 2.0 bar) to 6.1 dB (Weyres BeKa jacket with inner bubble curtain with 7 bar).

No.	System	Noise mitigation system	Distance 750 m (MP1.1)		Difference without/with noise mitigation system (median over MP1.1, MP2.1, MP3.1, MP4.1)	
			SEL [dB]	L_{peak} [dB]	ΔSEL [dB]	ΔL_{peak} [dB]
1	1	IHC NMS with bubble curtain	161.0	183.2	5.6	6.9
2		IHC NMS without bubble curtain	161.7	184.1	5.1	6.0
3	2	Menck FHSM with 1.0 bar	162.8	185.4	5.0	4.5
4		Menck FHSM	162.2	184.8	4.4	5.1

		with 2.0 bar				
5	3	Weyres LBC	164.2	188.2	4.2	4.0
6	4	Weyres BeKa 0 bar	162.3	184.8	5.9	7.4
7		Weyres BeKa 5 bar	162.4	184.6	5.9	7.6
8		Weyres BeKa 7 bar	162.2	184.6	6.1	7.6
9	5	Elmer HSD M ring	162.4	186.3	5.0	6.2
10		Elmer HSD O ring	162.2	185.2	4.2	7.3
11		Elmer HSD I ring	162.4	186.7	5.4	5.8
12		Elmer HSD MO ring	161.2	184.9	5.4	7.6
13		Elmer HSD MI ring	162.0	186.3	4.9	6.2
14		Elmer HSD I ring	162.0	184.6	5.4	7.9
15		Elmer HSD MOI ring	162.0	184.7	5.4	7.8
16	Reference	IHC NMS reference	166.8	190.1	-	-
17		Menck FHSM reference	167.0	189.9	-	-
18		Weyres LBC + BeKa reference	168.6	192.2	-	-
19		Elmer HSD reference	168.2	192.5	-	-

Table 10: Summary of the potential noise mitigation of the five tested noise mitigation systems, incl. variations. Additionally, the single event exposure level (SEL) and the L_{peak} at the StUK 3-compliant measurement position MP1.1 are shown.

However, in the previous sections a) to e), it was shown that noise mitigation is highly dependent upon frequency. In addition, larger dispersion occurs for particular noise mitigation values as a result of repetitions or at various measurement positions.

In order to compare all noise mitigation systems, Figure 61 shows a graph summarising the potential noise mitigation or sound transmission suppression (difference between third-octave spectra with and without noise mitigation measures) of all systems.

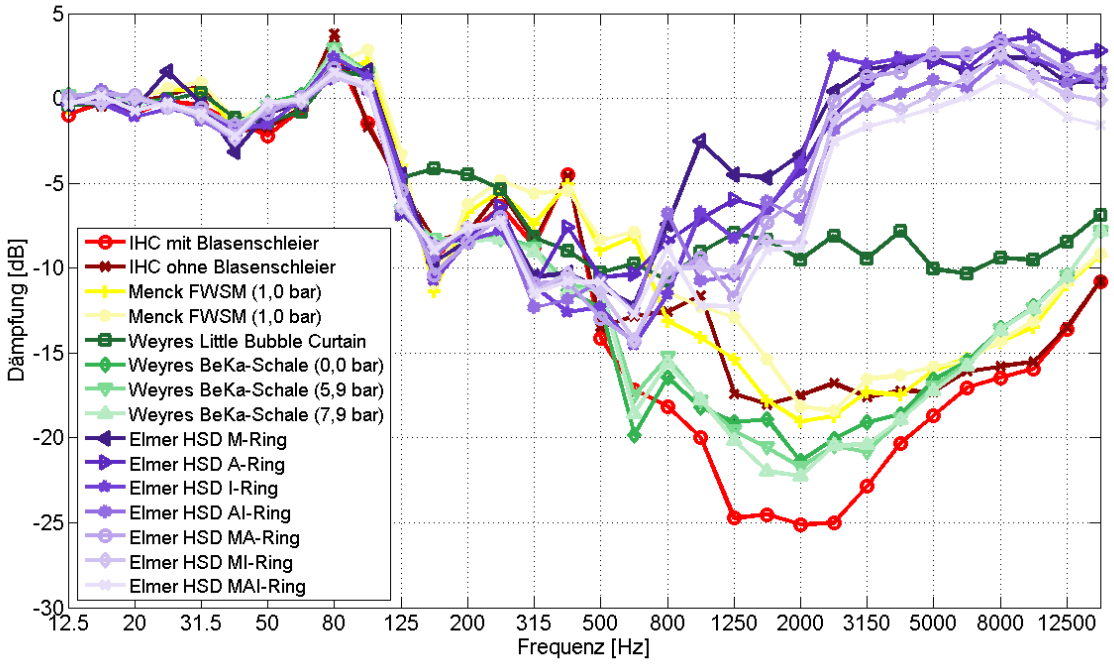

Daempfung [dB]	Damping [dB]
Frequenz [Hz]	Frequency [Hz]
IHC NMS mit Blasenschleier	IHC NMS with bubble curtain
IHC NMS ohne Blasenschleier	IHC NMS without bubble curtain
Menck FWSM (1,0 bar)	Menck FHSM (1.0 bar)
Menck FWSM (1,0 bar)	Menck FHSM (1.0 bar)
Weyres Little Bubble Curtain	Weyres little bubble curtain
Weyres BeKa –Schale (0,0 bar)	Weyres BeKa jacket (0.0 bar)
Weyres BeKa –Schale (5,9 bar)	Weyres BeKa jacket (5.9 bar)
Weyres BeKa –Schale (7,9 bar)	Weyres BeKa jacket (7.9 bar)
Elmer HSD M-Ring	Elmer HSD M ring
Elmer HSD A -Ring	Elmer HSD O ring
Elmer HSD I -Ring	Elmer HSD I ring
Elmer HSD AI-Ring	Elmer HSD OI ring
Elmer HSD Ma-Ring	Elmer HSD MO ring
Elmer HSD MI-Ring	Elmer HSD MI ring
Elmer HSD MAI-Ring	Elmer HSD MOI ring

Figure 61: Summary of the sound transmission suppression or difference spectrum with and without NMS (media value over measurement positions MP1.1, MP2.1, MP3.1 and MP4.1) of the tested noise mitigation measures.

8.6.2. Results of noise mitigation in the near field

Section 8.6.1 presented the results of noise mitigation of all systems measured in the far field (375 m to 750 m distance). This section will outline the results of measurement position MP5 in the near field of the pile (13 m).

The third-octave spectra of the reference condition (without noise mitigation system) of the measurement position MP5 at different hydrophone heights above ground are juxtaposed in Figure 62.

There are significant differences in the third-octave spectra measured at different heights above ground. The low-frequency fractions tend to decrease markedly as the distance from the sediment increases. This effect amounts to up to 20 dB (e.g. at f = 125 Hz).

In Figure 63 the sound transmission loss is shown for a representative noise mitigation measure from the near field at different heights.

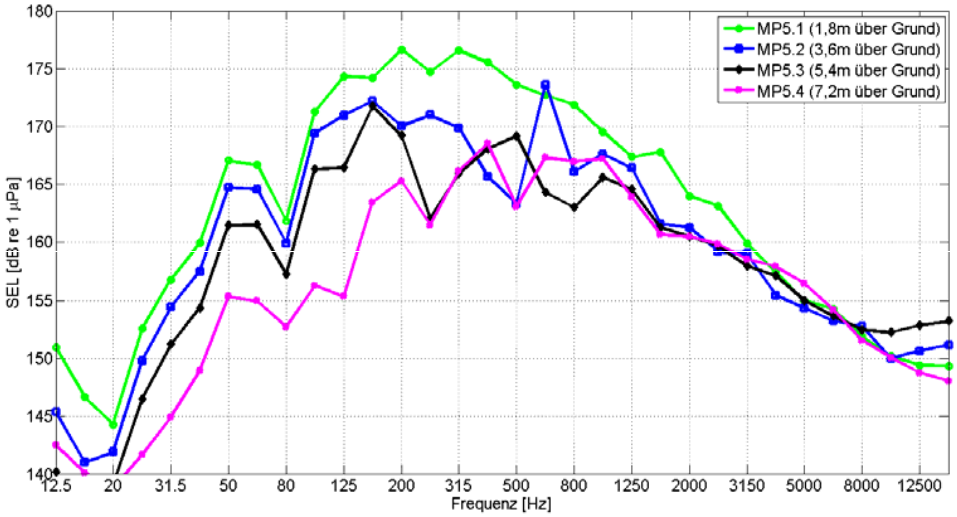

Figure 62: Represented are the third-octave spectra of the reference condition (without noise mitigation system) measured at the measurement position MP5 at different heights (hydrophone height 1.8 m, 3.6 m, 5.4 m and 7.2 m; distance from pile 13 m).

Frequenz [Hz]	Frequency [Hz]
MP5.1 (1,8m ueber Grund)	MP5.1 (1.8 m above ground)
MP5.2 (3,6m ueber Grund)	MP5.2 (3.6 m above ground)
MP5.3 (5,4m ueber Grund)	MP5.3 (5.4 m above ground)
MP5.4 (7,2m ueber Grund)	MP5.4 (7.2 m above ground)

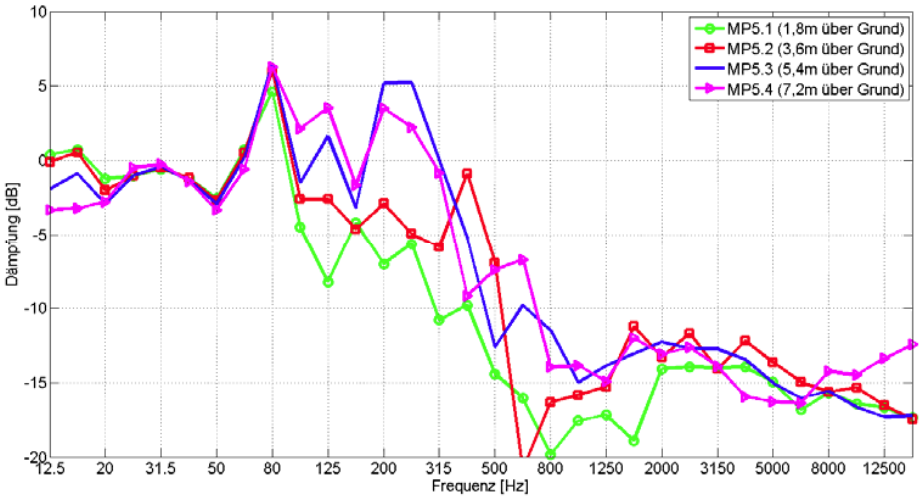

Figure 63: Represented is the difference spectrum (spectral sound transmission loss) for a representative noise mitigation system (with and without noise mitigation system) measured at the measurement position MP5 at different heights (hydrophone height 1.8 m, 3.6 m, 5.4 m and 7.2 m; distance from pile 13 m).

Daempfung [dB]	Attenuation [dB]
Frequenz [Hz]	Frequency [Hz]
MP5.1 (1,8m ueber Grund)	MP5.1 (1.8 m above ground)
MP5.2 (3,6m ueber Grund)	MP5.2 (3.6 m above ground)
MP5.3 (5,4m ueber Grund)	MP5.3 (5.4 m above ground)
MP5.4 (7,2m ueber Grund)	MP5.4 (7.2 m above ground)

There are significant differences of up to 10 dB in the difference spectrum with and without a noise mitigation system measured at MP5 at different heights. In the frequency range 100 Hz $\leq$ f $\leq$ 500 Hz, it is evident that the sound attenuation diminishes and in some cases even assumes negative values as the hydrophone height above ground increases.

The third-octave spectra with and without noise mitigation system are represented below with reference to Section 8.6.1 along with the related sound transmission loss, independent of frequency, for the measurement position MP5.1 (near field 13 m distant, 1.8 m above ground). The resulting broad-band reduction values ΔSEL can be found in the summary table in Section 8.8.

a) System 1: IHC NMS

The IHC NMS system was tested once with a bubble curtain between the test pile and IHC NMS system and once without a bubble curtain. The bubble curtain was produced by compressor at an air pressure of 7.0 bar.

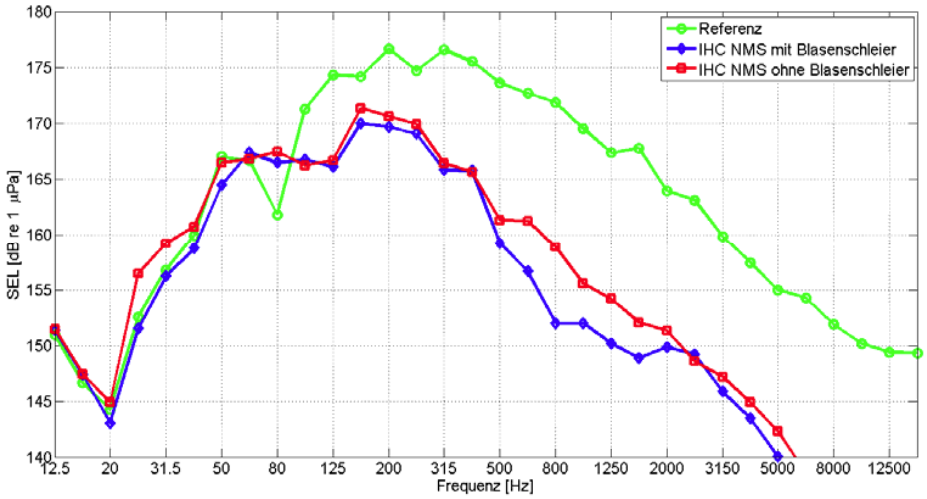

Figure 64: Represented are the third-octave spectra measured at the measurement position MP5.1 (hydrophone height 1.8 m, distance from pile 13 m) with and without noise mitigation system for the IHC NMS system with and without inner bubble curtain

Frequenz [Hz]	Frequency [Hz]
Referenz	Reference
IHC NMS mit Blasenschleier	IHC NMS with bubble curtain
IHC NMS ohne Blasenschleier	IHC NMS without bubble curtain

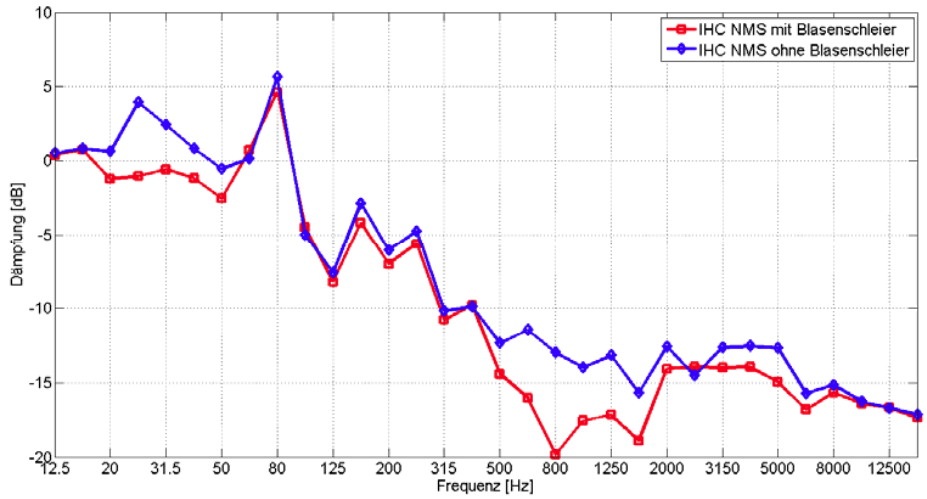

Figure 65: Difference spectrum pertaining to this (sound transmission loss) of the respective measurement condition.

Daempfung [dB]	Attenuation [dB]
Frequenz [Hz]	Frequency [Hz]
IHC NMS mit Blasenschleier	IHC NMS with bubble curtain
IHC NMS ohne Blasenschleier	IHC NMS without bubble curtain

b) System 2: Menck Fire Hose

The noise mitigation system of the Menck company (“fire hose method”) was implemented using two different constant air pressures of 1.0 and 2.0 bar generated by compressor in the two closed fire hose rings.

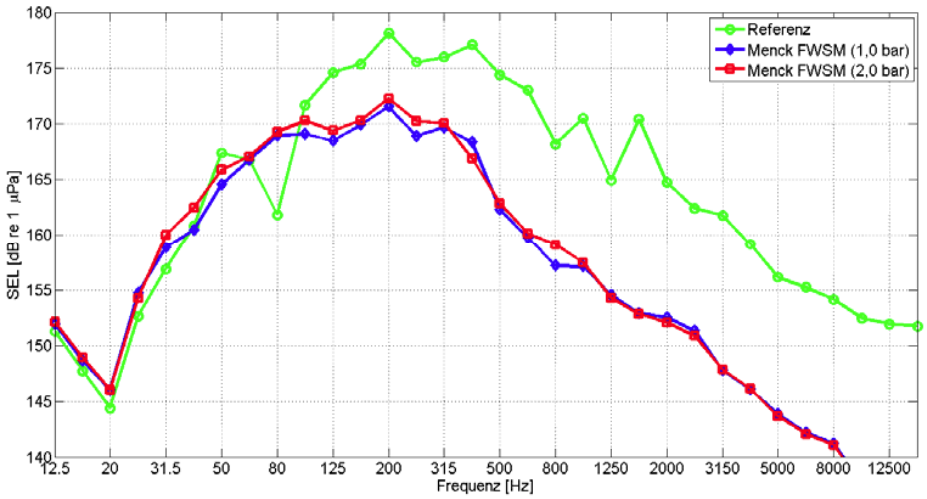

Figure 66: Represented are the third-octave spectra measured at the measurement position MP5.1 (hydrophone height 1.8 m, distance from pile 13 m) with and without noise mitigation system for the fire hose method from Menck with two different air pressures

Frequenz [Hz]	Frequency [Hz]
Referenz	Reference
Menck FWSM (1,0 bar)	Menck FHS (1.0 bar)
Menck FWSM (2,0 bar)	Menck FHS (2.0 bar)

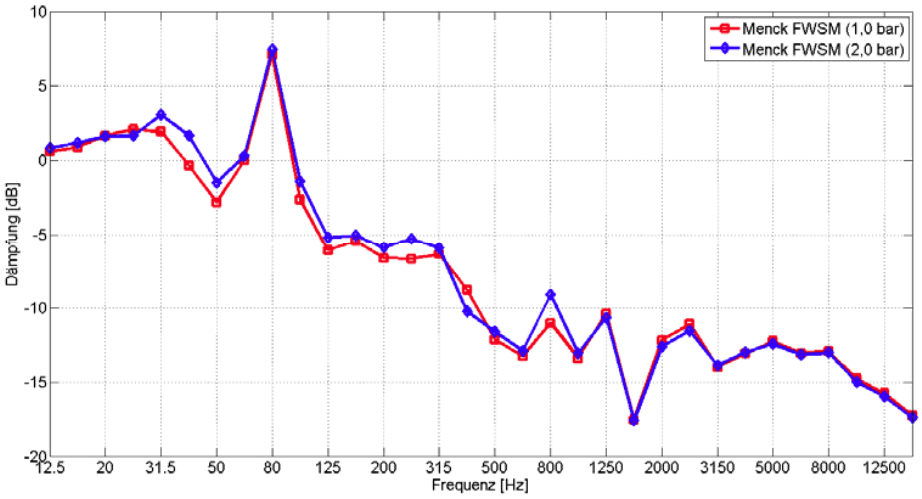

Figure 67: Difference spectrum pertaining to this (sound transmission loss) of the respective measurement condition.

Daempfung [dB]	Attenuation [dB]
Frequenz [Hz]	Frequency [Hz]
Menck FWSM (1,0 bar)	Menck FHS (1.0 bar)
Menck FWSM (2,0 bar)	Menck FHS (2.0 bar)

c) System 3: Weyres Little Bubble Curtain

The LBC was tested with only one air pressure (compressor, 7.9 bar).

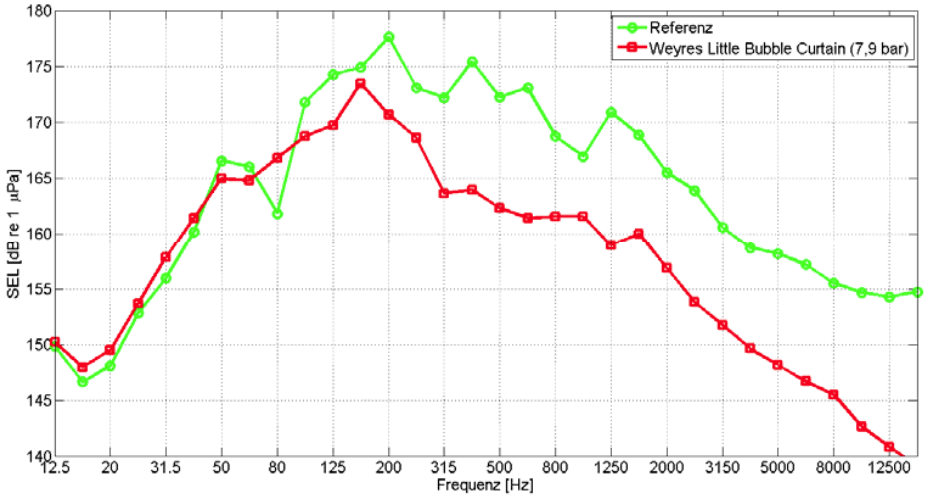

Figure 68: Represented are the third-octave spectra measured at the measurement position MP5.1 (hydrophone height 1.8 m, distance from pile 13 m) with and without noise mitigation systems for the Little Bubble Curtain of the Weyres company

Frequenz [Hz]	Frequency [Hz]
Referenz	Reference
Weyres Little Bubble Curtain (7,9 bar)	Weyres Little Bubble Curtain (7.9 bar)

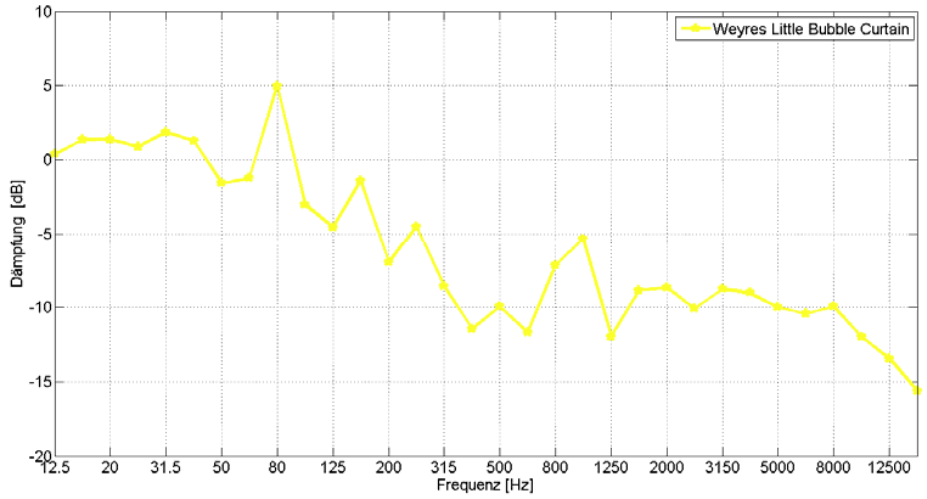

Figure 69: Difference spectrum pertaining to this (sound transmission loss) of the respective measurement condition

Daempfung [dB]	Attenuation [dB]
Frequenz [Hz]	Frequency [Hz]

d) System 4: BeKa Jacket

Three variations of the BeKa Jacket were tested: i) + ii) with inner bubble curtain at an air pressure of 2.9 and 7.0 bar at the compressor and iii) without bubble curtain. A fourth variation with pumping out of the water between the BeKa Jacket and the test pile was not carried out for safety reasons.

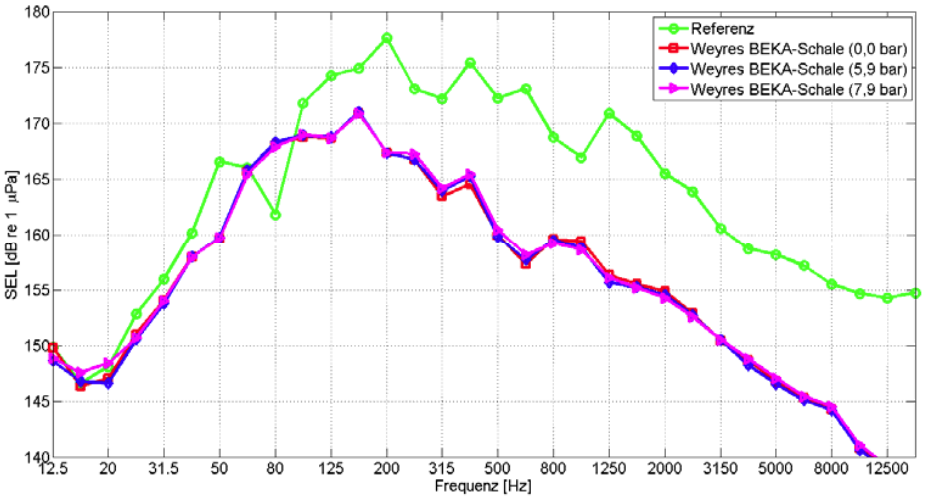

Figure 70: Represented are the third-octave spectra measured at the measurement position MP5.1 (hydrophone height 1.8 m, distance from pile 13 m), with and without noise mitigation systems, for the BeKa Jacket with and without the inner bubble curtain from Weyres

Frequenz [Hz]	Frequency [Hz]
Referenz	Reference
Weyres BEKA-Schale (0,0 bar)	Weyres BeKa Jacket (0.0 bar)
Weyres BEKA-Schale (5,9 bar)	Weyres BeKa Jacket (5.9 bar)
Weyres BEKA-Schale (7,9 bar)	Weyres BeKa Jacket (7.9 bar)

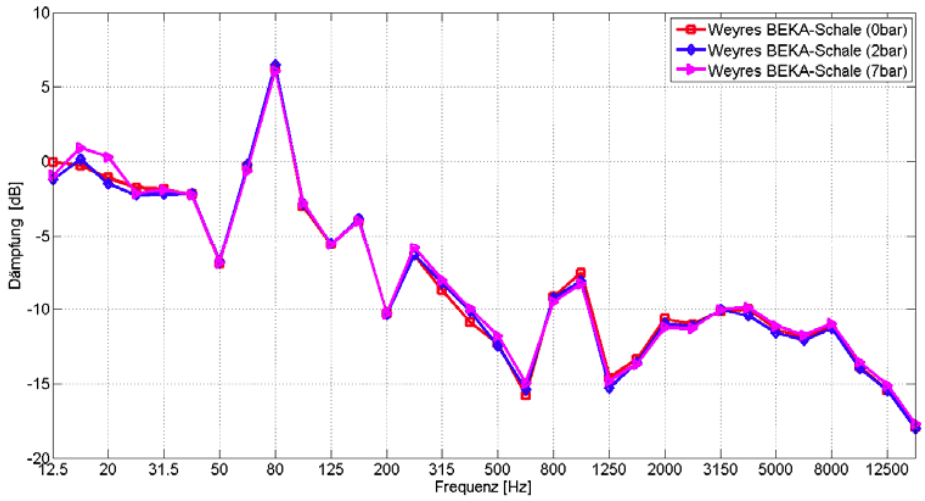

Figure 71: Difference spectrum pertaining to this (sound transmission loss) of the respective measurement condition

Daempfung [dB]	Attenuation [dB]
Frequenz [Hz]	Frequency [Hz]
Weyres BEKA-Schale (0 bar)	Weyres BeKa Jacket (0 bar)
Weyres BEKA-Schale (2 bar)	Weyres BeKa Jacket (2 bar)
Weyres BEKA-Schale (7 bar)	Weyres BeKa Jacket (7 bar)

e) Elmer Hydro Sound Damper

The Elmer Hydro Sound Damper had three different rings (I – inner ring; M – middle ring; A – outer ring), which were lowered and tested in all permutations. This gave rise to seven possible variations in all.

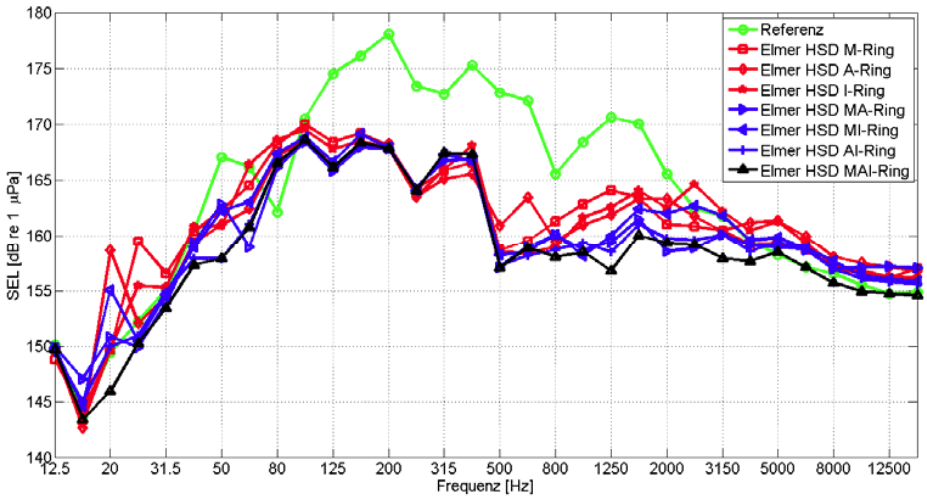

Figure 72: Represented are the third-octave spectra measured at the measurement position MP5.1 (hydrophone height 1.8 m, distance from pile 13 m) with and without noise mitigation system for the Elmer Hydro Sound Damper. The three rings (I – inner ring; M – middle ring; A – outer ring) resulted in seven possible variations

Daempfung [dB]	Attenuation [dB]
Frequenz [Hz]	Frequency [Hz]
Referenz	Reference
Elmer HSD M Ring	Elmer HSD M Ring
Elmer HSD A Ring	Elmer HSD O Ring
Elmer HSD I Ring	Elmer HSD I Ring
Elmer HSD MA Ring	Elmer HSD MO Ring
Elmer HSD MI Ring	Elmer HSD MI Ring
Elmer HSD AI Ring	Elmer HSD OI Ring
Elmer HSD MAI Ring	Elmer HSD MOI Ring

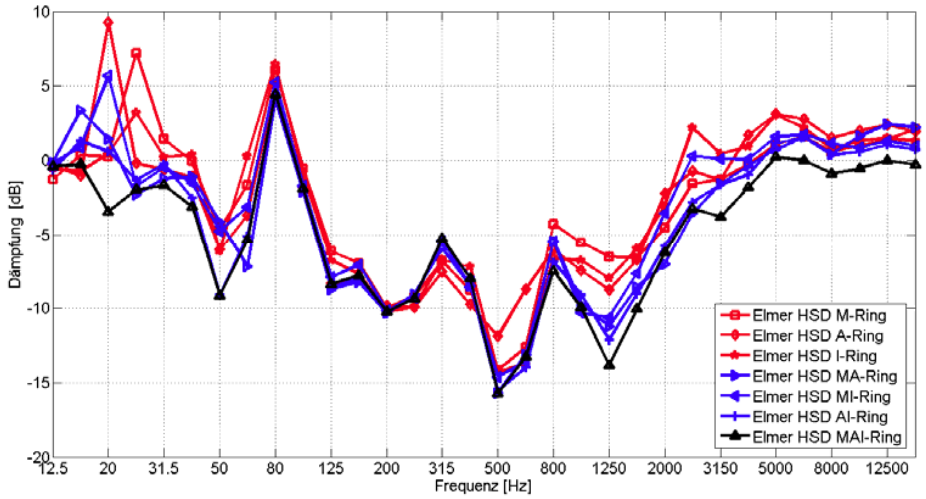

Figure 73: Difference spectrum pertaining to this (sound transmission loss) of the respective measurement condition

Daempfung [dB]	Attenuation [dB]
Frequenz [Hz]	Frequency [Hz]
Elmer HSD M Ring	Elmer HSD M Ring
Elmer HSD A Ring	Elmer HSD O Ring
Elmer HSD I Ring	Elmer HSD I Ring
Elmer HSD MA Ring	Elmer HSD MO Ring
Elmer HSD MI Ring	Elmer HSD MI Ring
Elmer HSD AI Ring	Elmer HSD OI Ring
Elmer HSD MAI Ring	Elmer HSD MOI Ring

8.7 Near field measurements TU BS (cf. Appendix 2)

In addition to the measurements by ITAP GmbH, TU BS carried out near-field measurements from a working pontoon. The complete report including numerical calculations can be read in Section 15, Appendix 2.

8.7.1 Measuring equipment used and measurement positions

The underwater noise measurements were carried out by IGB-TUBS on all 4 measuring days at a similar position. The measuring system used for the measurements was produced by Bruel & Kjaer and consists of two type 8103 hydrophones for this application. These are connected to a LanXI module (3052-B-3/0) via a Nexus signal conditioner (type 26920S2). This module is controlled from a laptop on which all measurement data are stored as sound pressure in Pascals. The sample rate of the hydrophone was 65.536 Hz. The measurements were carried out at a position at a distance of approx. six metres from the Brodten pile at different depths (H1 at 6 m depth, H2 at 4 m depth) (see Figure 74). On account of the short distance between the Brodten pile and the hydrophones, the measurements can be termed near-field measurements.

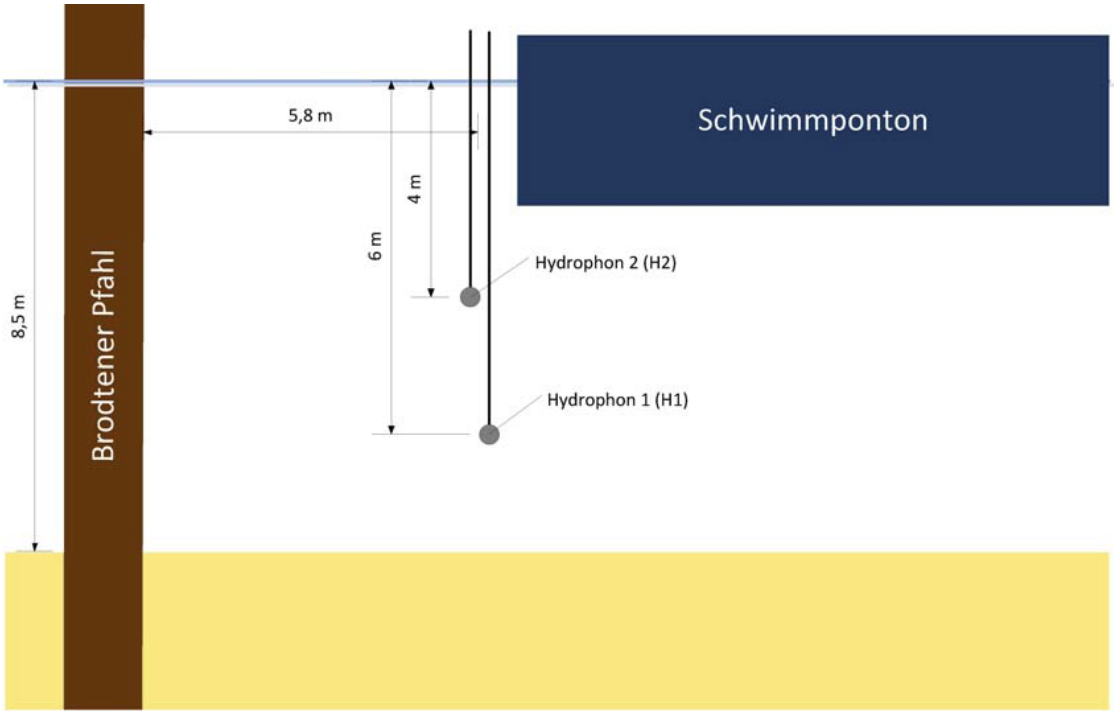

Figure 74: Measurement positions and distances of the IGB TUBS hydrophones from the Brodten pile

Schwimmponton	Floating pontoon
Hydrophon	Hydrophone
Brodtener Pfahl	Brodten pile

8.7.2 Evaluation procedure for underwater noise measurements

The sound attenuation effect was tested in 3 series of impacts respectively (100, 200 and 300 kNm impact energy) for each noise mitigation system. Each series of impacts consisted of 20 individual blows. The results of underwater noise measurement shown below refer exclusively to the series of blows with an impact energy of 300 kNm, as it is only at this impact energy that reference blows without NMS also exist for all NMS used.

Each of the 20 individual blows in the series of impacts was cut out of the signal sequences recorded for a length of 0.12 seconds. Figure 75 shows the signal time sequences of hydrophones H1 and H2 recorded on measuring day 4 at a reference impact with 300 kNm impact energy as an example. The impact pulse of the hammer is clearly recognizable after roughly 4 milliseconds and shows up as a maximum positive sound pressure of approx. 120 kPa in the sequence. A signal sequence of the reference impacts of this kind appeared characteristic on all measuring days. Furthermore, no basic difference can be detected between the hydrophones H1 and H2.

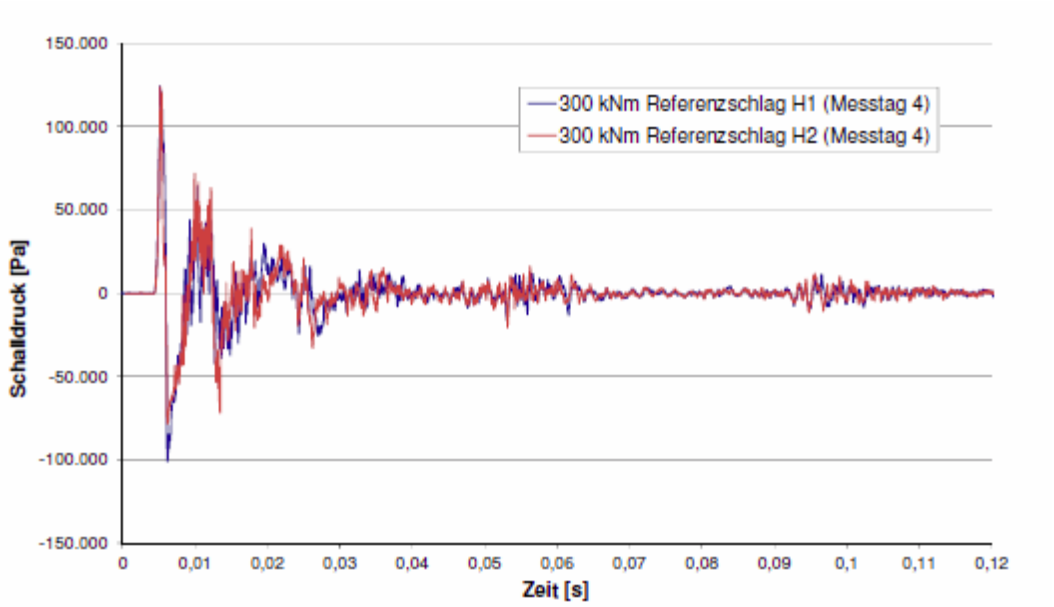

Figure 75: Comparison of signal time sequences of the hydrophones H1 and H2 at a reference impact of 300 kNm on the fourth measuring day

Schalldruck [Pa]	Sound pressure [Pa]
Zeit [s]	Time [s]
300 kNm Referenzschlag H1 (Messtag 4)	300 kNm reference impact H 1 (measuring day 4)
300 kNm Referenzschlag H2 (Messtag 4)	300 kNm reference impact H 2 (measuring day 4)

The SEL and the L_{Peak} were determined for every individual blow. The set value of p_0 = 1 µPa (dB re 1 µPa) was used as the reference value p_0 for waterborne sound.

The result of these calculations is shown separately for the hydrophones H1 and H2 in the following figure for the reference impacts on measuring day 4. An SEL of 194 dB and an L_{Peak} of 222 dB were established for both hydrophones. This diagram also reflects the extremely good reproducibility and comparability of the individual pile-driving blows.

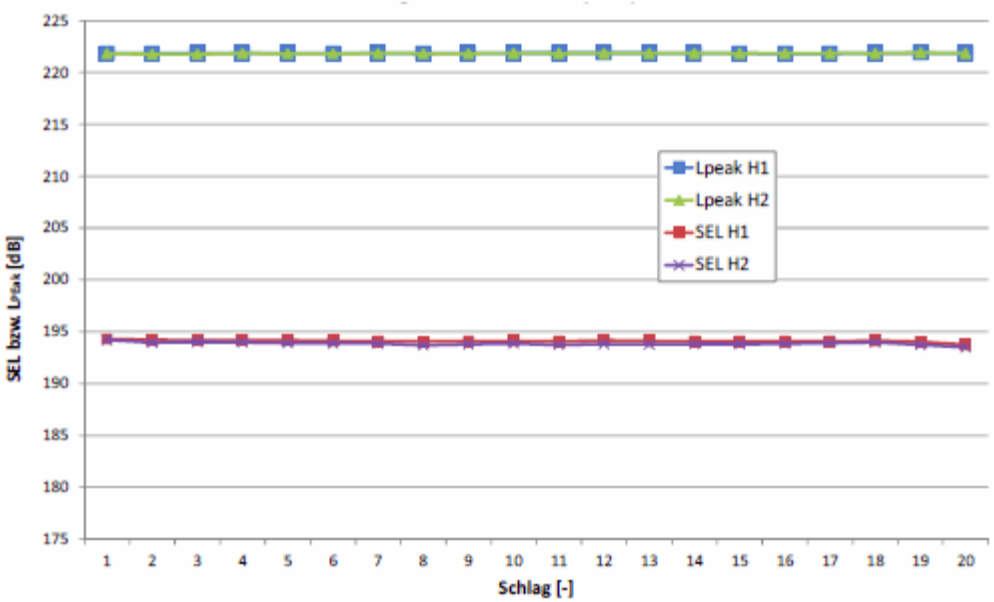

Figure 76: SEL and L_{Peak} determined for each individual impact (H1 and H2) with the reference impacts on measuring day 4

SEL bzw. Lpeak [dB]	SEL and Lpeak [dB]
Schlag [-]	Impact [-]
Lpeak H1	Lpeak H1
Lpeak H2	Lpeak H2
SEL H1	SEL H1
SEL H2	SEL H2

8.7.3 Results of underwater noise measurements

Using the level determination of the individual blows with an impact energy of 300 kNm described above, an assessment can be made of the attenuation potential of the individual systems. This evaluation is shown in Table 11. The average noise levels of hydrophone H1, which were determined from the individual blows, are given. The sound reduction of each system was related to the reference measurement carried out on the same measuring day.

System	L_{peak} [dB]	SEL [dB]	Reduction L_{peak} [dB]	Reduction SEL [dB]
Test day 1				
IHC NMS with 7 bar	206.0	184.2	13.6	7.6
IHC NMS without compressed air	206.0	184.8	13.6	7.0
IHC Reference	219.7	191.8		
Testtag 2				
Menck Firehose 1bar	208.3	183.6	13.7	10.9
Menck Firehose 2bar	210.4	184.8	11.6	9.6
Menck Reference	221.9	194.5		
Testtag 3				
Weyre Little Bubble Curtain	213.1	187.3	8.8	8.0
Weyres BEKA Jacket 7.9bar	204.8	179.6	17.0	15.7
Weyres BEKA Jacket 5.0bar	204.2	179.6	17.6	15.7
Weyres BEKA Jacket without compressed air	204.1	179.3	17.8	15.9
Weyres Reference	221.8	195.3		
Testtag 4				
HSD Middle	216.3	186.1	5.6	8.0
HSD Middle/Outer	213.9	183.3	7.9	10.8
HSD Inner/Middle/Outer	211.2	180.7	10.7	13.4
HSD Inner/Outer	214.5	182.3	7.4	11.8
HSD Outer	216.0	184.7	5.9	9.5
HSD Inner	216.2	185.1	5.7	9.0
HSD Inner/Middle	216.0	184.1	5.8	10.0
HSD Reference	221.8	194.1		

Table 11: Overall result of the IGB-TUBS underwater noise measurements in the near field (distance = 6.0 m) at an impact energy of 300 kNm

The levels of the reference measurements are approximately identical (approx. 222 dB) in the case of the Menck, Weyres and HSD systems (measuring days 2-4). A level that was 2 dB lower was only measured for the IHC system. A similar correlation results likewise when evaluating the third-octave analysis of the reference impacts (Figure 77). Here too it is evident that the SEL in the individual third octaves on measuring days 2 to 4 matches very well.

The sound reduction of the individual systems at a distance of 6 m from the pile is between 7.0 dB and 15.9 dB SEL.

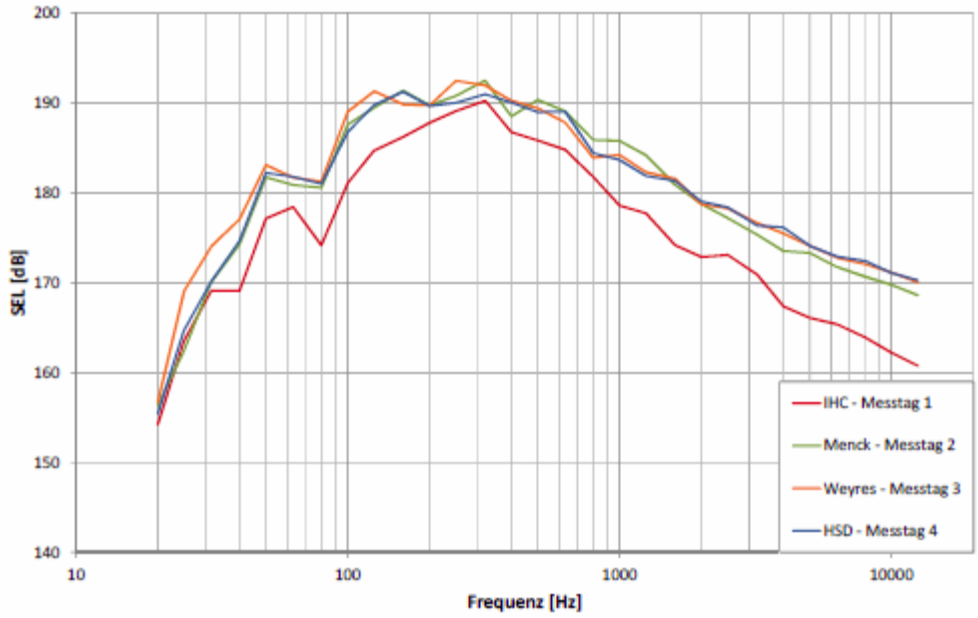

Figure 77: Third-octave analysis of the reference impacts over the 4 measuring days

Frequenz [Hz]	Frequency [Hz]
IHC-Messtag 1	IHC-Measuring day 1
Menck – Messtag 2	Menck – Measuring day 2
Weyres – Messtag 3	Weyres – Measuring day 3
HSD – Messtag 4	HSD – Measuring day 4

The following Figures 78 to 81 show the third-octave analyses when using the individual noise mitigation systems compared with the respective reference measurement (without system). Here the background area shown in white marks the noise mitigation produced with reference to the third octave. With the systems from IHC and Menck, maximum reductions of 20 dB and 18 dB are achieved, while 24 dB is achieved with the BeKa Jacket from Weyres and 23 dB with the Hydro Sound Damper (HSD) system.

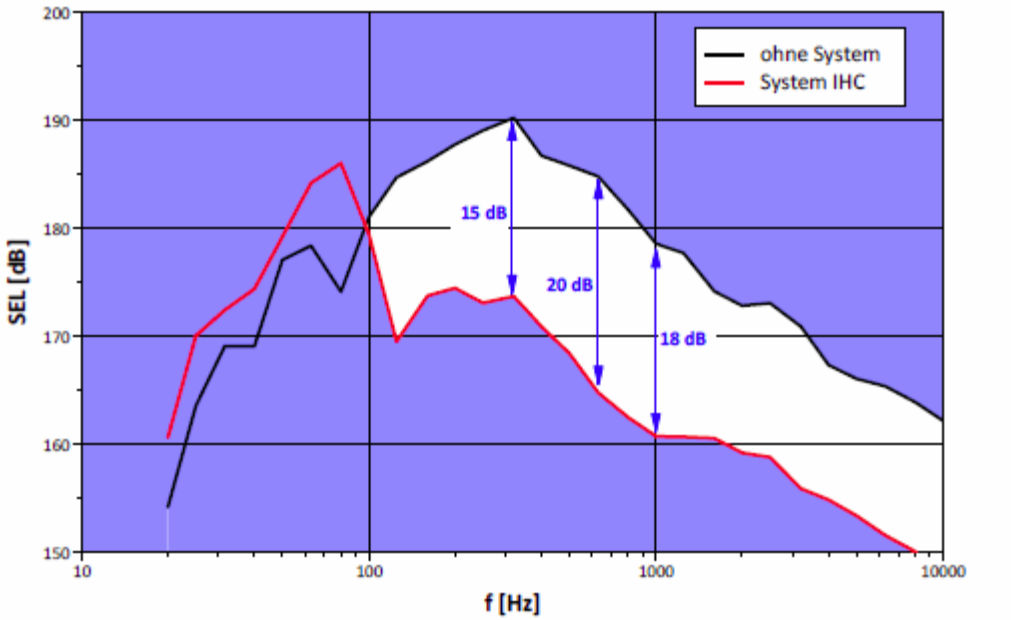

Figure 78: Third-octave analyses with the use of the IHC system (7 bar) and the reference measurement without noise mitigation (measuring day 1)

Ohne System	Without system
System IHC	System IHC

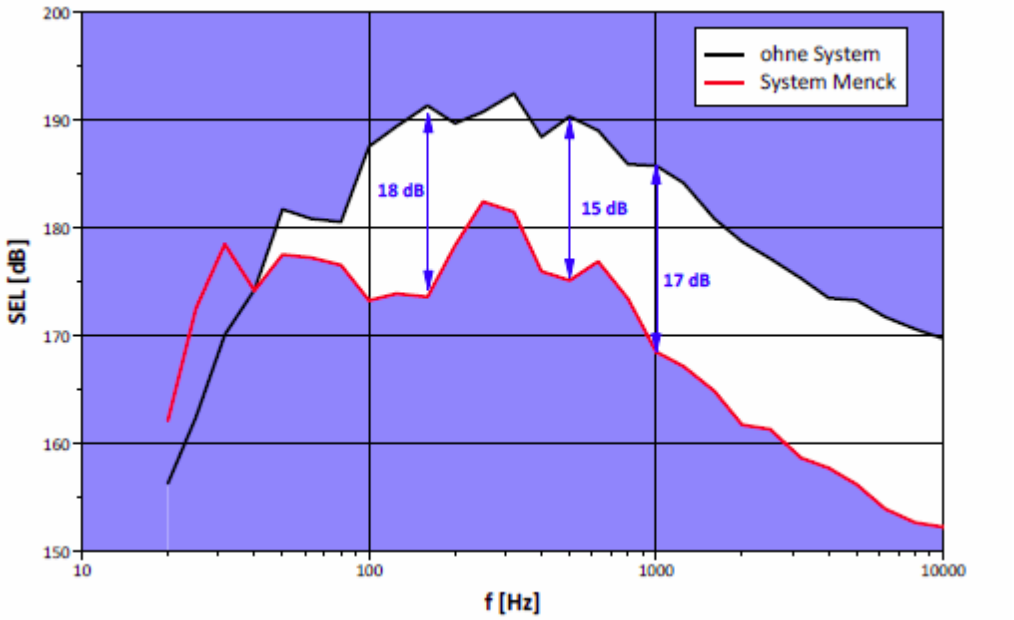

Figure 79: Third-octave analyses with the use of the Menck system (fire hose, 1 bar) and the reference measurement without noise mitigation (measuring day 2)

Ohne System	Without system
System Menck	System Menck

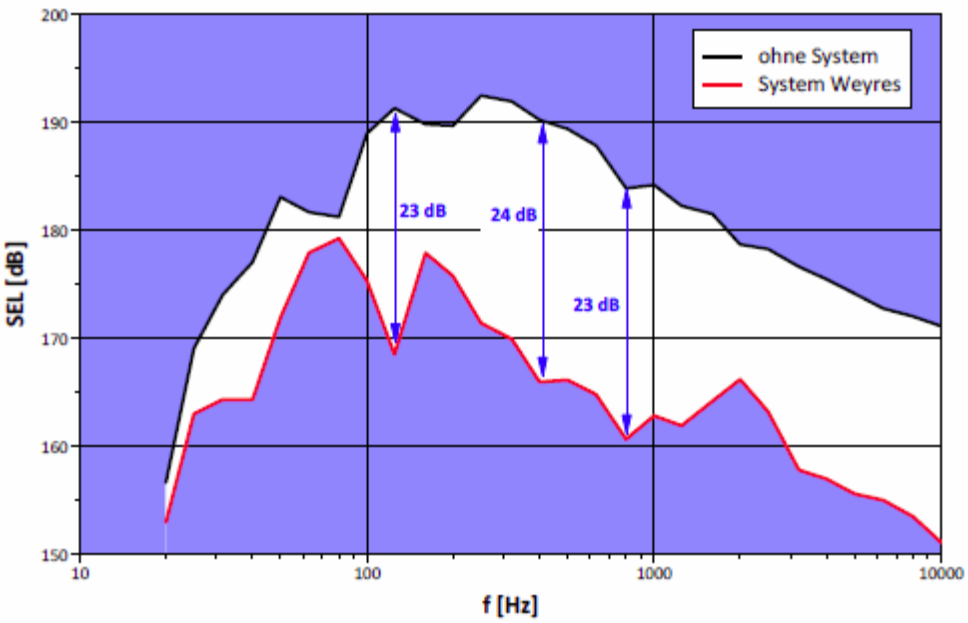

Figure 80: Third-octave analyses with the use of the Weyres system (BeKa Jacket, 0 bar) and the reference measurement without noise mitigation (measuring day 3)

Ohne System	Without system
System Weyres	System Weyres

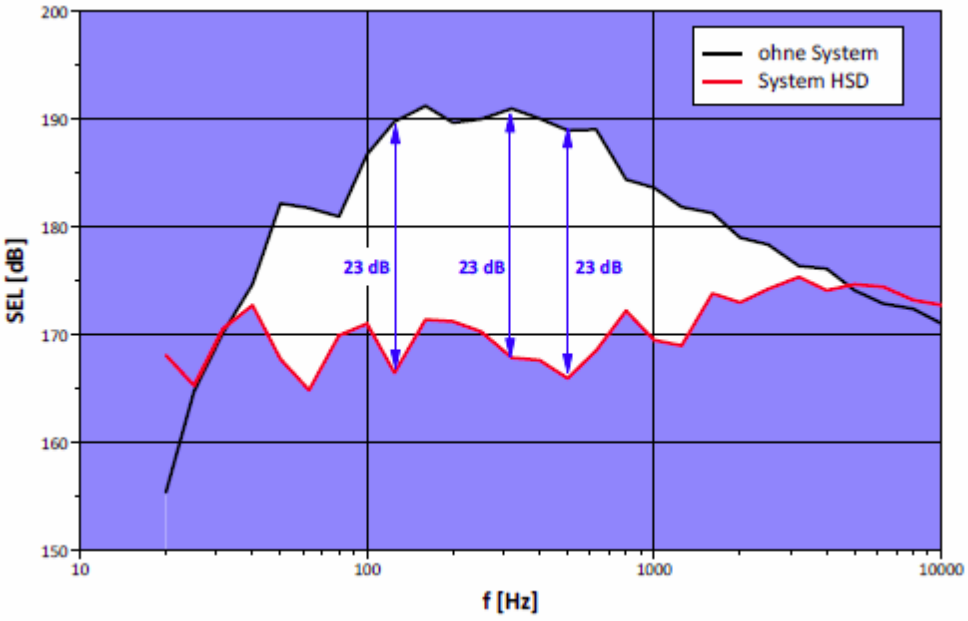

Figure 81: Third-octave analyses with the use of the HSD system (3 nets) and the reference measurement without noise mitigation

Ohne System	Without system
System HSD	System HSD

8.8 Comparison of far-field and near-field measurements

The near- and far-field measurements of underwater noise carried out during pile driving in the ESRa project with and without noise mitigation systems produce significant differences in some cases in the sound transmission loss (difference in single event exposure level with and without noise mitigation system - ΔSEL) measured in the near and far field. In the far field (distance 375 m to 750 m) the measurements are between 4.2 dB and 6.1 dB depending on the noise mitigation system used. In contrast to this, depending on the distance from the pile, values of 5.4 dB to 7.6 dB (distance 13 m) and 7.0 dB to 15.9 dB (distance 6.0 m) are produced for the sound transmission loss in the near field. The sound transmission losses measured for each noise mitigation system are summarised in Table 12 as a function of the distance from the pile. It is evident that, as the distance between measurement position and pile decreases, the sound transmission loss increases considerably. The reason for the increase in attenuation cannot be clearly explained at present. From a scientific viewpoint, this factor is highly interesting. Possible attempts at an explanation by the project partners go in two directions:

(1) as the distance from the pile decreases, the influence of a ground coupling or sound radiation from the sediment into the water is lessened and

(2) for acoustic measurements in the near field, not only the knowledge of the sound pressure p but also the knowledge of the particle velocity v is required, as the acoustic output in the near field is divided into an active component and a reactive component. Sound pressure measurements in the near field are thus associated with high levels of measuring uncertainty.

Both approaches have been the subject of contentious discussion by the project partners. The phenomena occurring could not be clarified conclusively. However, it can be put on record that the sound radiation of a pile to be driven is far from straightforward and further basic research is necessary to explain the above behaviour.

No.	System	Noise mitigation system	ΔSEL [dB] Difference with/without noise mitigation system		
			Near field		Far field
			Distance 6 m	Distance 13 m	Distance 375 – 750 m
1	1	IHC NMS with bubble curtain	7.6	7.3	5.6
2		IHC NMS without bubble curtain	7.0	6.4	5.1
3	2	Menck FHS with 1.0 bar	10.9	6.4	5.0
4		Menck FHS with 2.0 bar	9.6	5.8	4.4
5	3	Weyres LBC	8.0	5.4	4.2
6	4	Weyres BeKa 0 bar	15.9	6.9	5.9

7		Weyres BeKa 5 bar	15.7	6.8	5.9
8		Weyres BeKa 7 bar	15.7	6.8	6.1
9	5	Elmer HSD M Ring	8.0	6.2	5.0
10		Elmer HSD O Ring	9.5	6.9	4.2
11		Elmer HSD I Ring	9.0	6.2	5.4
12		Elmer HSD MO Ring	10.8	7.5	5.4
13		Elmer HSD MI Ring	10.0	6.8	4.9
14		Elmer HSD OI Ring	11.8	7.4	5.4
15		Elmer HSD MOI Ring	13.8	7.6	5.4

Table 12: Summary of the noise mitigation potentials (∆SEL) of the five noise mitigation systems tested, including variations, as a function of the distance between pile and measurement position. The measurements in the far field are used for ∆SEL median values over four measurement positions at a distance of between 375 m and 750 m, in the near field individual results.

8.9 Measuring uncertainties and tolerances

The hydrophones used and the geophone used have a high reproducibility of $\leq \pm$ 1 dB. Normally, however, in offshore field measurements, even when the sea is calm, non-systematic measuring uncertainty in the range of $\geq$ 2 dB is to be expected in the case of repeat measurements.

The measuring results shown in this section should be regarded as conservative observations of the noise mitigation potentials of the individual systems. Due to the median formation carried out by ITAP over up to four measurement positions in the far field, “rogue values” in the noise reduction (sound transmission loss), which may be due to external boundary conditions, are less strongly evaluated in a positive and negative direction.

9. Discussion of the results

The results from Section 8 give rise to the following three open points, which are to be dealt with in the discussion below:

1. Comparison between the *Brodten pile* (location for ESRa) and other project locations

2. State of the science in the field of noise mitigation concepts and noise mitigation systems

3. How can the noise mitigation systems tested from ESRa be improved?

The first point aims to clarify whether the *Brodten pile* is fundamentally suitable or not on account of its boundary conditions for a round-robin test of noise mitigation systems. In the second part (Section 9.2), the noise mitigation potentials of the systems tested from ESRa are compared with those from the literature. In the last part (Section 9.3), hypotheses are generated from a scientific viewpoint as to how the existing systems could be improved for future use.

9.1 Comparison between the Brodten pile (location for ESRa) and other project locations

9.1.1. Boundary conditions Brodten pile

The Brodten pile has an overall length of approx. 78 m, of which 65.0 m are in the sediment (embedded length), 8.5 m in the water and approx. 5.5 m of the pile protrudes above the waterline. These conditions are generally unusual. In addition, the pile has firmly coalesced with the sediment and it is not expected that the pile will be driven further in by further pile driving.

The water depth at a distance of 1 km surrounding the pile is between 5.4 m and 11.4 m, so that a very flat area of water close to the shore must be assumed.

In Figure 82 the third-octave spectra of pile-driving operations in the construction of the offshore wind farms alpha ventus (North Sea) [5], Baltic II (Baltic Sea) [25] are shown compared with the measurement data on the test pile *Brodten pile* in the far field (several 100 metres distant). The thin lines each represent individual measurements, while the related wider line represents the median of the individual measurements. In the measurements shown, the boundary conditions were completely different, i.e. different pile lengths, pile thicknesses (wall thickness), impact energies, water depths etc.

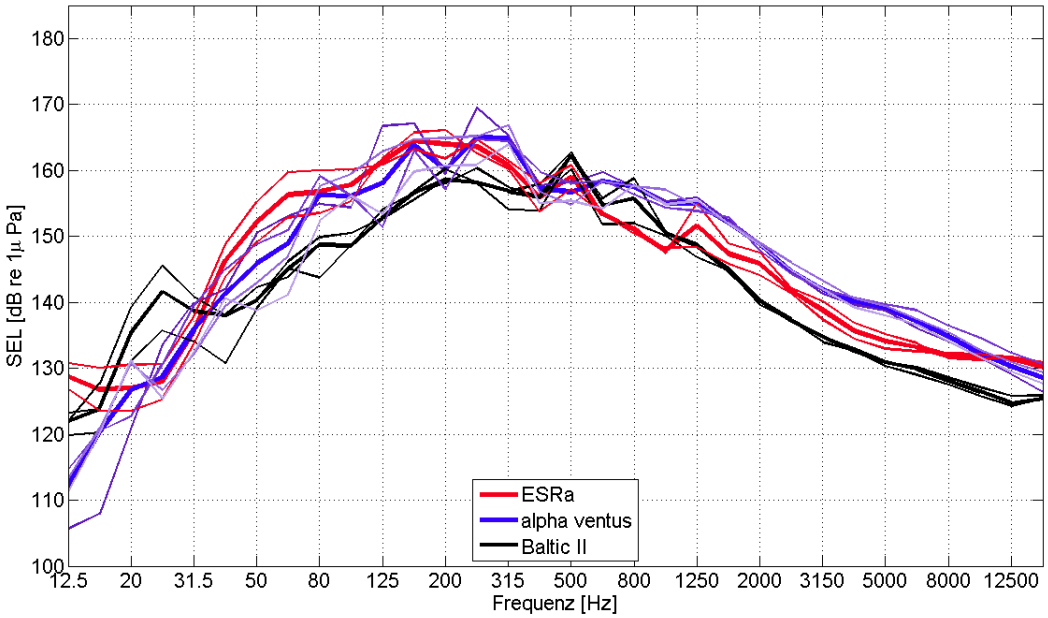

Figure 82: Represented are the third-octave spectra at distances of between 500 m and 1,000 m from the respective pile during different pile-driving operations. The thin coloured lines each represent individual measurements, while the thick coloured lines identify the median values.

Frequenz [Hz]	Frequency [Hz]

In Figure 83 a third-octave spectrum (model spectrum) averaged from several measurements by ITAP GmbH in the far field is shown, which is used for forecasting purposes.

The most energy during the pile-driving operations in the far field is to be found in the frequency range between 100 and 500 Hz (approx. 750 m). There are no greater differences whatsoever in the third-octave spectra between the pile-driving spectra represented in Figure 82 and in relation to the model spectrum from Figure 83.

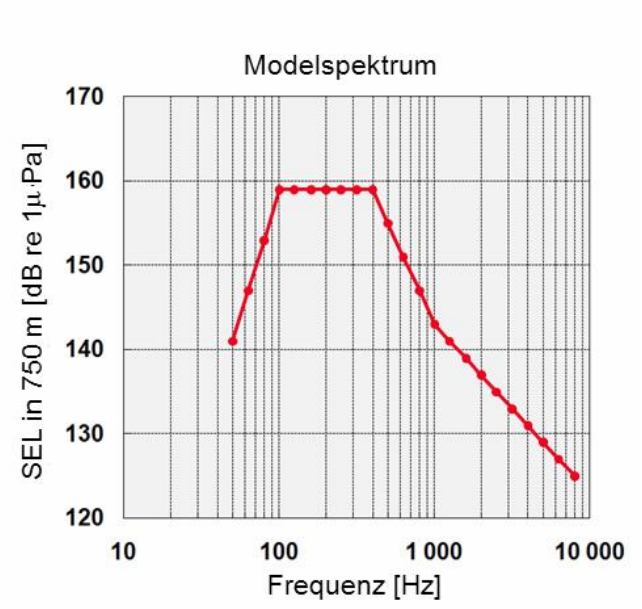

Figure 83: Model spectrum for a pile-driving impact in the far field for forecasting purposes. The idealized model spectrum is based on several measurements with various pile-driving activities by ITAP GmbH

Modelspektrum	Model spectrum
Frequenz [Hz]	Frequency [Hz]

9.1.2 Ground coupling (“preblow”)

In Figure 84, the time signal of one pile-driving acoustic impulse with and without a noise mitigation system respectively is shown at a distance of 750 m (MP1.1).

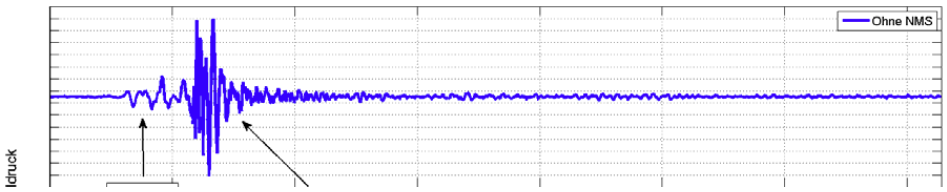

Figure 84: Time function (time signals) of an underwater noise pile-driving pulse at a distance of 750 m from the test pile and 1.8 m from the sediment, with a pile-driving energy of 300 kJ used.

Schalldruck	Sound pressure
Zeit [s]	Time [s]
Ohne NMS	Without NMS
Mit NMS	With NMS
Preblow	Preblow
Ramschlag	Pile-driving impact

After approx. 0.125 s it is clear in the top image (without noise mitigation system) that the portion of the sound (pile-driving impact) arriving purely via the water is present at the hydrophone in pulse form. In addition, a second component

exists, which is virtually sinusoidal (about 70 – 80 Hz) and arrives at the hydrophone approx. 0.05 s before the “actual” pile-driving impact.

In the literature [e.g. [9]], it was previously assumed that this component is produced on vibrations in the sediment due to the pile-driving impact on the pile. The vibrations of the sediment likewise connect to the water. Since the speed of sound *v* of the pile (steel, *c* between 2,000 and 5,000 m/s^2) and of the sediment (*c* between 1,600 and 2,000 m/s^2) is higher than the speed of sound in the water (*c* ~ 1,500 m/s^2) , this component reaches the hydrophones in the “far field” faster than the pure waterborne sound portion (pile-driving impact). This phenomenon is often described as “preblow” and characterises the ground coupling between the pile and the sediment. This effect is observed in all pile-driving operations in the North Sea and the Baltic [9]. The amplitude of the “preblow” in the case of piles that can still be driven in only amounts to approx. 1/10 of the amplitude of the pure pile-driving impact, however. In this case, the factor without noise mitigation system is only around 2.5 to 3, i.e. the “seismic” component is particularly pronounced in the case of this pile. This result was likewise measured in measurement at the *Brodten pile* in 2006.

In the lower image in Figure 84, the time function is represented with a noise mitigation system. The time sequence of the pile-driving pulse resembles that of the reference condition (without noise mitigation system). It is evident, however, that the pure underwater noise portion is considerably reduced in amplitude by the noise mitigation system. By contrast, the “seismic” component (ground coupling or “preblow”) remains virtually the same.

The time signal of the geophone (vibrations of the sediment) at the measurement position MP5.5 (13 m distant from the pile) is represented in Figure 85.

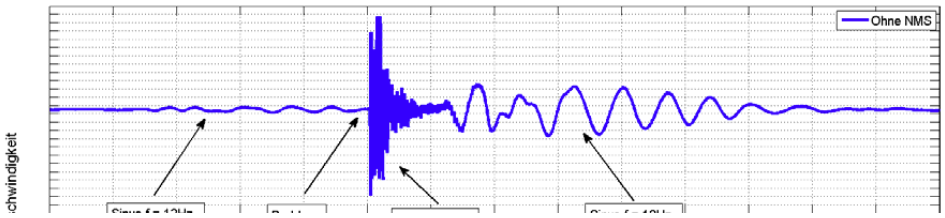

Figure 85: Time function (time signals) of the geophone (vibration) of a pile-driving pulse at a distance of 13 m from the test pile at the sediment with a driving energy of 300 kJ used.

Schwinggeschwindigkeit	Vibration speed
Zeit [s]	Time [s]
Ohne NMS	Without NMS
Mit NMS	With NMS
Sinus f – 12 Hz	Sinus f – 12 Hz
Preblow	Preblow

Ramimpuls	Pile-driving impact

In a comparison of Figure 84 (underwater noise in the far field) and Figure 85 (vibration of the sediment in the near field), it is clear that the vibration time signal is much longer. At the beginning and at the end of the time signal of a pile-driving impact, virtually sinusoidal long vibrations appear with a frequency around 12 Hz upon sediment vibration. The “actual” pile-driving pulse is roughly comparable with that of the underwater noise signal. It is assumed that the sinusoidal 12 Hz vibration is an eigenmode of the pile, which is propagated in the direction of the sediment upon the pile-driving impact (first sine oscillation before the actual pile-driving pulse) and is reflected at the end of the pile (second sine oscillation after the actual pile-driving pulse).

In the results of the noise reduction potentials of all noise mitigation measures tested in this study (Section 8.6), negative attenuations arise due to the noise mitigation systems in the range $63 < f < 100$ Hz. This effect is to be attributed to the ground coupling, i.e. the sound radiation from the sediment into the water. As investigations in 2006 [9] have already shown, the ground coupling at the Brodten pile is particularly strong. This is probably the result of the great penetration depth of the pile and the fact that the pile has coalesced with the sediment. A further influence on the increased sound radiation above the ground could be the additional compression of the sediment around the pile due to the static masses of the noise mitigation systems installed. In Figure 86, therefore, the difference between the third-octave spectra with and without noise mitigation system of the vibration speed is represented for each of the four test days. It is clear that on the first three days the sediment vibrations in the frequency range $63 < f < 100$ Hz likewise exhibit an increase of up to 5 dB with noise mitigation system. This increase with a very similar amplitude is also found in the difference spectra of the underwater noise measurements for the measurement systems tested on the first three days (IHC NMS, Menck FHS and Weyres BeKa Jacket), Figure 61. All the systems tested impose a not inconsiderable static load on the sediment around the pile. For the fourth measuring day, on the other hand, a difference in the vibration speed with and without noise mitigation measure of up to – 12 dB resulted. The system tested was the Elmer HSD system, which has a much smaller static mass than the other systems. Similar results are also obtained for the Weyres LBC, which likewise has a smaller mass than the other systems. The differences between with and without noise mitigation systems in the underwater noise (Figure 61) are likewise smaller for both the Elmer HSD system and the Weyres LBC than for the other systems. It can be concluded from this that the static mass of the noise mitigation system used and the associated static load transmission into the sediment may influence the ground coupling and ground radiation. Similar results can be observed in the use of a steel pipe as noise mitigation system in the studies from 2006 [9].

It should thus be assumed that the strong ground coupling in the present investigations is caused by the great penetration depth of the pile including coalescence and the static preloading of the noise mitigation systems used.

It can thus assumed that the ground coupling at the Brodten pile is clearly more strongly pronounced than in the case of piles which can still be driven deeper in deeper water. For this reason the noise mitigation potentials in the broad-band single event exposure level of the underwater noise measurements in the far field (Table 10 in Section 8.6.1) are compared with the noise mitigation potentials measured in the near field (MP5.1; Section 8.6.2) in Table 13. Since the ground coupling is low-frequency, the noise mitigation potentials in the far field exclusive to the low-frequency range (f < 125 Hz) are also represented in addition to the aforementioned variables.

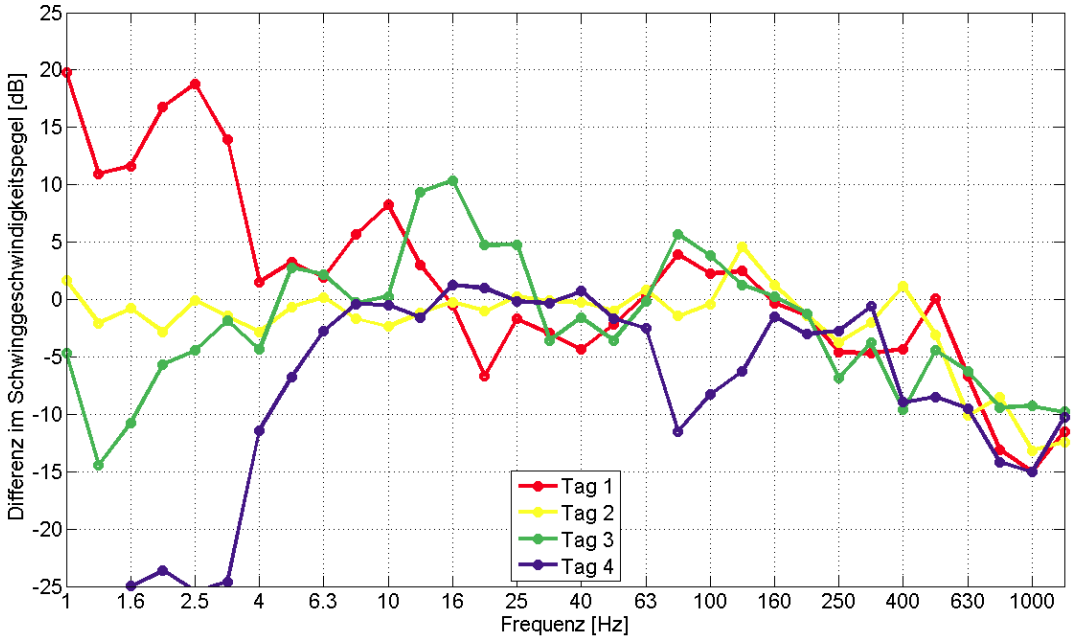

Figure 86: Attenuation of the vibration speed level (vibrations in the sediment; at a distance of 13 m from the pile with and without noise mitigation system on the four investigation days (MP5.5). On days 1 and 2 the same measurement position was used. On days 3 and 4, due to the different position of the stilt pontoon in front of the pile, the positions were changed. (A vibration speed of 10 mm/s corresponds to a vibration speed level of 140 dB).

Differenz in Schwinggeschwindigkeitspegel [dB]	Difference in vibration speed level [dB]
Frequenz [Hz]	Frequency [Hz]
Tag	Day

It is clear from Table 13 that without a possible ground coupling (column 5), i.e. exclusive of all frequencies < 100 Hz, the noise mitigation potentials rise **by 2 to 3 dB** for each system tested. This is a purely theoretical maximum estimate of the influence of the ground coupling. In column 6 of Table 13, the noise mitigation values measured (SEL broad-band) in the near field (MP5.1, 13 m distant) are represented. Due to the small distance between pile and measurement position, the influence of a possible ground coupling should also

be reduced. The noise mitigation values are higher by up to 2.0 dB than in the far field over the entire frequency spectrum (Table 13, column 4).

It can be assumed from this that the ground coupling a) is low-frequency by nature and b) can exert an influence of up to 3.0 dB on the noise reduction of noise mitigation systems in this case.

The influence of the ground coupling is normally much smaller and is only higher in individual third-octave bands, but in broad-band terms there are no significant influences during the pile-driving process (at the beginning and end). This is confirmed by measurements on a pile in the construction of the Baltic II wind farm, Figure 87.

No.	System	Noise mitigation system	ΔSEL [dB] Difference with/without noise mitigation system		
			12,5 – 16,000 Hz	125 – 16000 Hz	12,5 – 16,000 Hz
			Median over MP1.1 – MP4.1 (Far field)		MP5.1 (Near field)
1	1	IHC NMS with bubble curtain	5.6	8.7	7.3
2		IHC NMS without bubble curtain	5.1	8.1	6.4
3	2	Menck FHS with 1.0 bar	5.0	7.2	6.4
4		Menck FHS with 2.0 bar	4.4	6.5	5.8
5	3	Weyres LBC	4.2	5.3	5.4
6	4	Weyres BeKa 0 bar	5.9	8.2	6.9
7		Weyres BeKa 5 bar	5.9	8.1	6.8
8		Weyres BeKa 7 bar	6.1	8.3	6.8
9	5	Elmer HSD M Ring	5.0	6.6	6.2
10		Elmer HSD O Ring	4.2	6.7	6.9
11		Elmer HSD I Ring	5.4	8.0	6.2
12		Elmer HSD MO Ring	5.4	7.2	7.5
13		Elmer HSD MI Ring	4.9	7.4	6.8
14		Elmer HSD OI Ring	5.4	7.0	7.4
15		Elmer HSD MOI Ring	5.4	7.5	7.6

Table 13: Summary of the noise mitigation potentials of the five noise mitigation systems tested, including variations, as a median over the far field measurements (MP1.1 to MP4.1). In addition, the mitigation potentials are represented without a possible ground coupling in the far field in the frequency range of 125 Hz upwards, and measured in the near field at the position MP5.1.

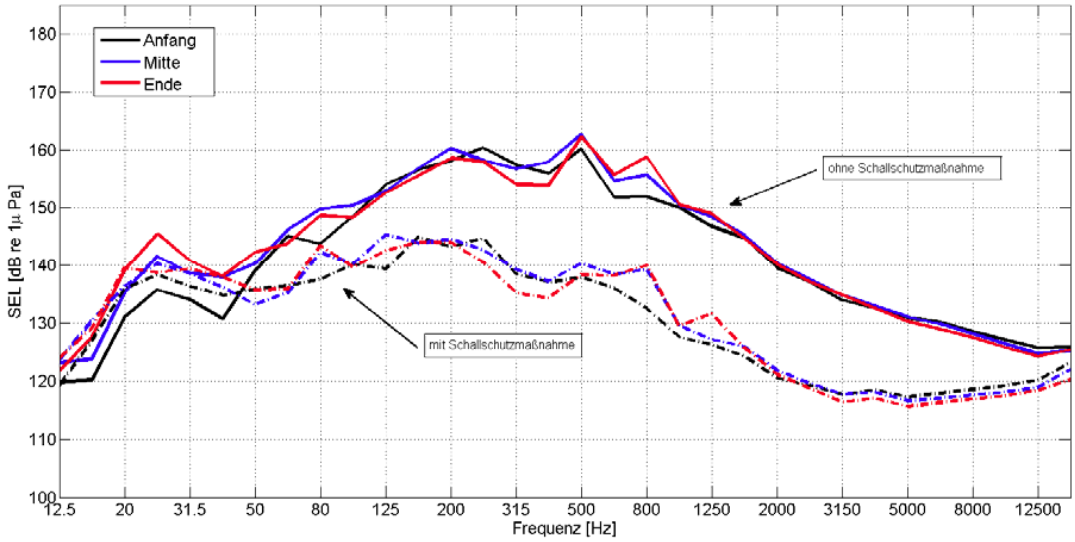

Figure 87: Third-octave spectrum during pile-driving operations at the Baltic II wind farm on a pile with and without a noise mitigation system (bubble curtain). The spectra are represented at the start of the grounding (i.e. introduction depth of a few metres), in the middle and at the end of grounding (i.e. scarcely any or no advance in pile driving).

SEL [dB re 1µPa]	SEL [dB re 1µPa]
Frequenz [Hz]	Frequency [Hz]
Anfang	Start
Mitte	Middle
Ende	End
Mit Schallschutzmassnahme	With noise mitigation system
Ohne Schallschutzmassnahme	Without noise mitigation system

It is evident that, when a noise mitigation system is used (here a bubble curtain), a ground coupling develops in the course of grounding around f = 80 Hz. Due to the small static mass of the noise mitigation system, the effect is in the range of 1 to 1.5 dB.

9.1.3 Comparison of an ESRa noise mitigation system at different locations

In the context of the Dutch research project FLOW (Far Large Offshore Wind), the IHC NMS was used by RWE Innogy GmbH at two North Sea locations (North Sea East and Ijmuiden) in collaboration with the IHC company and TU Delft when pile-driving the met masts there [26].

Both met masts have a diameter of 3.35 m at a water depth of 25 m. An IHC S800 hammer was used. The NMS has an outer diameter of 4.57 m. The impedance layer had roughly the same dimensions as for ESRa, but in contrast to the system for ESRa the two steel sheets of the NMS were acoustically decoupled by plastic holders.

The measuring results for the broad-band SEL are shown in Figure 88. Reductions of 9 dB are achieved for the location North Sea East and 11 dB for the location Ijmuiden. It should be noted with regard to the comparison that the pile for the North Sea East location was able to become embedded for several weeks before the NMS was used as part of a restrike test.

A comparison of the results obtained here shows very good correspondence with the measurement values of the NMS at ESRa if the ground coupling, in accordance with the recommendation in the previous section, is excluded at 2-3 dB (Table 13, column 5). If the improved decoupling of the two steel sheets of the NMS is assessed in addition at -1 dB, the corrected results of ESRa at ΔSEL = 8.7 dB lie between the corrected values of the FLOW test of 8 – 10 dB.

The tests under FLOW were thus able to confirm and validate the results of ESRa indirectly.

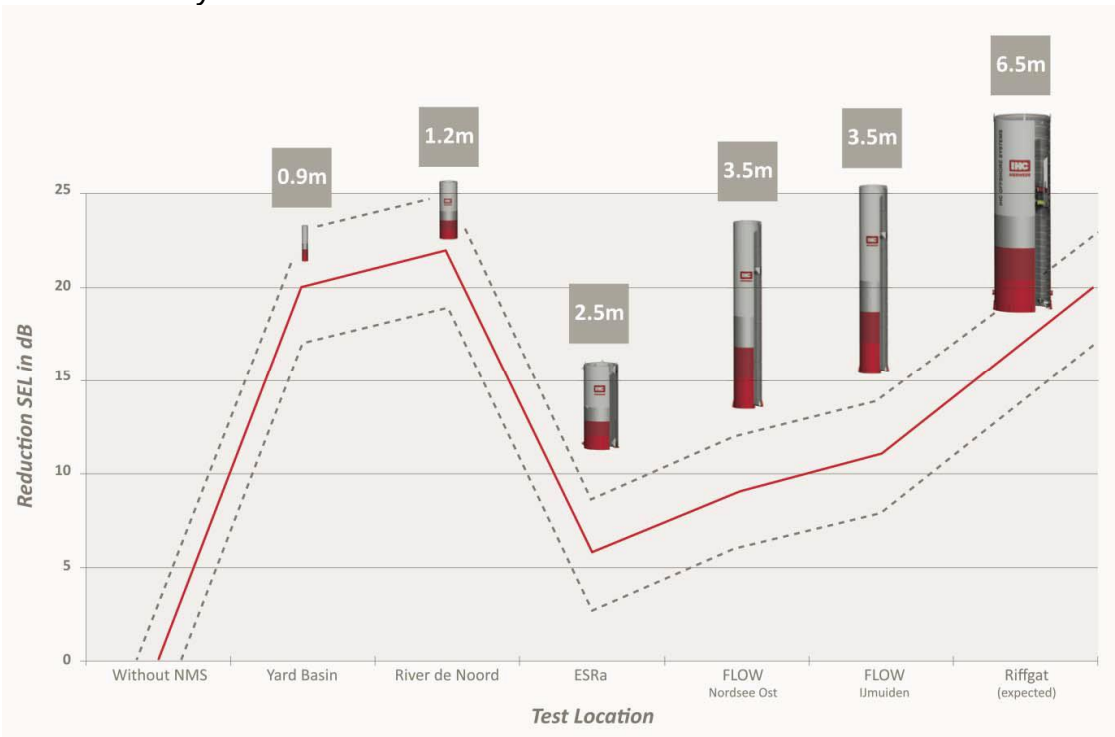

Figure 88: ΔSEL reductions achieved with the IHC NMS at different locations (by courtesy of IHC)

9.1.4. Influence of the water depth

Another striking feature in the frequency-engendered noise reduction potentials of the individual noise mitigation systems (Figure 61) is the almost identical attenuation of the underwater noise by about 10 dB, regardless of the system, at a frequency of about 160 Hz. An exception to this is the Weyres Little Bubble Curtain (LBC).

It is known from theory that the continuous noise radiation in water is dependent on the speeds of noise of the sediment and of the water, as well as the level of the water:

$$f_g = \frac{C_{water}}{4h} \sqrt{\frac{1}{1-\left(\frac{C_{water}}{C_{sediment}}\right)}} \quad [Hz] \qquad \text{Equation 9.1}$$

where:
f_g is the limit frequency for the radiation of noise under continuous excitation [Hz]
h is the water depth [m]
C_{water} Speed of noise in water [m/s]
$C_{sediment}$ Speed of noise in sediment [m/s]

Strictly speaking, the approximation formula 9.1 applies only to continuous excitation in water, and not to pulsed excitation. For this reason, noise below the limit frequency f_g is to be measured in the case of pile-driver impacts (e.g. Figure 44).
If the following peripheral conditions are taken into account: Water depth h = 8.5 m (measured), C_{water} = 1485 m/s and (estimated) $C_{sediment}$ = 1600 m/s, then, according to Equation 6.1 a limit frequency of approx. 163 Hz is derived.

All the noise mitigation systems referred to above, with the exception of the Weyres LBC, have a more or less rigid connection between sediment and water surface (steel tube, hoses, or nets). It may be considered that, due to the pulse-form excitation caused by the pile-driving, these noise mitigation systems are excited to a natural vibration (resonance) with f_g. It may therefore be considered that the noise mitigation around the 160 Hz mark is not attributable to the means of effect of the individual noise mitigation measures, but rather caused by the given peripheral conditions of the pile (water depth, speeds in sediment and water), and the connection between the water surface and sediment. This hypothesis could explain the almost identical attenuation of all the noise mitigation measures tested.

9.1.5 Interim result

The following conclusions may be drawn from the discussion hitherto:

- Pile-driving spectra with the *Brodten Pile* are similar to those at comparator locations
- *Brodten Pile*: Earth coupling at 80 < f < 100 Hz is strongly marked
- First local maximum in frequency-dependent attenuation with all NMS (except for LBC) at f = 160 Hz is present.

From this the following hypotheses can be derived:

Hypothesis 1: Attenuation at f = 160 Hz is attributable to the water depth and the NMS used.
Hypothesis 2: Noise mitigation systems “work” in close proximity, i.e. no attenuation of the soil coupling is to be anticipated

9.2 State of the science in the sector of noise mitigation concepts and noise mitigation systems

9.2.1 Noise mitigation systems in overview

Figure 89 illustrates the frequency-dependent reduction (noise throughput attenuation) of the pile due to the BeKa shell (ESRa Project) with internal bubble curtain, at 7.9 bar, in comparison with the large bubble curtain in use at Fino3 [12], the small staged bubble curtain at alpha ventus [5], a bubble curtain on the Baltic II project, and a tube with foamed material coating (UFO Plan research project) on the *Brodten Pile* [9]. (A more detailed description of the noise mitigation systems being used can be obtained from the secondary literature).

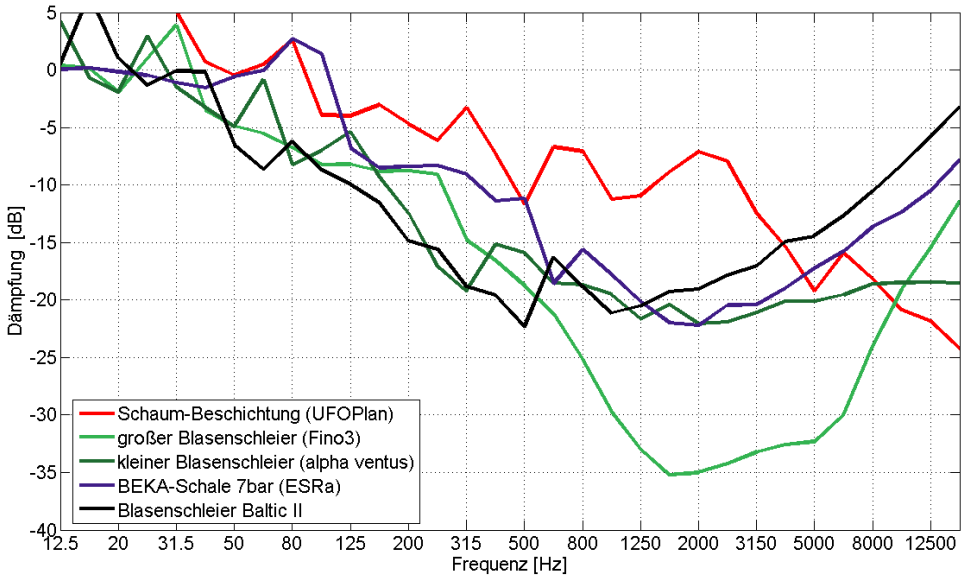

Figure 89: Frequency-dependent reduction in pile-driving noise due to different noise mitigation measures from the literature [5], [9], [12], and from the present research project.

Dämpfung [dB]	Attenuation [dB]
Frequenz [Hz]	Frequency [Hz]
Schaum-Beschichtigung (UFOPlan)	Foam coating (UFO Plan)
Grosser Blasenschleier (Fino3)	Large bubble curtain (Fino3)
Kleiner Blasenschleier (alpha ventus)	Small bubble curtain (alpha ventus)
BEKA-Schale 7bar (ESRa)	BEKA shell 7bar (ESRa)
Blasenschleier Baltic II	Baltic II bubble curtain

In the frequency range between 60 and 100 Hz, clear differences arise between the BeKa shell and the foam coating on the one hand, and the various different bubble curtains (FINO3, alpha ventus, and Baltic II). The foam coating was likewise tested in 2006 as part of a research project on the Brodten Pile, under conditions close to those in this project. With both the systems demonstrated on the Brodten Pile a “negative” attenuation is exhibited in this frequency range; i.e. there is more energy present in the water with this noise mitigation system than without. This is attributable to a strong ground feedback. By contrast, the bubble curtains referred to above have an attenuation of 5 to 10 dB in both the North Sea and the Baltic.

In the frequency range between 125 and 500 Hz, the various different bubble curtains likewise exhibit a higher noise reduction (5 to 10 dB) than the BeKa shell.

At higher frequencies, with the large bubble curtain at FINO3, the reduction increases to as much as 35 dB. By contrast with this, the noise mitigation potential with the BeKa shell and the other bubble curtains used in this frequency range is of the order of 20 dB, and is therefore comparable.

The reduction in the single event level (SEL) with the small bubble curtain at alpha ventus amount in broad band to 8.0 to 12.0 dB, and with the large bubble curtain at FINO3 to 10.0 to 14.0 dB. The small guided bubble curtain tested at ESRa (Weyres LBC) exhibits a reduction potential from 4.0 to 5.0 dB. These values, at least up to the LBC, are heavily dependent on the prevailing current, however, since in both cases the bubble curtains were not guided; i.e. they were caused to drift by the current. This means that under the most unfavourable weather conditions it may happen that a sharp reduction in underwater noise takes place on one side of the pile (in the direction of the current), while there is no measurable reduction on the opposite side. In addition to this, the decreasing water pressure towards the surface causes a v-shaped profile among the bubbles.

Another difference between the bubble curtain in the BeKa shell or the LBC respectively and the other bubble curtains referred to earlier is that the bubble curtain in the BeKa shell or the LBC is located directly at the pile and is guided to a limited width of about 20 to 30 cm. By contrast with this, bubble rings formed at the water surface at FINO3 and alpha ventus, several metres in diameter, which in part were at a perceptible distance from the driven pile.

There are only a small number of findings with regard to the effect of the bubble curtains and their essential variables (e.g. air volume, bubble size, and bubble distribution) [2]. It is suspected, however, that the directed noise energy which is radiated inwards in the bubble curtain is radiated outwards without specific direction by multiple reflections, and therefore has the effect of a reduction in the noise energy. It seems probable that the multiple reflection on several adjacent air bubbles in the water also causes wavelengths to be reflected, which are related to the width of the bubble curtain. In other words, the more the bubble curtain broadens out in a v–shape towards the surface of the water, the lower

the frequencies which can be attenuated. It is not possible at the present time, however, to conduct an exact analytical calculation of this phenomenon.

Added to this is the fact that the air bubbles in the water “take effect” predominantly on the acoustic pressure and not on the speed, with the result that it may be assumed that the effect of a bubble curtain is greater at some distance (close to far field radiation conditions) than in the close field range.

In order to improve the noise mitigation potential (broad-band) of the noise mitigation systems tested, a higher attenuation of the hydro-noise in the 100 to 500 Hz range is required, since it is in this range that the most energy is contained in respect of pile-driving noise; Figure 83.

9.3 How can the noise mitigation systems tested from ESRa be improved?

From Figures 51 to 60 there can be seen, for each noise mitigation system tested, with the exception of the Weyres LBC system, striking minimum values in the difference spectrum of the underwater noise measurements with and without a noise mitigation system. This means that at these frequencies the individual noise mitigation system has resulted in a particularly high reduction in the underwater noise. The question which arises is whether the dimensioning of the individual systems has an influence on these frequencies and, if so, what influence. For this reason, Figure 90 takes the example of the IHC NMS system to illustrate the passage of the noise through the double-walled tube.

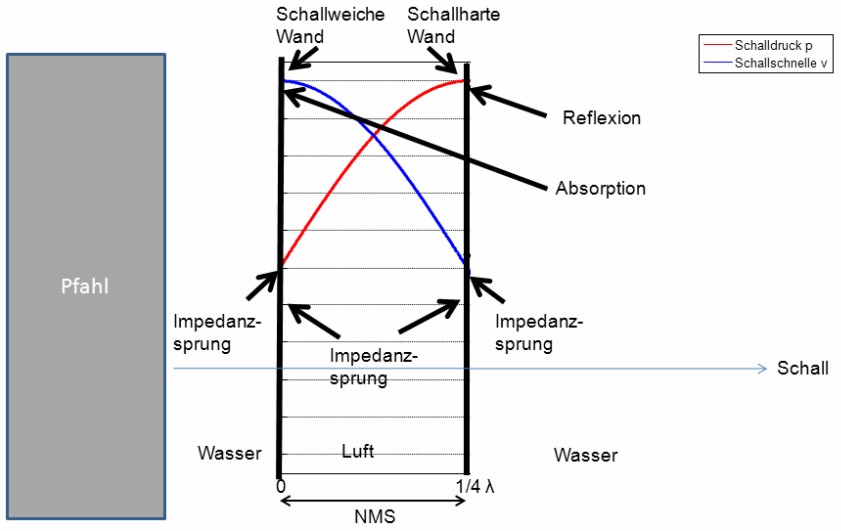

Figure 90: Schematic representation, using the example of the IHC NMS system. The noise is irradiated out from the pile and runs through, in succession, the media of water, steel, air, steel, and then water again.

Pfahl	Pile
Schallweiche Wand	Sound absorbing wall
Schallharte Wand	Sound reflecting wall
Schalldruck p	Acoustic pressure p
Schallschnelle v	Sound speed v
Reflexion	Reflection
Absorption	Absorption
Impedanz sprung	Impedance jump
Schall	Noise
Wasser	Water
Luft	Air
NMS	NMS

Next, an propagation of noise outwards from the pile into the water takes place. The sound waves then impinge on a steel tube (the inner tube of the IHC NMS

system) and therefore on a jump in the sound characteristic impedance Z of the medium. A second impedance jump occurs at the transition from the steel tube to the interior air chamber between the double-walled tube. Further impedance jumps occur at the transition from air to steel tube (outer tube) and steel tube to water. The principle is known from theory that at every impedance jump in the dissemination medium a part of the noise is reflected, and a part is transmitted [e.g. [28], [3]]. At the impedance jump from the steel tube (inner tube) to air, it is to be assumed, because of the different materials, that this involves a soft sound termination, and the reflection factor will accordingly lie in the range of -1. This means that the speed v is at its maximum at the transition from steel to air, and the acoustic pressure p is at its minimum. The transition from air to the outer steel tube is a hard sound termination. The reflection factor is close to 1. This means that the acoustic pressure p is at its maximum, and the sound speed v is at a minimum. In the situation in which the distance interval between the two tubes corresponds to a quarter wavelength (*lambda*/4), the acoustic pressure is at its maximum at the outer steel tube and is strongly reflected (hard sound termination), or only slight fractions of the sound are transmitted.

It can be derived from a rough calculation from the frequency-resolved difference spectra (one-third octave spectra), and the approximate data from the manufacturers with regard to the thicknesses of their noise mitigation systems, that on every occasion on which a quarter wavelength (*lambda*/4) corresponds to the interval between two impedance jumps (first soft sound, then hard sound) in the noise mitigation system (e.g. the distance between the tubes with the IHC NMS system or with the BeKa shell), a local maximum is present in the noise reduction.

It can therefore be assumed that, due to the various different impedance jumps and the fact that first a soft sound and then a hard sound termination is applied in the noise mitigation system, a type of *lambda*/4 resonator comes into being, which minimizes the passage of the noise at certain specific frequencies.

9.4 Outcome

In Section 9.3 a possible explanatory formulation was presented with regard to the noise mitigation systems tested. Due to the small number of experiments and variations within this project, the remarks made hitherto can only be drawn on as a hypothesis or an attempt at an explanation, and more extensive systematic investigations and variation are required in order to optimize noise mitigation in pile-driving.
In the event that the principle of a *lambda*/4 resonator is confirmed by extensive experimentation, the dimensioning of the noise mitigation measures is to be optimized in relation to the individual frequency range with the highest energy input when pile-driving in water. In addition to this, by the suitable introduction of additional materials, such as porous absorbers or materials with different sound characteristic impedances (sliding impedance adaptation), the noise passage can be minimized by the noise mitigation systems. In this context attention is to be paid as to whether the materials have an influence on the speed of the sound (e.g. porous absorber) or on the acoustic pressure p (e.g. impedance jump).

Another point still unresolved is the location, including the manner of effect, of the noise mitigation systems used. From the theory (e.g. piston irradiators) it is known that the acoustic pressure p runs ahead of the sound speed v in the close vicinity, i.e. near the source. In the close vicinity the phase displacement is 90º. In the far field area, both noise field values are in phase [28]. This results from the fact that the sound speed is composed of an effect part and a blind part. The blind part drops off perceptibly in the close vicinity, in proportion to the distance from the source. This also means, however, that in the close vicinity there is no real noise energy conveyance, and this does not take effect until in the far area. From the theory, for air the boundary between close vicinity and far area is assumed to be about 2 *lambda*, depending on the frequency.

The underwater noise from pile driving impacts, presents, as a rule, a marked energy maximum in the range between 100 and 500 Hz. This means that the wavelength of 100 Hz, at a sound speed of approx. 1,500 m/s, corresponds to about 15 m, and at 500 Hz to about 3 m. At the present time it is not adequately known from theory or from measurements where the transition from close vicinity to far field lies with regard to the driving of a pile. If, as a first approximation, 2 *lambda* (up to 10 *lambda*) is assumed, then, depending on the frequency, one will certainly be in the acoustic close vicinity within the first 6 to 30 m around the pile.

(It may be mentioned at this point that a pile is not to be regarded as a piston irradiator during the driving process. The precise effect and propagation effect of a pile is at present a subject for ongoing and forthcoming research projects).

The bubble curtains used in this research project were all positioned very compactly at the pile, and were all delimited in their width or guided, e.g. by tubes or deflector plates. This could be a reason why the use of the bubble curtains with the Weyres BeKa shells and the IHC NMS did not bring about any

increase, or only slight, in the attenuation (only) at high frequencies. Detailed investigations and inter-relationships between air volume, bubble size, width of the bubble curtain, and their effect on noise reduction are not available at present, however.

Another point is that the results from the measurements in the far field do differ perceptibly from the results in the close vicinity. It is clear that the spectra (of the pile-driving noise) exhibit substantially more energy in the close vicinity at high frequencies than at low frequencies, and that therefore the typical energy maximum 100 Hz <= f <= 400 Hz tends to shift towards frequencies of up to 800 Hz.

A consideration of the difference spectra (with and without noise mitigation measures) measured in the far field and close vicinity reveals that the broad-band passage attenuation (*delta* SEL) is slightly raised. The reason for this is not at present known. It may be surmised, however, that the influence of the phase displacement between the acoustic pressure p and sound speed v makes itself felt in the close vicinity.

From the discussion the following working hypotheses may therefore be derived for further research and development formulations:

Hypothesis 1: Attenuation of the NMS (ESRa) with f = 160 Hz is attributable to the water depth.

Hypotheses 2: NMS “take effect” in the close vicinity; i.e. no ground feedback attenuation is to be anticipated.

Hypothesis 3: By the dimensioning (*lambda*/4) and means of effect (speed or pressure) of the NMS tested, a clear improvement of the *delta* SEL is to be attained.

Accordingly, systematic investigation of both the effect principle and the influence of the distance from the pile of the noise mitigation measures should be undertaken by way of more extensive experiments and measurements.

10. Summary and Outlook

Within the framework of the ESRa research project at the Brodten Pile in Lübeck Bay (Baltic Sea), the handling and means of effect of five different noise mitigation systems for the construction of pile-driven offshore wind power installations have been tested in a ring experiment.

itap GmbH is required to work out an appropriate measurement and evaluation concept for underwater noise measurements on the basis of the existing StUK 3 concept, and to carry out and evaluate the measurements.

The measurements provided the following results:

- The evaluation of the underwater noise measurements has shown that, in principle, effective noise protection can be achieved with the five different noise mitigation systems. The broad-band reduction of the single event level (SEL) amounts to 4.2 to 6.1 dB. The noise reduction, by contrast, is heavily frequency-dependent. The noise mitigation systems tested have a high noise mitigation potential in the high frequency range (f > 500 Hz), while in the low-frequency range it has only a slight reduction potential.

- At the Brodten Pile, a particularly powerful ground feedback effect occurs due to the dimensions of the pile and the fact that the pile has grown to become fixed. In qualitative terms, however, this effect is to be assessed at 1.0 to 3.0 dB, with the result that it is to be anticipated that the noise mitigation systems used would result in noise mitigation potentials of 7-9 dB at other piles which have not grown fixed.

- For the first time, measurements have been taken of the sediment vibrations in the vicinity of the pile. These measurements have provided valuable indications about the ground feedback of the pile.

- A large databank of pile-driving noise measurements in the close vicinity and far area (>650 data records) has been generated.

- A better understanding of noise propagation has been achieved, and also of the means of effect of the individual noise mitigation concepts.

- In order to increase the *delta* SEL, it would be necessary, with the noise mitigation concepts tested, to improve the attenuation on the frequency range 100 < f < 500 Hz.

- It has been shown that, with the reduction of the distance interval between the measurement position and the pile, the noise passage attenuation increases appreciably (both close and far field). The reason for the increase in attenuation cannot at present be unambiguously explained.

From the discussion the following formulations and hypotheses can be derived for the optimization of the noise mitigation systems.

The attenuation of the NMS (ESRa) at f = 160 Hz is attributable to the depth of the water. The NMS “take effect” in the close vicinity; i.e. no attenuation of the ground feedback is to be anticipated. A perceptible improvement of the *delta* SEL is to be achieved by the dimensioning (l*amba*/4) and the means of effect (speed or pressure) of the NMS tested.

A systematic examination should therefore be conducted in further investigations and measurements of the effect principle and of the influence of the distance from the pile of the noise mitigation systems. It can be determined, however, that the noise propagation from a pile which is to be driven is far from trivial. The propagation and the possible effect of ground feedback are at present still unclear from the scientific point of view, and are increasingly becoming the focus for research (e.g. Project BORA, sponsored by the BMU (Federal Ministry of the Environment), since it is only from a knowledge of the close and far fields that a complete modelling of the noise propagation of a driven pile will be possible. With the present state of the art, no model exists which can correctly simulate the noise propagation of a pile in the close and far fields in both phenomenological and physical terms.

Accordingly, from the ESRa results the following prospect can be derived for the research and development work to be carried out in the middle and long term:

- The know-how from ESRa should be used in order to improve existing noise mitigation systems in a consistent manner. In the case of the IHC NMS this has already been implemented for the Riffgat Project.

- Improved noise mitigation systems should be tested with a real installation process (running pile).

- A detailed investigation of the acoustic vicinity should be carried out, with the distribution of pressure and speed.

- Phenomenologically and physically motivated models are to be developed in order to simulate the propagation from a pile which is to be driven.

- The influence of the ground feedback should be systematically investigated.

If the development work described is implemented successfully, it may be possible in the future, on the basis of models, to develop effective noise mitigation systems individually for a particular location and a structure type.

11. Literature, Guidelines, and Aids Used

[1] BSH (2007) Standard: Investigation into the effects of offshore windfarm installations on the marine environment (StUK3). Federal Office for Navigation and Hydrography, Hamburg

[2] Nehls G. and Betke K. (Draft 2011): Presentation and evaluation of the effects of noise emissions caused by offshore pile-driving on marine mammals. Commissioned by the Wind Energy Offshore Forum

[3] Meyer E. and Neumann EG. (1979) Physical and technical acoustics, Vieweg Publishing House, Braunchweig

[4] Thiele R. and Schellenstede G. (1980): Standard values for propagation attenuation in the North Sea. FWG Report 1980-7, Research Institute of the Federal Armed Forces for Water-borne Noise and Geophysics

[5] Betke K. and Matuschek R. (2011): Measurements of underwater sound in the construction of wind energy installations in the offshore test field “alpha ventus”. Concluding report for the StUK3 monitoring project of 20.05.2011

[6] Urick R. (1983): Principles of underwater sound, 3rd edition. Peninsular Publishing, Los Altos

[7] ISD, DEWI, ITAP (2007): Standard procedure for the determination and evaluation of the burden on the marine environment due to noise immision from offshore wind energy installations. Concluding report for the BMU “Schall 2” Project (FKZ 0327528A). Federal Ministry for the Environment, Protection of Nature, and Reactor Safety, Berlin

[8] CRI, DEWI, ITAP (2004): Standard procedure for the determination and evaluation of the burden on the marine environment due to noise immision from offshore wind energy installations. Concluding report for the BMU Project (FKZ 0327528A). Federal Ministry for the Environment, Protection of Nature, and Reactor Safety, Berlin

[9] Schultz-von Glahn, M., Betke K., Nehls, G. (2006): Reduction of underwater sound during pile-driving work for offshore wind power installations – Practical testing of different procedures under offshore conditions, UFOPLAN Ref. No. 205 53 113, Concluding Report, Office of the Environment, Berlin

[10] ISD, DEWI, ITAP (2007): Investigation of noise mitigation measures at FINO 2. Concluding report for the research project 0329947b. Federal Ministry for the Environment, Protection of Nature, and Reactor Safety, Berlin

[11] LU Hannover/DEWI/ITAP (2007-2010): Conception, testing, realization, and checking of low-noise construction projects and noise-reducing measures in the establishment of offshore wind energy installations, Project “Schall 2” (FKZ 0327645a).

[12] Griessmann T., Rustmeier J., Betke K., Gabriel J., Neumann T., Nehls G., Brandt M., Diedrichs A., and Bachmann J. (2010): Research and application of noise minimization measures during pile-driving at FINO3 – Monopiles. Hannover, concluding report for the BMU project “Noise at FIO3”, FKZ0325077

[13] LU Hannover/Menck (2007-2010): Composite project within the framework of alpha ventus. Research into the noise mitigation system “Little bubble curtain” in the alpha ventus test field

[14] Wilke F. and Kloske K. (2011): Project: Evaluation of systems for reducing pile-driving noise on an offshore test pile. (Project description PTJ 41V6069)

[15] Marine Programme Ocean View (Sea Map): Chart extract Lübeck Bay.

[16] TAGU/HIOCHTIEF Consortium: Site installation planning, Project ESRa

[17] IHC (2012): ESRa System Specification IHC tube (Noise Mitigation Screen)

[18] Menck (2012): ESRa System Specification, fire hose method

[19] Weyres (2012): ESRa System Specification, Little Bubble Curtain

[20] Weyres (2012): ESRa System Specification, BeKa Shell

[21] TU Braunschweig/Dr. Elmer (2012): ESRa System Specification, Hydro Sound Damper

[22] BioConsult SH (2011): ESRa research project – Examination in respect of type protection legislation, NATURA 2000 – Preliminary test, preliminary test of compatibility in accordance with Article 34 BNatSchG

[23] Betke K. Schultz-von Glahn M., Matuschek R. (2004): Underwater noise emissions from offshore wind turbines. In: Proceedings of the joint congress CFA/DAGA’04, pp. 591-592, Strasbourg

[24] Gattermann J. and Zahlmann J. (2011): Pile driving monitoring on the ESRa Project, Braunchweig, Measurement Report No. 11297 by TU Braunschweig

[25] Schultz-von Glahn M. and Gerke P. (June 2011): Measurement of hydro-noise emissions during test pile driving at the offshore wind park EnBW Baltic 2,

and measurement and evaluation of the effectiveness of noise mitigation measures. itap report No. 653-10-svg

[26] TNO (2012): Measurements of the acoustic insertion loss of the IHC Underwater Piling Noise Mitigation Screen, TNO-DV 2012 C017

[27] Nehls G., Betke K. and Ros M. (2007): Assessment and costs of potential engineering solutions for the mitigation of the impacts of underwater noise arising from the construction of offshore windfarms. Husum

[28] Veitl (1996): Technical Acoustics

12. Schedule of Figures

Figure 1: Signature time signal of underwater sound with a pile-driving blow as measured at a distance of approx. 100 metres. 17

Figure 2: The test pile in the vicinity of Travemünde 21

Figure 3: Geographical position of the test pile in Lübeck Bay (source: [14]) 22

Figure 4: Map section of Lübeck Bay [15] indicating the test pile near the Brodten-Ost cardinal buoy 22

Figure 5: Position of the exclusion around the test pile 23

Figure 6: Hammer specification MHU 270 T (source: www.menck.com) 25

Figure 7: Hammer placed on the pile (photo: Patrice Kunte) 26

Figure 8: Stilt-mounted pontoon RHR 1 with equipment (photo: Patrice Kunte) 27

Figure 9: Mooring of the stilt-mounted pontoon in the port of Neustadt, construction site plan [16] 27

Figure 10: Air compressor used (source: www.compair.de) 28

Figure 11: Noise Mitigation Screen from IHC, schematic layout 30

Figure 12: IHC NMS during installation (photo: Patrice Kunte) 30

Figure 13: View of the intermediate space between pile/NMS during the operation of the bubble curtain (photo: Patrice Kunte) 31

Figure 14: Menck fire hose system when lifting from the deck of the working platform (left) and during installation at the pile (right) (photo: Patrice Kunte) 31

Figure 15: Detail view of the lower end of the NMS with the connections of the fire hoses (photo: Patrice Kunte) 32

Figure 16: Sea fastening of the fire hose system (photo: Patrice Kunte) 33

Figure 17: Schematic representation of the components of the fire hose system 34

Figure 18: Retracted and telescopically extended LBC system (photo left: Patrice Kunte, photo right: Weyres) 35

Figure 19: Ring lines generating the bubble curtain in the area of the ground trough, with 50 mm foam cladding (source: Weyres) 36

Figure 20: Little bubble curtain – LBC, from Weyres, in operation (photo: Patrice Kunte) 36

Figure 21: BeKa jacket, Weyres, schematic design drawing 37

Figure 22: Two-part structure of the BeKa jacket, Weyres (photo: Patrice Kunte) 39

Figure 23: BeKa jacket during installation (photo: Patrice Kunte) 40

Figure 24: Application examples and variants of nets with hydro noise dampers (source: TU Braunschweig/Dr. Elmer) 40

Figure 25: Interaction of an HSD balloon for scattering and propagation of sound waves (source: TU Braunschweig/Dr. Elmer) 41

Figure 26: HSD test system with a net (retracted, half lowered and fully lowered) (source: TU Braunschweig/Dr. Elmer) 42

Figure 27: Design drawing of the ESRa HSD platform (source: TU Braunschweig/Dr. Elmer) 44

Figure 28: Constructing the inner net with double-layer air-filled HSD balloons (source: TU Braunschweig/Dr. Elmer) 44

Figure 29: Constructing the middle net with HSD foam elements (source: TU Braunschweig/Dr. Elmer) 45

Figure 30: Constructing the outer net with single-layer HSD balloons (source: TU Braunschweig/Dr. Elmer) 45

Figure 31: The entire HSD platform over the test pile (photo: Patrice Kunte) 46

Figure 32: Scientific muscle strength lowers the inner net (photo: Patrice Kunte) 46

Figure 33: Schematic layout of the experiment (not to scale) 49

Figure 34: Autonomous measurement systems of ITAP GmbH for measuring underwater sound at measurement positions MP1 to MP4. Top: photo; bottom: schematic diagram 50

Figure 35: Measuring system (“array”) consisting of one geophone and four hydrophones (MP5). Left: photo; right; schematic diagram 51

Figure 36: Measuring positions used 53

Figure 37: Measurement position of acceleration (right) and expansion sensor (left) at the Brodten Pile 54

Figure 38: Details of measurement recorder, pile energy measurement (photo: Patrice Kunte) 54

Figure 39: Schematic time diagram of the experiment sequence per measurement day 59

Figure 40: FFH area: “1931-301 Baltic Coast at Brodten Bank” 62

Figure 41: Predicted single event exposure level at a depth of 2 m along the stretches 1 and 2 63

Figure 42: Predicted single event exposure level at a depth of 8 m northeast of the pile 63

Figure 43: Water properties (temperature – red line; salinity – green; speed of sound – blue) during a representative measurement. 65

Figure 44: Third-octave spectra of the reference measurements (no noise mitigation system) at measurement position MP1.1 (750 m distance, 1.8 m hydrophone height) with a driving energy of 300 kJ on the four different measurement days. 66

Figure 45: Third-octave spectra of a reference measurement (no noise mitigation system) at measurement positions MP1.1, MP2.1, MP3.1, MP4.1 and MP5.1 (hydrophone height 1.8 m above sediment) with a driving energy of 300 kJ. 67

Figure 46: Single event level LE or SEL (summary level) as a function of the impact energy and the distance interval 68

Figure 47: The median values of the third-octave spectra measured at the measurement positions MP2.1, MP3.1 and MP4.1 (hydrophone height 1.8 m, distance to pile 375 m) with and without noise mitigation system as a function of the selected impact energy 69

Figure 48: Associated difference spectrum of the respective measuring condition (respective median over measurement positions MP1.1, MP2.1, MP3.1 and MP4.1). 70

Figure 49: Single event exposure level LE or SEL (total level) as a function of the hydrophone height above ground and the distance to the test pile when pile driving without noise mitigation system (impact energy 300 kJ). 71

Figure 50: Single event exposure level LE or SEL (total level) as a function of the distance to the test pile when pile driving without noise mitigation measures (impact energy 300 kJ). In addition, the expected (calculated) single event exposure level according to Thiele & Schellenstede [4] is shown as a function of distance. 73

Figure 51: The median values of the third-octave spectra measured at measurement positions MP2.1 and MP3.1 (hydrophone height 1.8 m, distance to pile 375 m) with and without noise mitigation system for the IHC NMS system, with and without inner bubble curtain 75

Figure 52: Corresponding difference spectrum (sound transmission suppression) of the respective measurement condition 75

Figure 53: The median values of the third-octave spectra measured at measurement positions MP2.1, MP3.1 and MP4.1 (hydrophone height 1.8 m, distance to pile 375 m) with and without noise mitigation system for the Menck fire hose method with two different air pressures. 76

Figure 54: Corresponding difference spectrum (sound transmission suppression) of the respective measurement condition. 76

Figure 55: The median values of the third-octave spectra measured at measurement positions MP2.1, MP3.1 and MP4.1 (hydrophone height 1.8 m, distance to pile 375 m) with and without noise mitigation system for the Weyres little bubble curtain 77

Figure 56: Corresponding difference spectrum (sound transmission suppression) of the respective measurement condition (respective median of measurement positions MP1.1, MP2.1, MP3.1 and MP4.1). 77

Figure 57: The median values of the third-octave spectra measured at measurement positions MP2.1, MP3.1 and MP4.1 (hydrophone height 1.8 m, distance to pile 375 m) with and without noise mitigation system for the BeKa jacket, with and without Weyres inner bubble curtain 78

Figure 58: Corresponding difference spectrum (sound transmission suppression) of the respective measurement condition (respective median of measurement positions MP1.1, MP2.1, MP3.1 and MP4.1). 78

Figure 59: The median values of the third-octave spectra measured at measurement positions MP2.1, MP3.1 and MP4.1 (hydrophone height 1.8 m, distance to pile 375 m) with and without noise mitigation system of the Elmer hydro sound damper. The three rings (I – inner ring; M – middle ring; O – Outer ring) offer seven different possibilities 79

Figure 60: Corresponding difference spectrum (sound transmission suppression) of the respective measurement condition (respective median of measurement positions MP1.1, MP2.1, MP3.1 and MP4.1). 80

Figure 61: Summary of the sound transmission suppression or difference spectrum with and without NMS (media value over measurement positions MP1.1, MP2.1, MP3.1 and MP4.1) of the tested noise mitigation measures. 90

Figure 62: Represented are the third-octave spectra of the reference condition (without noise mitigation system) measured at the measurement position MP5 at different heights (hydrophone height 1.8 m, 3.6 m, 5.4 m and 7.2 m; distance from pile 13 m). 83

Figure 63: Represented is the difference spectrum (spectral sound transmission loss) for a representative noise mitigation system (with and without noise mitigation system) measured at the measurement position MP5 at different heights (hydrophone height 1.8 m, 3.6 m, 5.4 m and 7.2 m; distance from pile 13 m). 84

Figure 64: Represented are the third-octave spectra measured at the measurement position MP5.1 (hydrophone height 1.8 m, distance from pile 13 m) with and without noise mitigation system for the IHC NMS system with and without inner bubble curtain 85

Figure 65: Difference spectrum pertaining to this (noise passage attenuation) of the individual measurement condition 85

Figure 66: Represented are the third-octave spectra measured at the measurement position MP5.1 (hydrophone 1.8 m, distance from pile 13 m), with and without noise mitigation system, for the fire hose method from Menck with two different air pressures 86

Figure 67: Difference spectrum pertaining to this (noise passage attenuation) of the individual measurement condition 86

Figure 68: Represented are the third-octave spectra measured at the measurement position MP5.1 (hydrophone 1.8 m, distance from pile 13 m), with and without noise mitigation system, for the Little Bubble Curtain from Messrs. Weyres 87

Figure 69: Difference spectrum pertaining to this (noise passage attenuation) of the individual measurement condition 87

Figure 70: Represented are the third-octave spectra measured at the measurement position MP5.1 (hydrophone 1.8 m, distance from pile 13 m), with and without noise mitigation system, for the BeKa shell, with and without the inner bubble curtain from Messrs. Weyres 88

Figure 71: Difference spectrum pertaining to this (noise passage attenuation) of the individual measurement condition 88

Figure 72: Represented are the third-octave spectra measured at the measurement position MP5.1 (hydrophone 1.8 m, distance from pile 13 m), with and without noise mitigation system, for the Elmer Hydro Sound Damper, The three rings (I – inner ring; M – Middle ring; A – Outer ring) resulted in seven possible variations 89

Figure 73: Difference spectrum pertaining to this (noise passage attenuation) of the individual measurement condition 90

Figure 74: Measurement positions and distance intervals of the IGB TUBS hydrophones at the Brodten Pile 91

Figure 75: Comparison of the signal time sequences of the hydrophones H1 and H2 at a reference impact with 300 kNm on the fourth day of measurements 92

Figure 76: SEL and Lpeak determined for each individual impact (H1 and H2) with the reference impact on the fourth day of measurement 93

Figure 77: Third-octave analysis of the reference impacts over the four days of measurement 95

Figure 78: Third-octave analysis with the use of the IHC system (7 bar) and the reference measurement without noise mitigation (measurement day 1) 96

Figure 79: Third-octave analysis with the use of the Menck system (fire hose, 1 bar) and the reference measurement without noise mitigation (measurement day 2) 96

Figure 80: Third-octave analysis with the use of the Weyres system (BeKa shell, 0 bar) and the reference measurement without noise mitigation (measurement day 3) 97

Figure 81: Third-octave analysis with the use of the HSD system (3 nets) and the reference measurement without noise mitigation 97

Figure 82: Represented are the third-octave spectra at distances of between 500 m and 1,000 from the individual pile during different pile-driving operations. The thin coloured lines each represent individual measurements, while the thick coloured lines identify the median values 101

Figure 83: Model spectrum for a pile-driving impact in the far field range for forecasting purposes. The idealized model spectrum is based on several measurements with various different pile-driving activities by itap GmbH 102

Figure 84: Time function (time signals) of a hydro-noise pile-driving pulse at a distance of 750 m from the test pile and 1.8 m from the sediment, with a driving energy used of 300 kJ 102

Figure 85: Time function (time signals) of the geophone (vibration) of a pile-driving pulse at a distance of 13 m from the test pile in the sediment, with a driving energy used of 300 kJ 103

Figure 86: Attenuation of the vibration speed level (vibrations in the sediment; at a distance of 13 m from the pile, with and without noise mitigation system, on the four investigation days (MP5.5). On days 1 and 2 the same measurement position was used. On days 3 and 4, due to the different location of the pontoon in front of the pile, the positions were changed. (A vibration speed of 10 mm/s corresponds to a vibration speed level of 140 dB) 105

Figure 87: Third-octave spectrum during pile-driving work at the Baltic II wind farm, on a pile without and with a noise mitigation system (bubble curtain). The spectra are represented at the start of grounding (e.g. introduction depth of a few metres), in the middle and at the end of the grounding (i.e. hardly any or no advance in driving) 107

Figure 88: delta SEL reductions achieved with the IHC NMS at different locations (source: IHC, with kind approval) 108

Figure 89: Frequency-dependent reduction in driving noise due to different noise mitigation arrangements from the literature [5], [9], [12], and from this present research project 110

Figure 90: Schematic experimental arrangement, with the example of the IHCNMS system. The noise is propagated from the pile and runs in turn through the media of water, steel, air, steel, and then water again 113

13. Schedule of Tables

Table 1: Overview of the main physical quantities and parameters used, and their units of measurements 11

Table 2: Soil conditions at the Brodten Ost test pile 24

Table 3: Weights of the test systems and comparison with a 9 m section of the test pile 47

Table 4: Test pile data 48

Table 5: Equipment units used 51

Table 6: Geographical location of the measurement positions used and their identification 53

Table 7: Results of the drive energy measurement for all NMS [24] 56

Table 8: Sequence of the noise mitigation systems used, with the individual variation possibilities 58

Table 9: List of the measurements taken (☺ = correct; - measurement not taken) 60

Table 10: Summary of the potential noise mitigation of the five tested noise mitigation systems, incl. variations. Additionally, the single event exposure level (SEL) and the Lpeak at the StUK 3-compliant measurement position MP1.1 are shown. 80

Table 11: Overall result of the IGB TUBS hydro-noise measurements in the close vicinity (distance = 6.0 m) with a pile-driving energy of 300 kNm 94

Table 12: Summary of the noise mitigation potentials (ΔSEL) of the five noise mitigation systems tested, including variations, as a function of the distance between pile and measurement position. The measurements in the far field are used for ΔSEL median values over four measurement positions at a distance of between 375 m and 750 m, in the near field individual results. 98

Table 13: Summary of the noise mitigation potentials of the five noise mitigation systems tested, including variations, as a median over the far field measurements (MP1.1 to MP4.1). In addition, the mitigation potentials are represented without a possible ground feedback in the far field range, in the frequency range of 125 Hz upwards, and measured in the close vicinity at the position MP5.1. 106

14. APPENDIX 1: Itap Noise Prognosis

Prognosis for the underwater noise incurred during pile-driving experiments at the “Brodten Pile”.

May 2011

Prepared by:

Klaus Betke, Rainer Matuschek (itap GmbH (Institute for Technical and Applied Physics)

Contents

1.	Outline of Task and Summary	Page 2
2.	Local and Technical Circumstances	3
3.	Procedure	4
3.1	Noise Propagation	4
3.2	Source Level	6
4.	Results	7
4.1	Sound Level as a Function of Distance	7
4.2	Cumulative Effect	9
4.3	Effect on Persons in the Water	10
5.	Literature	12

1. Outline of Task and Summary

Within the framework of the research project entitled Evaluation of Systems for Pile-driving Noise Mitigation (ESRa), the intention is to investigate a number of different methods for mitigating underwater noise in offshore pile-driving work. To this end, it is intended to conduct pile-driving experiments at a test pile in Lübeck Bay. With pile-driving work of this nature, loud noises are engendered under water, which can exert an effect on marine fauna. BioConsultSH were commissioned with the task of assessing this influence, and itap calculated the noise level to be anticipated for this.

By way of example, two propagation routes were examined, one to the shoreline and one in the direction of the open sea. What is referred to as the UBA precautionary value, a single event level (SEL) of a pile-driving impact of 160 dB re 1 µPa, was not attained in the most unfavourable direction, at a distance of 1.5 to 2 km from the pile. At the Brodten shoreline, the SEL at a water depth of 2 m was 140 dB re 1 µPa or less. At Barendorf (Mecklenburg Vorpommern), the forecast SEL is higher, and does not drop until 200 to 300 m off the coastline, to less than 150 dB re 1 µPa. In addition to this, up to a distance of about 3 km from the shore it is approximately constant at 150 to 155 dBa re 1 µPa.

2. Local and Technical Circumstances

The test pile is located in Lübeck Bay at E, in the vicinity of Travemünde, about 2.4 km north-east of the Brodten shoreline (Fig. 1m Fig. 2). It was erected in the 1980's by Menck GmbH in order to test pile-driving equipment. The pile is a steel tube of 2.2 m in diameter and 50 mm wall thickness. It projects 5.5 m out of the water, and according to Menck it is embedded more than 60 m into the sea bed. It is not to be anticipated, or scarcely, that it can be driven any further into the ground by pile-driving impacts. For the experiments a ram of the type Menck MHU 270T was provided, with a maximum impact energy of 300 kJ.

Fig. 1. The test pile in the vicinity of Travemünde. The white cover is intended to make it more visible to shipping and is removed for pile-driving experiments (photos from autumn 2005).

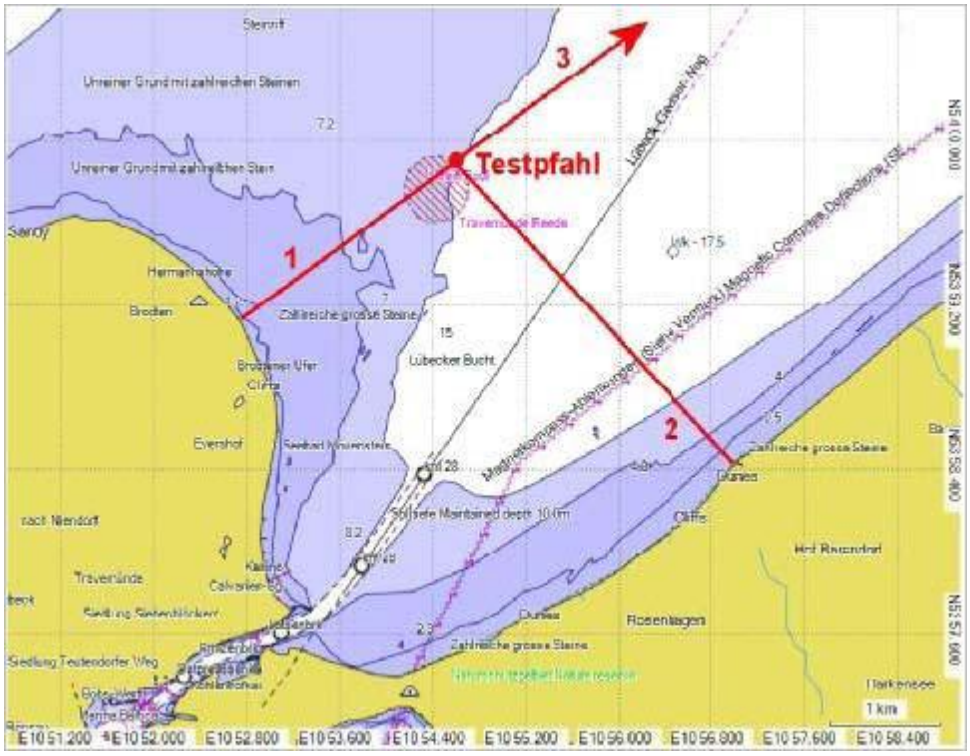

Fig. 2. Geographical position of the test pile. The red lines indicate the directions for which the noise propagation was calculated by way of example; see Sections 3 and 4.

Testpfahl	Test pile

3. Procedure

The noise levels to be expected were calculated by way of example for the propagation routes entered in Fig. 2:

1. Direction of Brodten shoreline, 235º, distance to shore 2.4 km
2. Direction of Barendorf, 135º, distance to shore 3.9 km
3. Direction of the open sea, 55º

For profile 1 and 2, the noise levels were calculated at a water depth of 2 m, and for profile 3 at 8 m.

3.1 Noise Propagation

For the calculation, the model “Range-dependent Water Depth Acoustic Model RAM” was used, which was developed by Michael D. Collins for the U.S. Naval Research Laboratory in Washington (e.g. Collins & Westwood 1991, Collins et al., 1996). This works according to the method of what is referred to as parabolic equation, PE. The program code is freely available. The depth profiles used are represented in Fig. 3; the approximate water depths were read off from the sea charts 35 (“Neustädt Bay”) and 37 (“Dahmeshöved to Wismar”). For the last 200 to 300 m of the noise propagation between the 2 m line and the shoreline, a constant water depth of 2 m was applied. In view of the fact that the broad-band level of pile-driving noise is largely determined by its low-frequency components below 1000 Hz, calculations were made in the octave frequency bands of 125 Hz to 2000 Hz. In addition, a constant noise speed over the water depth of 1485 m/s was assumed and constant sediment over the propagation path, characterized by a sound speed of 1600 m/s.

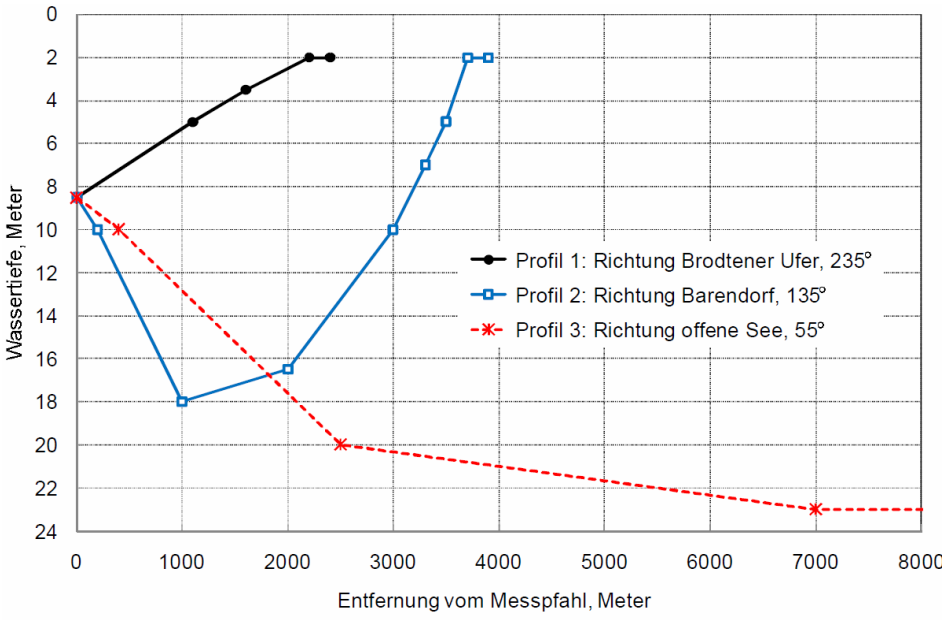

Fig. 3. Water depths assumed for the calculation of the noise propagation

Wassertiefe, Meter	Water depth, metres
Entfernung vom Messpfahl, Meter	Distance from measurement pile, metres
Profil 1: Richtung Brodtener Ufer,235°	Profile 1: Direction of Brodten shoreline, 235º
Profil 2: Richtung Barendorf, 135°	Profile 2: Direction of Barendorf, 135 º
Profil 3: Richtung offene See 55°	Profile 3: Direction of the open sea, 55 º

Apart from the PE, the "Thiele formula" was also used for the calculation:

$$TL = (16.07 + 0.185\ F)\ (lg\ (R) + 3) + (0.174 + 0.046\ F + 0.005\ F2)\ R$$

where TL is the propagation attenuation in dB, F = 10 log(f / kHz, and R is the distance in km. TL relates to a distance of 1 m from the noise source, conceived as being a point; i.e. for R = 1 m, TL = 0 dB. This approximation formula for the noise propagation is based on measurements by Thiele and Schellstede (1980) in specific areas of the North Sea, and, strictly speaking, only applies to that location and only under winter conditions with good intermixture of water, without a striking sound speed profile. The formula can, however, be readily adopted also for other areas for comparisons and for overlapping calculations.

3.2 Source Level

Taking as a basis the measurements available for underwater pile-driving noise in the North Sea, for the pile diameter of 2.2 m and an impact energy of 300 kJ a broad-band SEL of an impact was taken of 168 dB re 1 µPa at a distance of 750 m. For the propagation calculation, as an interim value, the source level is needed, i.e. the value at a fictitious distance of 1 m. This was calculated with the aid of the Thiele formula, and is listed in Table 1 for the frequency bands under consideration. In this context, the idealized form of the spectrum in Fig. 4 was adopted.

Octave band, Hz	125	250	500	1000	2000	Total
SEL in 750 m, dB re 1 µPa	163.7	163.7	160.9	149.1	142.0	168.0
SEL in 1 m dB re 1 µPa	205.3	206.8	205.3	195.2	190.0	210.8

Table 1. Frequency-dependent source levels of pile-driving noise used for the prognosis, based on a broad-band value of 168 dB re 1 µPa at a distance of 750 m from the ram.

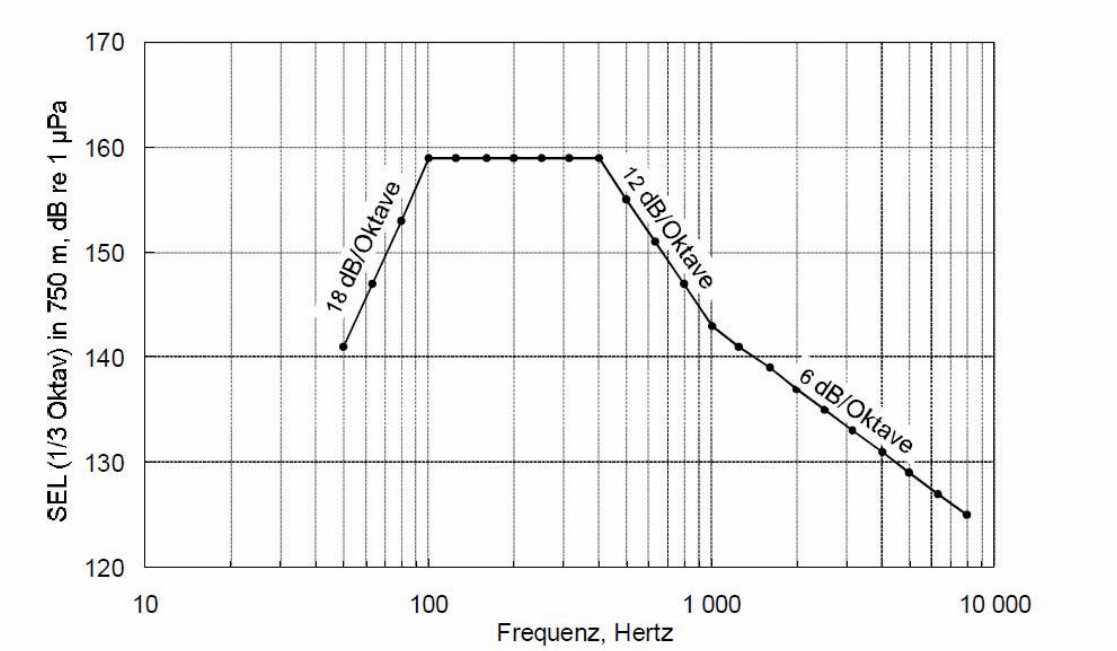

Fig. 3. Model spectrum of a ram impact used for the calculation of the noise propagation

SEL (1/3 Oktav) in 750m, dB re 1µPa	SEL (1/3 octave) at 750 m, dB re 1 µPa
Frequenz, Hertz	Frequency, Hertz
18 dB/Oktave	18 dB/Octave
12 dB/Oktave	12 dB/Octave
6dB/Oktave	6dB/Octave

4. Results

4.1 Sound Level as a Function of Distance

Fig. 5 shows the results of a propagation calculation based on the PE model for the paths 1 and 2. Represented is the single event level (SEL) of a ram impact at a receiver at a depth of 2 m. In the westerly direction (path 1) the noise level decreased continuously; in the vicinity of Brodten, the SEL falls at 700 m from the coastline to below 150 dB re 1 µPa. At the beach, it then falls further to some 130 dB re 1 µPa. In the south-easterly direction (135º) the noise level initially drops sharply in a similar manner over the first 1000 metres from the ram pile, but then remains up to 3500 m at 150 to 155 dB re 1 µPa, and only at 200 to 300 m off the coastline drops to below 150 dB re 1 µPa.

The levels referred to decrease towards the surface of the water, in other words if the reception depth is less than 2 m. As the depth increases, by contrast the level increases slightly, at a depth of 8 m by some 3 dB in relation to the value at a depth of 2 m.

In the direction of the open sea (path 3, Fig. 6), the noise level decreases steadily as the distance from the ram increases. In line with the formula, the precautionary value developed by the Federal Office of the Environment, of 150 dB re 1 µPa, is no longer attained at about 1.6 km.

In Figs. 5 and 6, by way of comparison, the result of the simple calculation with the Thiele formula is drawn in. Because this does not take account of any water depth profiles, it cannot provide any realistic values for the stretches in the direction of the coast. For direction 3, by contrast, it does provide a usable approximation up to a distance of some 2 km.

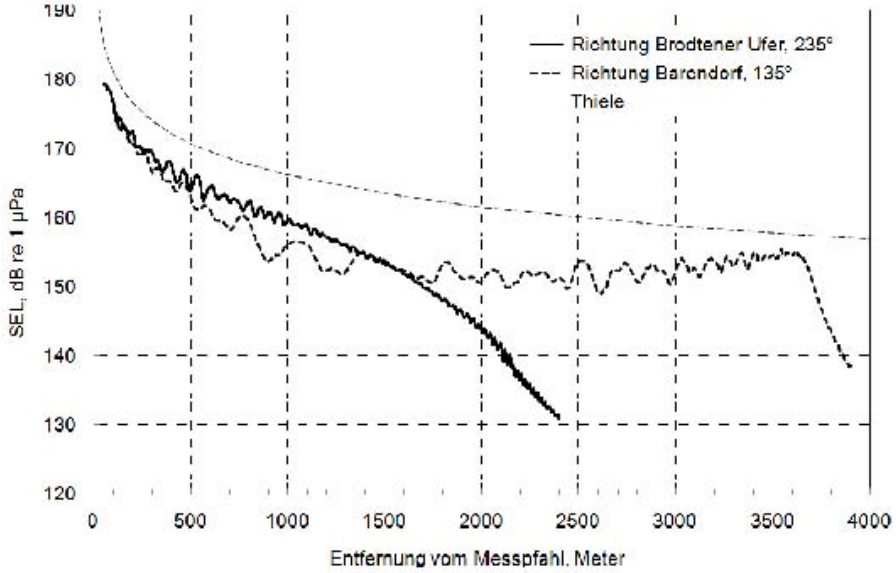

Fig. 5. Prognosticated single event level at 2 m depth along stretches 1 and 2

Entfernung vom Messpfahl, Meter	Distance from measurement pile, metres
Richtung Brodtener Ufer, 235°	Direction of Brodten shoreline, 235º
Richtung Barendorf, 135°	Direction of Barendorf, 135º

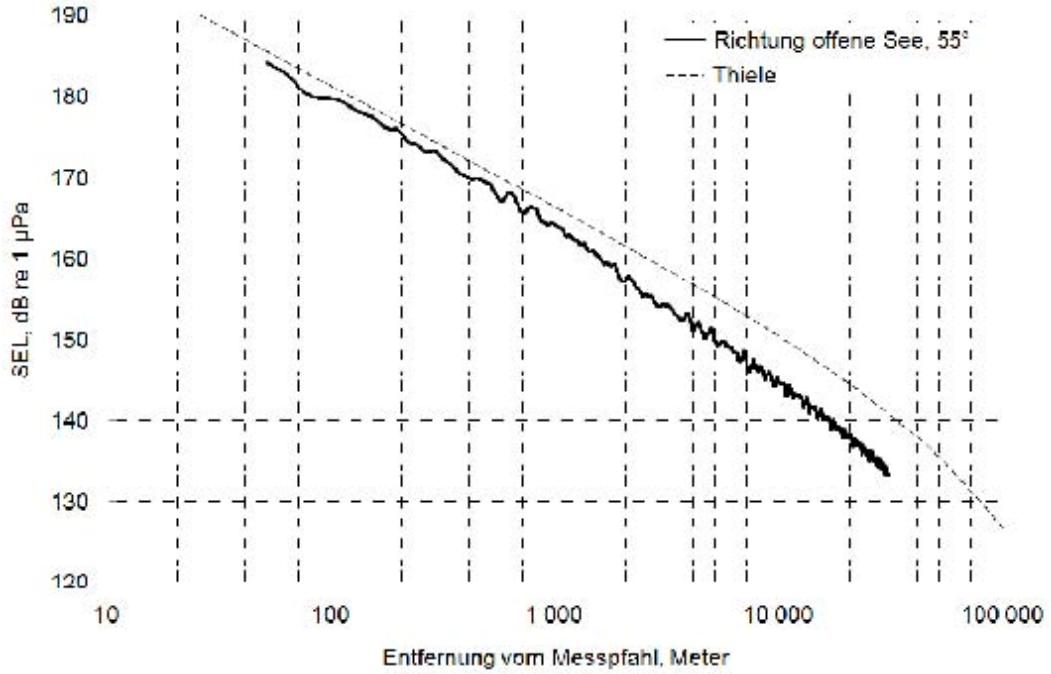

Fig. 6. Prognosticated single event level at 8 m depth in the north-east direction from the pile

Entfernung vom Messpfahl, Meter	Distance from measurement pile, metres
Richtung offene See, 55°	Direction of open sea, 55º

4.2 Cumulative Effect

For the biological effect of pile-driving noise, it is not only the level of an individual impact which is determinant, but also the duration of effect and the number of impacts. It is not possible to produce exact forecasts about the duration, due to the experimental nature of the work. Sequences of impacts of some minutes in duration are to be anticipated, or some 10 impacts, during which the noise is measured, with extended periods of rearranging the equipment both before and after.

For the onset of damage to hearing, at least, characterized by a permanent threshold shift (PTS), as well as for a temporary threshold shift (TTS), noise values are given in the literature for the “cumulative SEL” (Southall et al., 2007). For the cumulative SEL, it is not a single noise pulse which is regarded as an ”event”, but a sequence of pulses. Accordingly, from the value SEL_{single} for an individual ram impact, the following is derived:

$$SEL_{cum} = SEL_{single} + 10\ lg(N)$$

where N is the number of ram impacts. In Fig. 7, values are shown for N = 1 (this is the curve from Fig. 6), N = 10, and N = 100, which according to the equation are increased by 10 dB and 20 dB respectively in relation to the curve for N = 1 ram impact.

In this connection, Southall et al. additionally proposed what is referred to as the M-weighting, a frequency weighting which, in a similar manner to the well-known A-weighting for airborne sound, is intended to make it possible for single-figure values to be calculated for the noise level, and, at the same time, to take account of the frequency dependency of hearing capacity. The M-weighting attenuates low frequencies in particular, with the result that M-weighted pile-driving noise levels are somewhat lower than unweighted levels. This can likewise be seen from Fig. 7. Southall et al. refer to several slightly different M-weightings. In this case, the curve M_{HF} was used for “high frequency cetaceans”, among which are the common porpoise. The weighting attenuates sound ranges below a frequency of some 200 Hz.

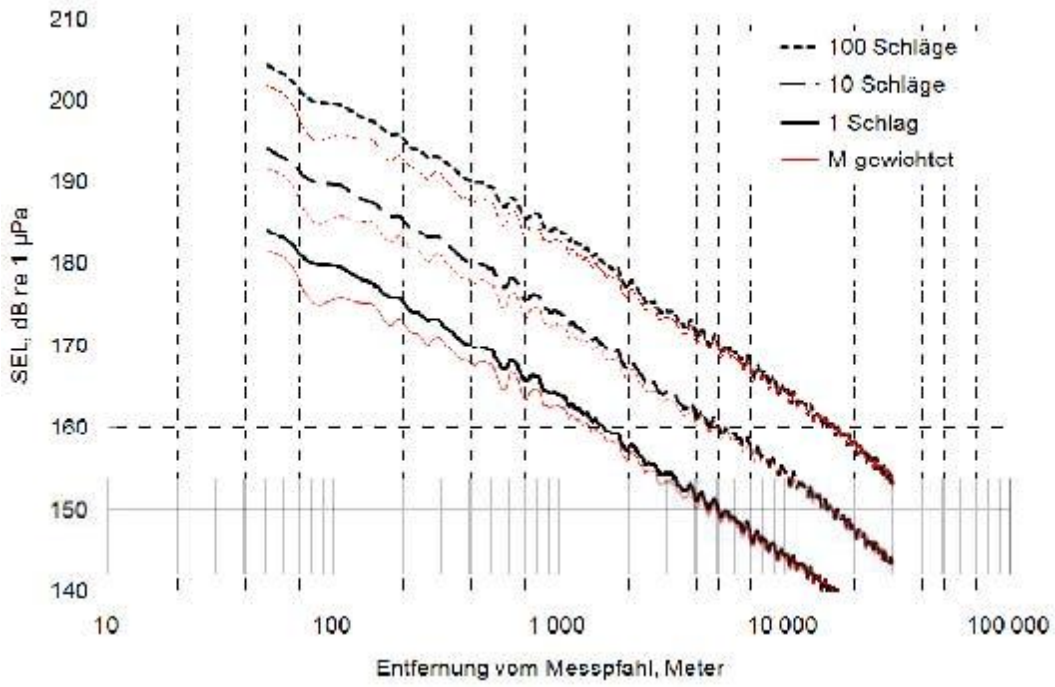

Fig. 7. Prognosticated cumulative SEL at a depth of 8 m in the north-easterly direction from the pile, for sequences of 10 and 100 impacts (the curve for one impact is the same as in Fig. 5)

100 Schlaege	100 impacts
10 Schlaege	10 impacts
1 Schlag	1 impact
M gewichtet	M-weighted
Entfernung vom Messpfahl, meter	Distance from measurement pile, metres

For a sequence of 10 impacts the TTS threshold value of 183 dB re 1 µPa (M-weighted) is accordingly attained or undercut respectively at 100 to 200 m from the ram, and at about 1 km for a sequence of 100 impacts. There is a lack of clarity, however, inasmuch as Southall et al. count TTS as “behavioural disturbance” reactions, and, with an increase in the level by 10 lg(N), the cumulative calculation method may not be adequate for these.

4.3 Effect on Persons in the Water

Data regarding the effect of underwater noise on human beings can hardly be found in the literature at all. A number of guidelines for divers do exist, such as provided by the NATO Undersea Research Centre NURC. Ainslie (2008) evaluated a number of such safety rules, and determined that the noise levels assessed as critical do in part differ sharply from one another. Moreover, it is unclear on what mean time periods etc. the values are based.

Ainslie comes to the conclusion that in the frequency range from 125 Hz to 4 kHz a level of 160 dB re 1 µPa should not be exceeded, whereby this level should be determined over 125 ms, which is approximately the time constant of the volume formation of human hearing. The figure is intended to apply to Navy divers; for leisure divers who are not forewarned, a lower value may well be advisable.

The value is intended to be for sonar signals or similar applications, but expressly not for short pulses such as the noise from pile-driving. A number of considerations are possible, however. The SEL of an impact event is defined as the level of a continuous noise of 1 s duration, which has the same energy content as the noise event. A pile-driving impact, however, is much shorter than 1 s, and in most cases also shorter than 125 ms, with the result that the L_{eq} (equivalent sustained noise level) at 125 ms mean time with one impact can amount to as much as

$$L_{eq\ 125\,ms} = SEL + 10\lg(1\ s/0.125\ s)dB = SEL + 9\ dB$$

in other words, 9 dB higher than the SEL. The precautionary value cited would therefore correspond to an SEL of a single ram impact of 151 dB re 1 µPa. As Fig. 4 shows, this value can be attained, off Barendorf, for example, at a distance of several hundred metres from the shore. This value, however, only occurs for brief periods with the impact sequence of the ram. No assessment basis is known for such repeated underwater noise pulses.

5. Literature

Ainslie MA (2008): Review of published safety thresholds for human divers exposed to underwater sound. TNO report TNO-DV 2007 A598. Nederlandse Organsatie voor toegepast naturwetenschappelijk onderzoek, April 2008

Collins MD, Westwood EK (1991): A higher-order energy-conserving parabolic equation for range-dependent ocean depth sound speed and density. J. Acoust. Soc. Am. 89, 10681075

Collins MD, Cederberg RJ, King DB, Chin-Bing SA (1996): Comparison of Algorithms for Solving Parabolic Wave Equations. J. Acoust. Soc. Am. 100, 178-182

Collins MD, User's guide for RAM versions 1.0 and 1.0p. U.S. Naval Research Laboratory, Washington

Southall BA, Bowles AE, Ellison WT, Finneran JJ, Gentry RL, Greene Jr CR, Kastak D, Ketten DR, Miller JH, Nachtigall PE, Richardson WJ, Thomas JA, Tyac PL (2007): Marine Mammal Noise Exposure Criteria: Initial Scientific Recommendations. Aquatic Mammals 33, 411-522

Thiele R., Schellstede G. (1980): Standard Values for Propagation Attenuation in the North Sea. FWG Report 1980-7, Research Institute of the Federal Armed Forces for Water-borne Noise and Geophysics

15. APPENDIX 2: TUBS Close Proximity Measurements

Energy and Hydro-noise Measurements in Close Proximity to the Pile, in the ESRa Research Project

February 2012

Prepared by:

Dr.-Ing. Jörg Gattermann, Dipl.-Ing. Benedikt Bruns, Dipl.-Ing. Christian Kuhn, Dipl.-Ing. Jörn Zahlmann (IGB-TUBS)
Dr.-Ing. Karl-Heinz Elmer (Neustadt a. Rbg.)

Determination of Inducted Energy

As part of the ESRa Project, during the tests dynamic test loadings accompanying the pile-driving were carried out in order to determine the energy inducted into the pile. The measurements serve to provide proof of the comparability of the tests.

With a dynamic test loading, the expansions and accelerations produced by the hammer impact are measured beneath the pile head. With these two measured values it is possible for the energy that is introduced to be determined in the plane of the measuring recorder. Fig. 1 below provides an impression of the sensors applied to the Brodten Pile.

Fig. 1: Measuring positions of the acceleration sensor (right) and expansion sensor (left) at the Brodten Pile

The tests at the Brodten Pile made provision for three series of impacts, with impact energy values of 100, 200, and 300 kNm. Each series of impacts consisted of 20 individual blows. Based on this arrangement, each noise mitigation system (NMS) was examined, and in each case also a reference measurement without a noise mitigation system. These various different NMS are not described in greater detail in this report. Figures 2 to 5 which follow provide a graphic summary of the energy calculated from the expansion and acceleration measured at the pile head. In each case, the energy is represented over the number of impacts. The two impacts with an energy of approx. 25 kNm were the pre-blows, and served to drive sealife away from the area around the Brodten Pile at the beginning of each test.

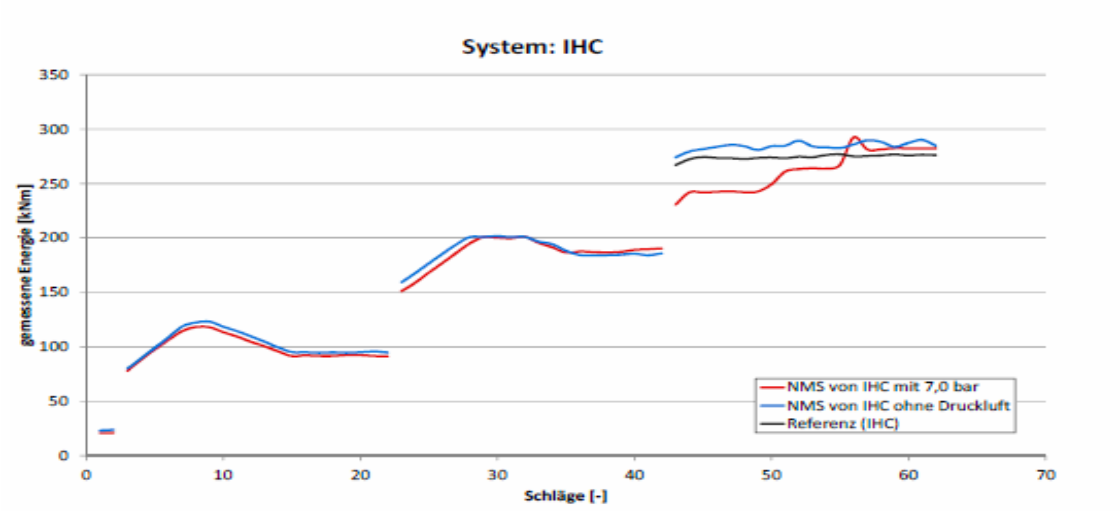

Abbildung 2: eingeleitete Schlagenergien beim System IHC (Messtag 1)

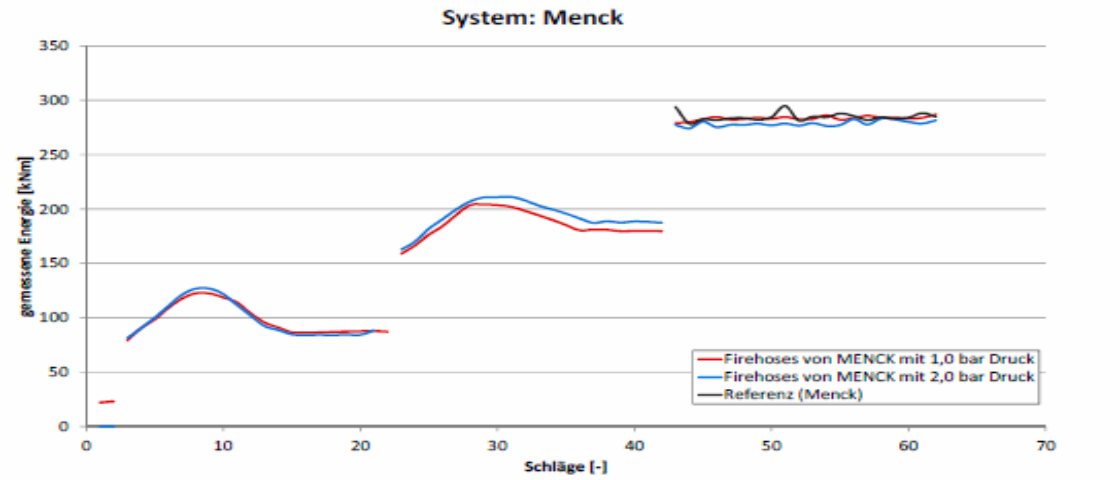

Abbildung 3: eingeleitete Schlagenergien beim System Menck (Messtag 2)

Figure 2: Inducted impact energy with the IHC system (measurement day 1)

Gemessene Energie [kNm]	Measured energy [kNm]
NMS von IHC mit 7,0 bar	NMS of IHC with 7.0 bar
NMS von IHC ohne Druckluft	NMS of IHC without compressed air
Referenz (IHC)	Reference (IHC)
Schlaege	Impacts

Figure 3: Inducted impact energy with the Menck system (measurement day 2)

Gemessene Energie [kNm]	Measured energy [kNm]
Firehoses von Menck 1,0 bar Druck	Fire hoses from MENCK at 1.0 bar pressure
Firehoses von Menck 2,0 bar Druck	Fire hoses from MENCK at 2.0 bar pressure
Referenz (Menck)	Reference (Menck)
Schlaege	Impacts

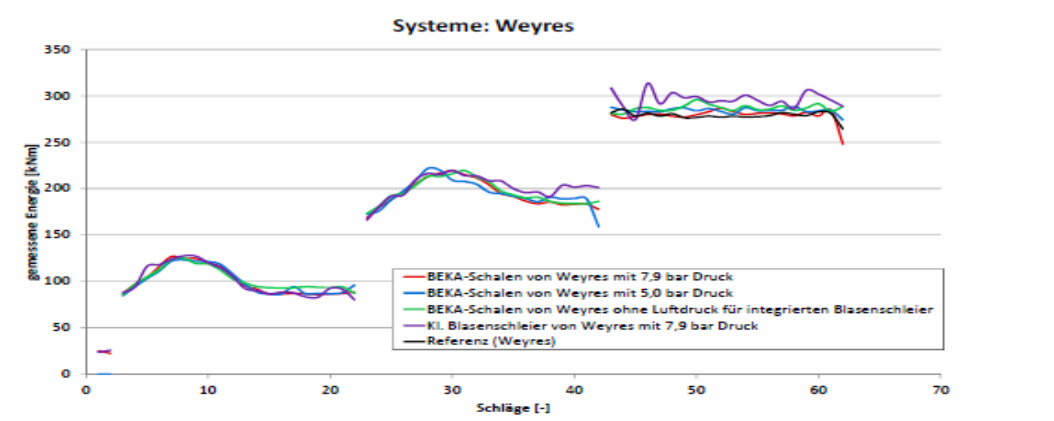

Abbildung 4: eingeleitete Schlagenergien bei den Systemen Weyres (Messtag 3)

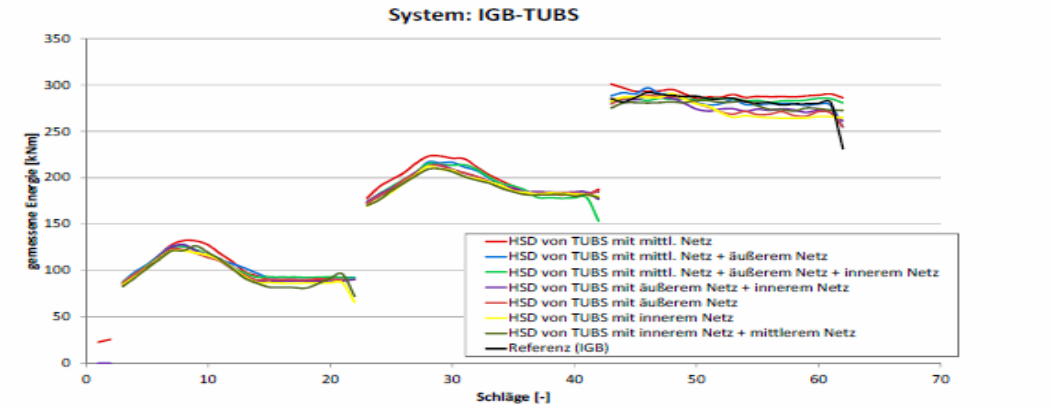

Abbildung 5: eingeleitete Schlagenergien beim System Hydroschalldämpfer (HSD) (Messtag 4)

Figure 4: Inducted impact energy with the Weyres systems (measurement day 3)

Systeme: Weyres	Systems: Weyres
Gemessene Energie [kNm]	Measured energy [kNm]
BEKA-Schalen von Weyres mit 7,9 bar Druck	BEKA shells from Weyres at 7.9 bar pressure
BEKA-Schalen von Weyres mit 5,0 bar Druck	BEKA shells from Weyres at 5.0 bar pressure
BEKA-Schalen von Weyres ohne Luftdruck fuer integrierten Blasenschleier	BEKA shells from Weyres without air pressure for integrated bubble curtain
Referenz (Weyres)	Reference (Weyres)
Kleinen Blasenschleier von Weyres mit 7,9 bar Druck	Little bubble curtain by Weyres with 7.9 bar pressure
Schlaege	Impacts

Figure 5: Inducted impact energy with the hydro noise attenuator system (HSD) (measurement day 4)

Systeme: IGB-TUBS	Systems: IGB-TUBS
Gemessene Energie [kNm]	Measured energy [kNm]
HSD von TUBS mit mittl. Netz	HSD from TUBS with middle net
HSD von TUBS mit mittl. Netz + aeusserem Netz	HSD from TUBS with middle net + outer net
HSD von TUBS mit mittl. Netz + aeusserem Netz + innerem Netz	HSD from TUBS with middle net + outer net + inner net
HSD von TUBS mit aeusserem Netz + innerem Netz	HSD from TUBS with outer net + inner net
HSD von TUBS mit aeusserem Netz	HSD from TUBS with outer net
HSD von TUBS mit innerem Netz	HSD from TUBS with inner net
HSD von TUBS mit innerem Netz + mittlerem Netz	HSD from TUBS with inner net + middle net
Referenz (IGB)	Reference (IGB)
Schlaege	Impacts

Hydro noise measurements

Measuring equipment used and measurement positions

The hydro noise measurements were carried out by IGB-TUBS on all four measurement days, in a similar position. The measurement system used for the measurements was produced by Messrs. Bruel & Kjaer, and for this application consisted of two hydrophones of type 8103. These were connected via a Nexus signal conditioner (type 26920S2) with a LanXI module (3052-B-3/0). The control for this module was provided by means of a laptop, on which all the measured data was stored as noise pressure in Pascals. The scanning rate of the hydrophone was 65.536 Hz. The measurements were taken at a distance of about six metres from the Brodten Pile, at different depths (H1 at depth of 6 m, H2 at 4 m) (see Fig. 6). Due to the short distance between the Brodten Pile and the hydrophones, the measurements could be designated as near-field (close vicinity) measurements.

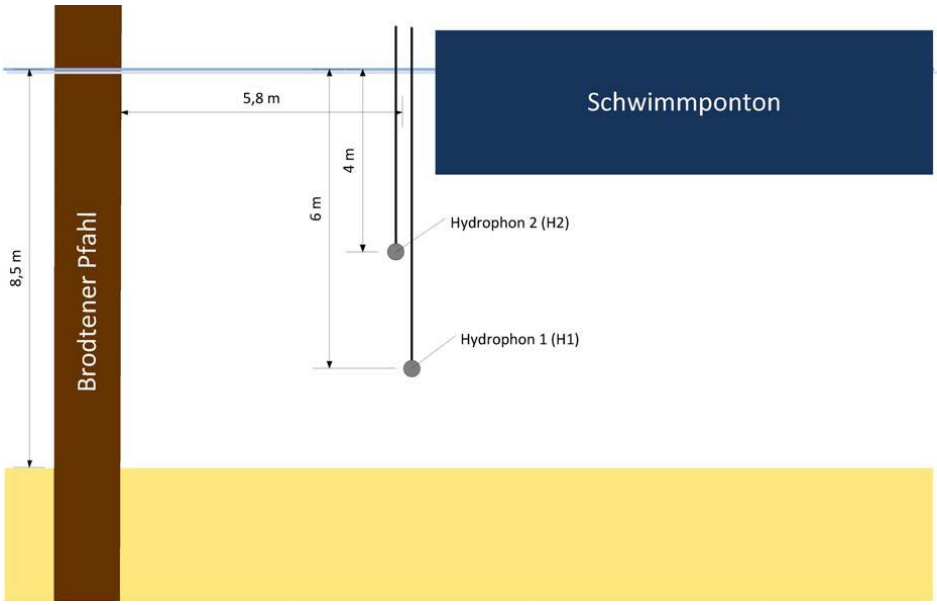

Fig. 6: Measurement positions and distances between the IGB-TUBS hydrophones and the Brodten Pile

Schwimmponton	Floating pontoon
Brodtener Pfahl	Brodten Pile
Hydrophone 1 (H1)	Hydrophone 1 (H1)
Hydrophone 2 (H2)	Hydrophone 2 (H2)

Assessment principle of hydro noise measurements

The noise mitigation effect was tested with every noise mitigation system with three series of impacts in each case (100, 200, and 300 kNm impact energy). Each series of impacts consisted of 20 individual blows. The hydro noise measurement results shown hereinafter relate exclusively to the series with an impact energy of 300 kNm, since it is only with this energy on all the NMS used that there also exist reference impacts without NMS.

From the signal sequences recorded, each of the 20 individual impacts of the impact series was cut out to a length of 0.12 seconds. By way of example, in Fig. 7 the signal-time sequences of the hydrophones H1 and H2 are represented with a reference impact with an impact energy of 300 kNm, which were recorded on measurement day 4. The impact pulse of the hammer can be clearly identified after about 4 milliseconds, which shows as the maximum positive sound pressure of approx. 120 kPa in the track. Such a signal track of the reference impacts proved to be characteristic on all the measurement days. Moreover, no substantial difference can be identified between the hydrophones H1 and H2.

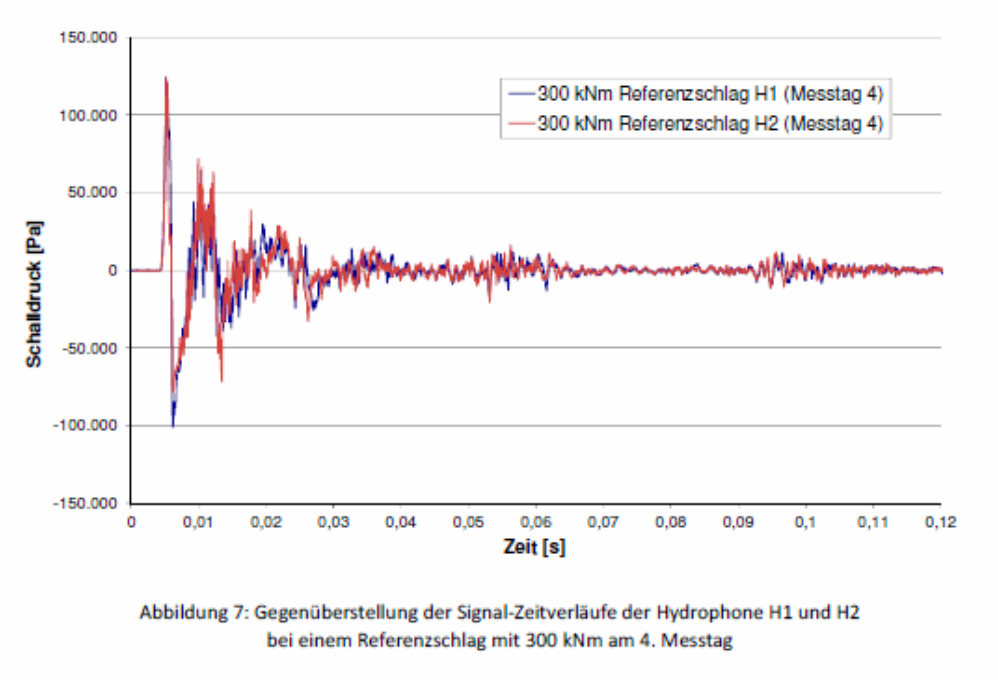

Abbildung 7: Gegenüberstellung der Signal-Zeitverläufe der Hydrophone H1 und H2 bei einem Referenzschlag mit 300 kNm am 4. Messtag

Fig. 7: Comparison of the signal-time tracks of hydrophones H1 and H2, with a reference impact of 300 kNm on measurement day 4

Schalldruck [Pa]	Sound pressure [Pa]
Zeit [s]	Time [s]
300 kNm Referenzschlag H1 (Messtag 4)	300 kNm reference impact H1 (measurement day 4)
330 kNm Referenzschlag H2 (Messtag 4)	300 kNm reference impact H2 (measurement day 4)

The SEL and the L_{peak} were determined for every individual impact in accordance with the following equations:

$$\mathrm{SEL} = 10\log\left(\frac{1}{T_0}\int_{T1}^{T2}\frac{p(t)^2}{P_0^2}dt\right) \text{ [dB]}$$

$$\mathrm{L_{peak}} = 20\log\left(\left|P_{peak}\right|/P_0\right) \text{ [dB]}$$

As the reference value p_0 for water-borne noise, the value determined for p_0 = 1 µPa (dB re 1 µPa) was used.

The results of these calculations are shown in the following figure separately for the hydrophones H1 and H2 for the reference impacts on measurement day 4. For both hydrophones an SEL of 194 dB and an L_{peak} of 222 dB are derived. This diagram also reflects the very good reproducibility and comparability of the individual impacts.

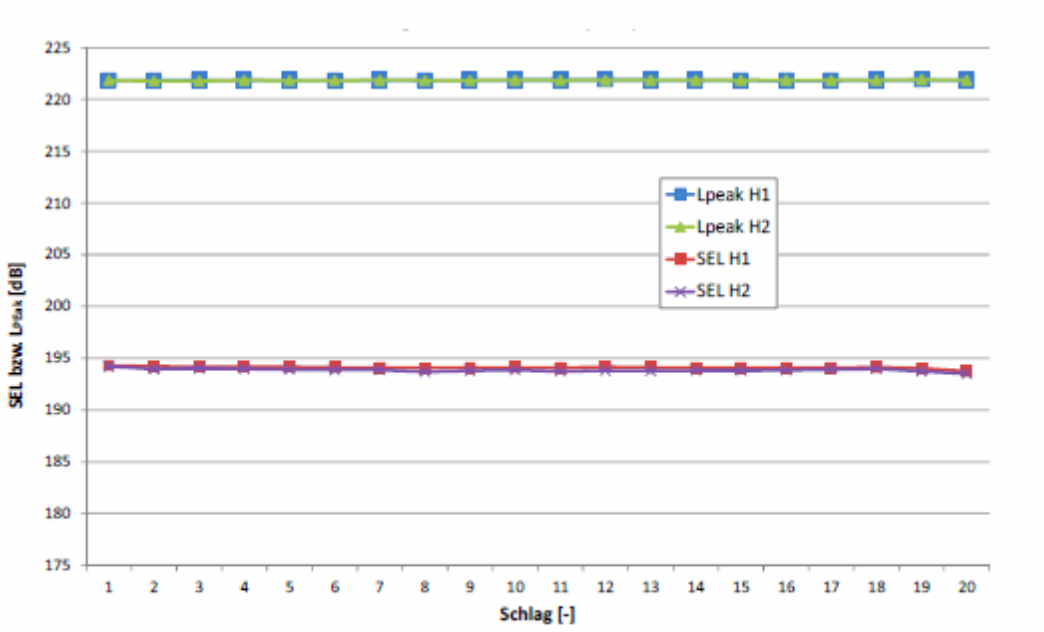

Abbildung 8: ermittelte SEL und L_{Peak} für jeden Einzelschlag (H1 und H2) bei den Referenzschlägen am Messtag 4

Fig. 8: SEL and L_{peak} determined for each individual impact (H1 and H2) with the reference impacts on measurement day 4

SEL bzw. L_{peak} [dB]	SEL and L_{peak} respectively [dB]
Schlag	Impact [-]

Results of the hydro noise measurements

With the level determination described heretofore for the individual impacts with an impact energy of 300 kNm, an assessment of the attenuation potential of the individual systems can be carried out. This assessment is summarised in Table 1. Listed are the noise levels detected from the hydrophone H1, which were determined from the individual impacts. The noise reduction of each system was related to the reference measurements carried out on the same measurement day.

Table 1: Overall result of the IGB-TUBS hydro noise measurements in the close vicinity (distance = 6.0 m) with an impact energy of 300 kNm

System	L_{peak} [dB]	SEL [dB]	L_{peak} [dB] reduction	SEL [dB] reduction
Test day 1				
INC NMS with 7 bar	206.0	184.2	13.6	7.6
IHC NMS without compressed air	206.0	184.8	13.6	7.0
IHC reference	219.7	191.8		

Test day 2				
Menck Fire hose 1 bar	208.3	183.6	13.7	10.9
Menck Fire hose 2 bar	210.4	184.8	11.6	9.6
Menck reference	221.9	194.5		
Test day 3				
Weyres small bubble curtain	213.1	187.3	8.8	8.0
Weyres BEKA shells, 7.9 bar	204.8	179.6	17.0	15.7
Weyres BEKA shells, 5.0 bar	204.2	179.6	17.6	15.7
Weyres BEKA shells, without compressed air	204.1	179.3	17.8	15.9
Weyres reference	221.8	195.3		
Test day 4				
HSD middle	216.3	186.1	5.6	8.0
HSD middle/outer	213.9	183.3	7.9	10.8
HSD inner/middle/outer	211.2	180.7	10.7	13.4
HSD inner/outer	214.5	182.3	7.4	11.8
HSD outer	216.0	184.7	5.9	9.5
HSD inner	216.2	185.1	5.7	9.0
HSD inner/middle	216.0	184.1	5.8	10.0
HSD reference	221.8	194.1		

The levels of the reference measurements are close to identical (approx. 222 dB) with the Menck, Weyres, and HSD systems (measurement days 2-4). Only with the IHC system was a level measured which was less by 2 dB. A similar relationship was likewise derived in the assessment of the third-octave analysis of the reference impacts (Fig. 9). In this case, too, it was shown that the SEL in the individual third-octaves had very good concordance on measurement days 2 to 4.

The noise reduction of the individual systems at a distance of 6 m from the pile amounts to between 7.0 dB and 15.9 dB SEL.

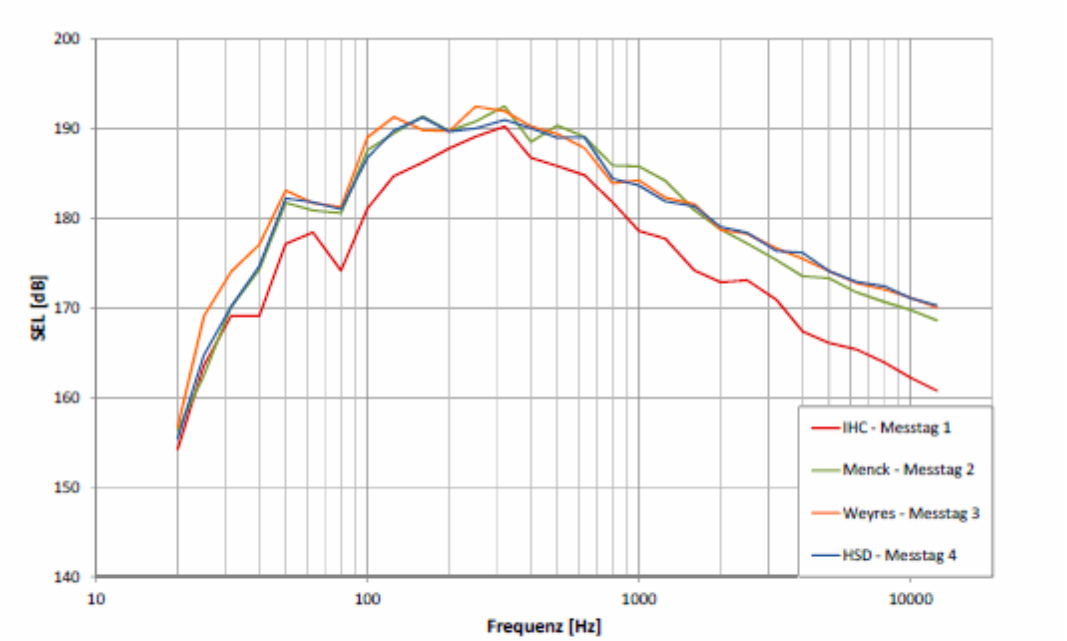

Abbildung 9: Terzanalyse der Referenzschläge an den 4 Messtagen

Fig. 9: Third-octave analysis of the reference impacts on the four measurement days

Frequenz [Hz]	Frequency [Hz]
IHC – Messtag 1	IHC – Measurement day 1
Menck – Messtag 2	Menck – Measurement day 2
Weyres – Messtg 3	Weyres – Measurement day 3
HSD – Messtag 4	HSD – Measurement day 4

In the following figures 10 to 13, the third-octave analyses are represented in the application of the individual noise mitigation systems in comparison with the individual reference measurement (without system). The area with the white background in this situation marks the noise reduction attained, related to the third octave. With the systems from IHC and Menck, maximum reductions were achieved of 20 dB and 18 dB respectively, with the BeKa shells from Weyres 24 dB, and with the hydro noise attenuator system (HSD) 23 dB.

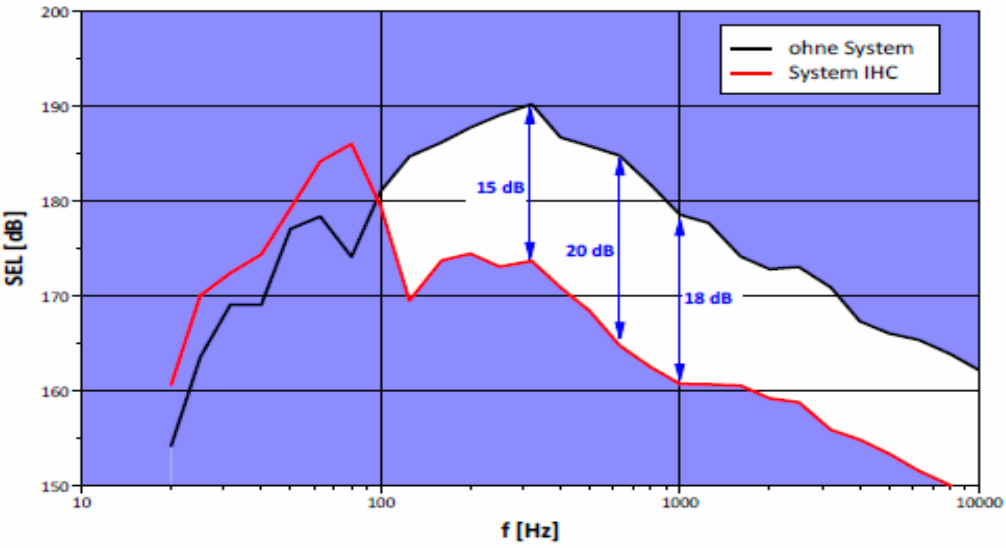

Abbildung 10: Terzanalysen beim Einsatz des IHC-Systems (7 bar)
und der Referenzmessung ohne Schallschutz (Messtag 1)

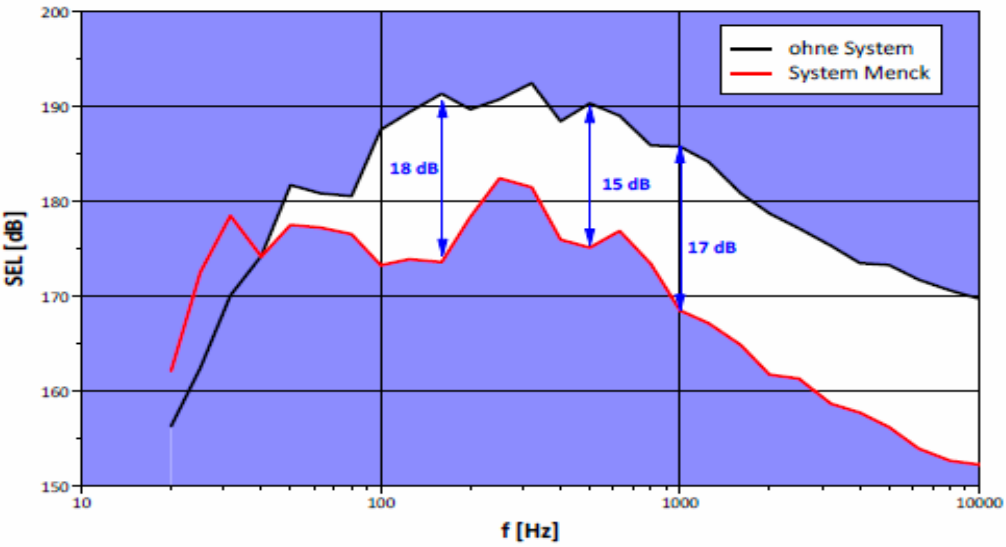

Abbildung 11: Terzanalysen beim Einsatz des Menck-Systems (Firehose, 1 bar)
und der Referenzmessung ohne Schallschutz (Messtag 2)

Fig. 10: Third-octave analysis with the use of the IHC system (7 bar) and the reference measurement, without noise protection (measurement day 1)

Ohne System	Without system
System IHC	IHC system

Fig. 11: Third-octave analysis with the use of the Menck system (fire hose, 1 bar) and the reference measurement, without noise protection (measurement day 2)

Ohne System	Without system
System IHC	Menck system

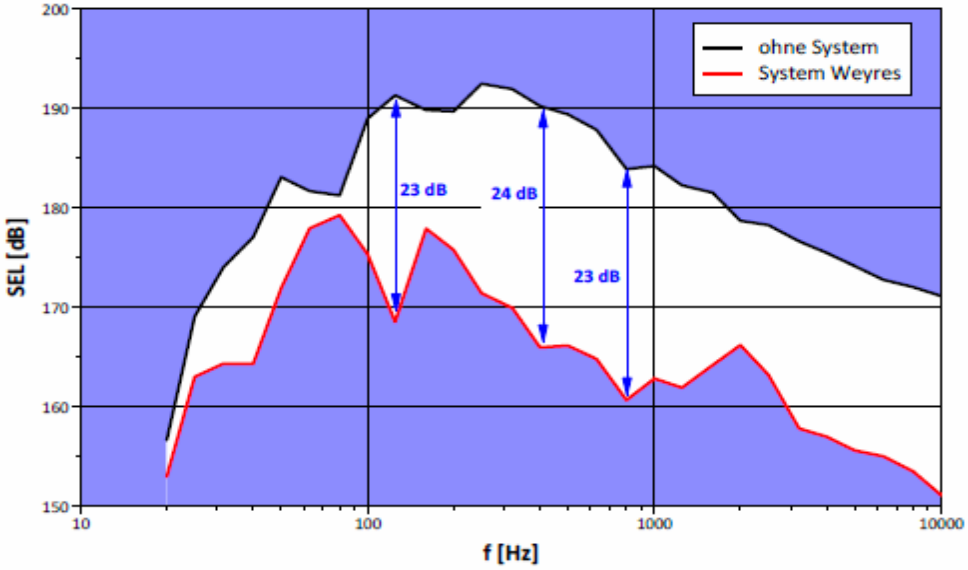

Abbildung 12: Terzanalysen beim Einsatz des Weyres-Systems (Beka-Schale, 0 bar)
und der Referenzmessung ohne Schallschutz (Messtag 3)

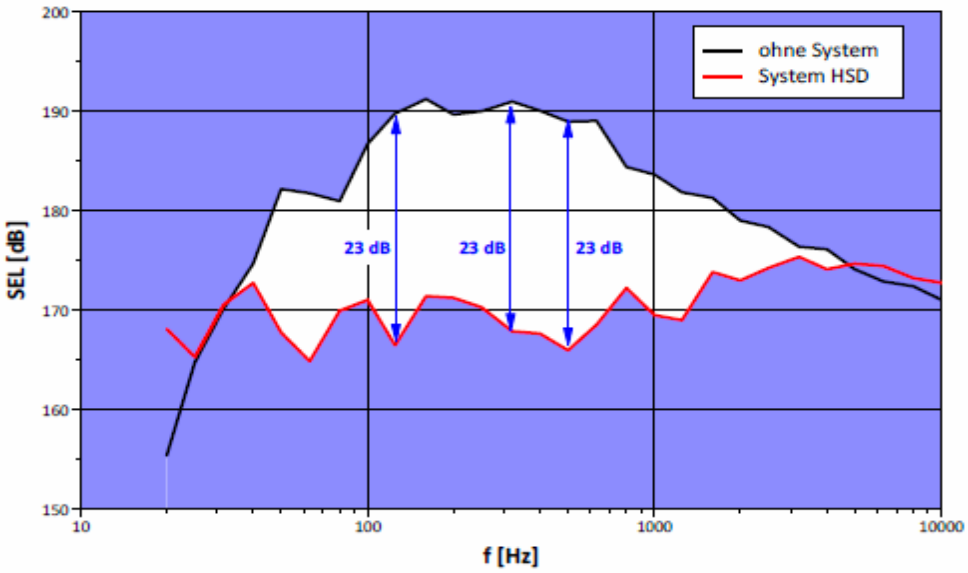

Abbildung 13: Terzanalysen beim Einsatz des HSD-Systems (3 Netze)
und der Referenzmessung ohne Schallschutz (Messtag 4)

Fig. 12: Third-octave analysis with the use of the Weyres system (BeKa shell, 0 bar) and the reference measurement, without noise protection (measurement day 3)

Ohne System	Without system
System Weyres	Weyres system

Fig. 13: Third-octave analysis with the use of the HSD system (3 nets) and the reference measurement, without noise protection (measurement day 4)

Ohne System	Without system
System Menck	Menck system

Summary and Assessment of the Results of the Hydro Noise Measurements

During the tests under the ESRa Project, hydro noise measurements were carried out by IGB-TUBS on four measurement days, at two different depths, and at a distance of approx. 6 m from the Brodten Pile. For all the individual impacts of the impact series with an impact energy of 300 kNm the peak levels LPeak and sum peak SEL were determined, as well as the third-octave analyses pertaining to them. In this context, very good reproducibility and therefore also good comparability of the measurements was attained.

The IHC system resulted in broad-band noise reductions of 7 to 8 dB (SEL) and approximately 14 dB in the LPeak. The additional use of compressed air had the result of increasing the attenuation effect by about 0.6 dB (SEL). The comparison of the third-octave analysis results in a noise reduction of maximum 20 dB at approximately 600 Hz.

With the Menck system, the imposition of 1 bar of compressed air produced the best result. The broad-band noise reductions were just on 11 dB (SEL) and 14 dB (LPeak) respectively. The third-octave analysis resulted in a maximum reduction of 18 dB at approximately 200 Hz.

The BeKa shells from Weyres produced noise reductions of 16 dB (SEL) and 18 dB (LPeak) respectively, whereby the use of compressed air did not lead to any substantial increase. The third-octave analysis resulted in maximum reductions of approximately 23to 24 dB in the frequency between 200 and 900 Hz. The small bubble curtain from Weyres came out comparatively worse, at 8 dB (SEL) and 9 dB (LPeak) respectively.

The hydro noise attenuators produced a broad-band noise reduction of 14 dB (SEL) and 11 dB (LPeak) respectively. The third-octave analysis resulted in maximum reductions of approx. 23 dB in the relevant level-determinant frequency range between 100 and 800 Hz with HSD elements which were set exclusively to 120 Hz.

Considerations with regard to Noise Propagation at the Brodten Pile

Pile-driving procedure with conventional noise irradiation

During the pile-driving operation with pulsed ramming, expansion waves are introduced into the pile in order to drive it into the ground in stages. The continuous expansion waves lead, in the case of offshore piles according to Figure 14, to the direct irradiation of hydro sound waves into the water and vibration waves in the ground.

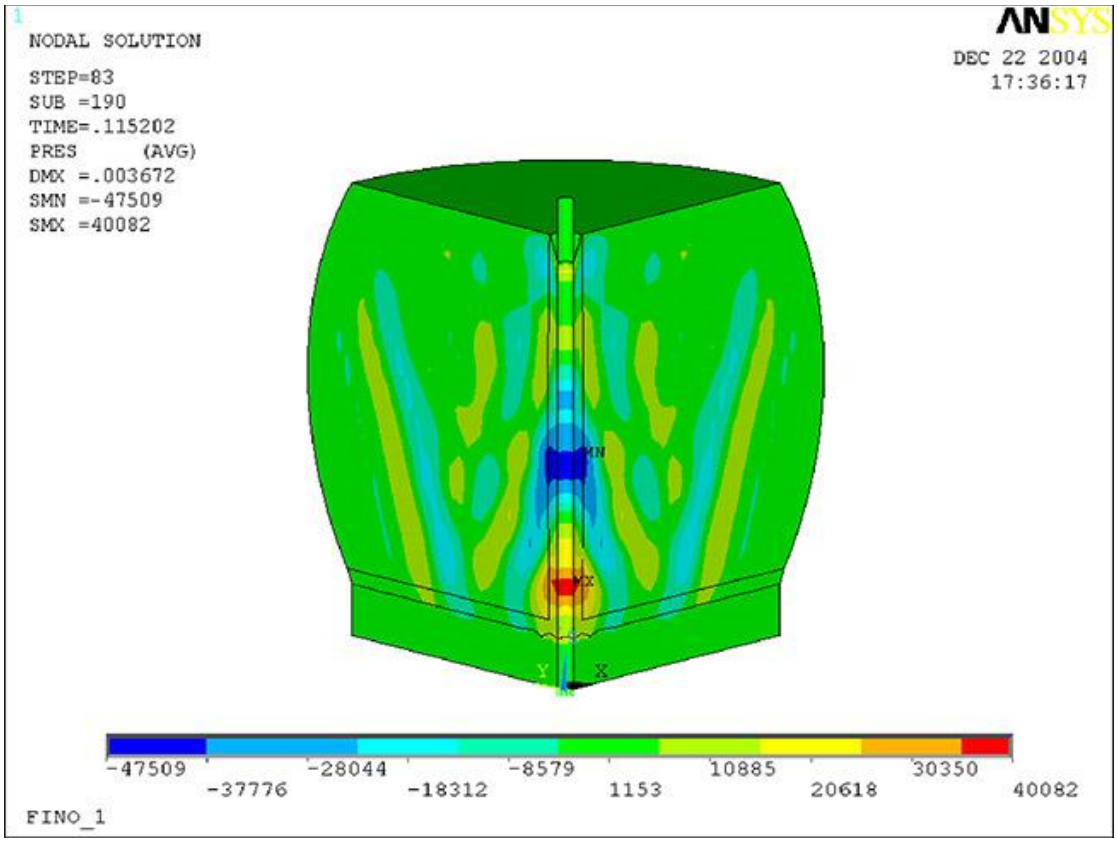

Figure 14: Deployment of an expansion wave in the pile, after Elmer et al. (2007), with the irradiation and propagation of the hydro noise in the water, and reflections at the foot of the pile and part reflections at cross-section transitions

In acoustic terms, the shallow water areas (10 – 50 m) of the locations of offshore windfarm installations represent wave conductors, in which the hydro sound waves as shown in Figure 14 are reflected and attenuated on both the sea bed as well as at the sea surface, and disperse in close to a cylindrical patterns. In this context, solely for geometric reasons, the noise energy, with the distance r, is divided over increasingly larger areas, such that the energy per surface area decreases cylindrically with 1 / r, in addition to the decrease due to the attenuation referred to above.

Depending on the jacket friction and the transfer of energy into the ground which has already taken place in the area of the foot of the pile, the expansion wave can be reflected once or more times in the pile, in particular when the integration depth of the pile is still low. Added to this are part reflections of the expansion wave with stepped piles, such as with the piles of the FINO1 jacket design, which forms the basis for the simulation according to Fig. 14.

With offshore pile-driving operations, overall, some 1% (up to 2% at greater depths of water) of the pile-driving energy is irradiated directly into the water, while the predominant part of the energy is conducted into the seabed. In this situation, the energy transfer due to sliding friction forces in the area of the pile jacket, as in Fig. 15, are substantially lower than with the high peak pressures required in the area of the pile foot.

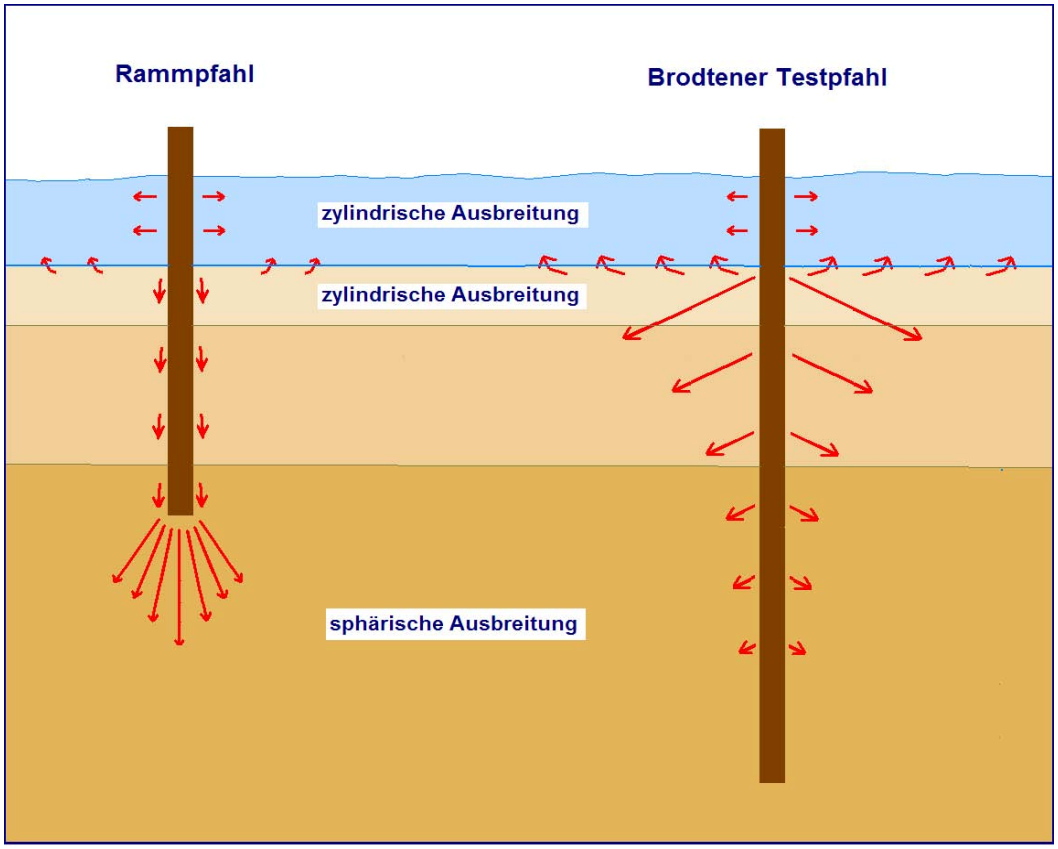

Abbildung 15: Ausbreitung Abstrahlung und Ausbreitung von Schall und Erschütterungen:
a) bei einem üblichen Offshore-Rammpfahl (links),
b) beim Brodtener Testpfahl (rechts).

Fig. 15: Dispersal, irradiation, and propagation of noise and vibrations
a) With a conventional offshore pile (left)
b) With the Brodten Test Pile (right)

Rammpfahl	Conventional pile
Brodtener Testpfahl	Brodten Pile

Zylindrische Ausbreitung	Cylindrical dispersal
Sphaerische Ausbreitung	Spherical dispersal

In principle, the pile-driving energy which is conducted into the ground disperses spherically in the direction of the deeper and more rigid layers of earth. With this spatial dispersal, the energy per surface area decreases very rapidly, with $1 / r^2$, in addition to the material attenuation in the ground.
Layered soils with clear differences in the wave propagation speed and the impedance of the individual layers likewise take effect as wave conductors, which, with distance, incur only a slowly decreasing cylindrical propagation of the waves. The water-saturated sediment layers of the seabed also play a special role, since with wave propagation speeds of some 1,600-1,700 m/s, they present slightly higher values in comparison with sea water, at about 1,500 m/s, and accordingly the noise energy contained in the upper layers can be transferred into the water as indirect hydro-noise.

Driving process at the Brodten Test Pile

This effect plays a decisive part at the Brodten Test Pile, as shown in Fig. 15b. At about 65 m, the Brodten Test Pile is embedded unusually deep into the seabed, and, as well as that, over the years it has become fully integrated with the subsoil as a result of incrustation in the ground, which contains limestone and marl. While with conventional pile-driving, according to Fig. 15a, the predominant part of the driving energy is conducted via the pile foot deep into the subsoil, with the Brodten Test Pile, as a result of the complete intermeshing of the pile with the ground, the whole of the driving energy remains in the upper layers of the seabed, is irradiated there, and leads to a substantial conductance of indirect hydro noise into the water.
The measurement of the IGS-TUBS at the head of the Test Pile shows in Figure 16, for one ram impact, the course of the conducted force in comparison with the product from the measured speed the pile impedance. The force curve of the ram shock and the response from the system points to a purely transient wave propagation process, with complete irradiation of the energy into the ground, without any reflections from the pile foot worth mentioning. Rather, according to the further time curve according to Fig. 16, the whole of the surrounding ground is excited to low-frequency vibrations of some 12 Hz and 21 Hz. These values can be read off from a corresponding frequency analysis.

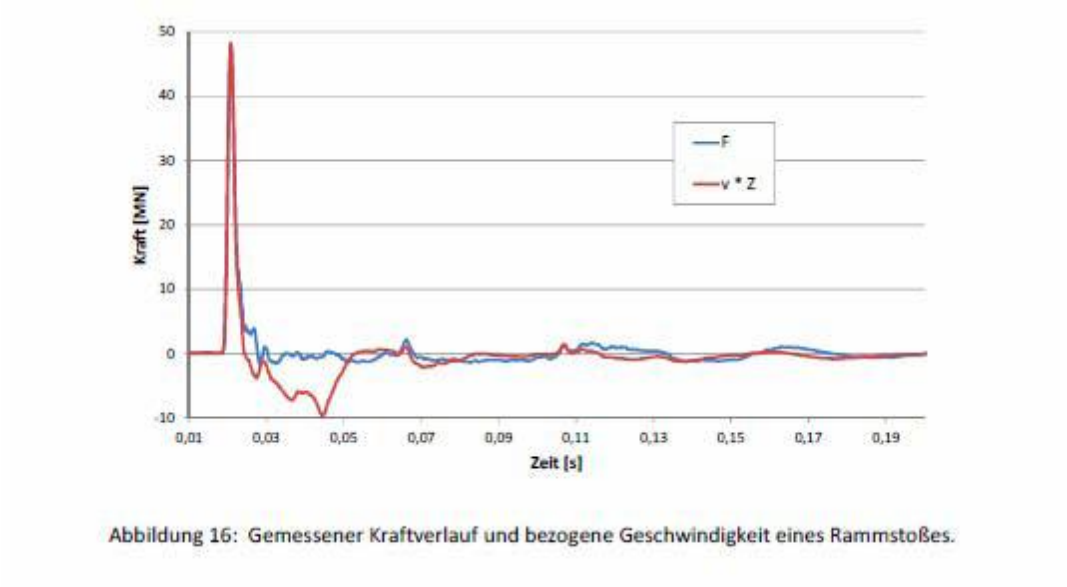

Fig. 16: Force curve measured, and related speed of a ram shock

Kraft [MN]	Force [MN]
Zeit [s]	Time [s]

With the incorporation of the adjacent sediment layer as the lower peripheral condition of the natural oscillation forms, the lowest natural frequency of the water column, and therefore the lower limit frequency of the shallow water area is assumed to be some 80 Hz. The low-frequency ground vibrations therefore do not propagate over the water, but over the upper soil layers. They can also have the effect at greater distances of a substantial indirect introduction of noise into the water.

Open noise mitigation systems, which can be flowed through, such as the hydro noise attenuators, influence and attenuate the bodies of water which surround them, and therefore also achieve substantial noise reductions close to the natural frequency of the water column or the lower limit frequency of 80 Hz respectively, as can be derived from the measurement results.

There are essentially two transfer routes for hydro noise during the driving of offshore piles:

1. The direct transfer of hydro sound waves in the shallow water area, which in this case, as a wave conductor, only conveys sound waves above the limit frequency of 80 Hz.

2. The indirect transfer and conducting of hydro noise over the seabed, which is very heavily dependent on the local circumstances and ground conditions.

At the Brodten Test Pile, due to the incrustation of the pile it is predominantly the indirect transfer path according to Fig. 15b which is of substantial significance, by

contrast with the situation with conventional offshore pile-driving procedures with penetrating piles.
Noise mitigation systems on the pile essentially influence the direct transfer path of the hydro noise into the water. This noise mitigation effect can be designated as a system-inherent noise mitigation, which can also be transferred to other situations largely independent of the local circumstances.

The indirect transfer path over the layered seabed is largely determined by local conditions, in particular with regard to the Brodten Test Pile. These influences on the hydro noise are therefore not transferable.

In order to exclude as far as possible the non-transferable locally-conditioned influences in the examination of noise mitigation systems, hydro noise measurements have been conducted by IGB-TUBS in the immediate vicinity of the Test Pile, in the acoustic near-field.

Acoustic near-field measurements

The measurements, at a distance of about 6 m from the noise-irradiating surface of the pile, are intended in particular to demonstrate the measured noise reductions as system-inherent and transferable properties of the different noise mitigation techniques, and reduce local influences.

With regard to the acoustics of airborne sound, near-field measurements at a distance interval of r < 2 *lambda* of sound pressure and sound speed, with the aid of sound intensity probes, in the localization and quantifying of sound sources have been common practice for more than 20 years (such as in the engine compartment of a car). In principle, however, these procedures are not yet available in the sector of hydro noise.

The background to the measurement procedure specially required in the acoustic near-field is the fact that in acoustics it is not the scalar sound pressure p [Pa] which represents the actual determinant value, but the vectoral sound intensity I [W/m^2]. The sound energy which passes through a surface element per time unit is defined as the sound intensity I, and is derived as a product from the effective values of sound pressure and sound speed:

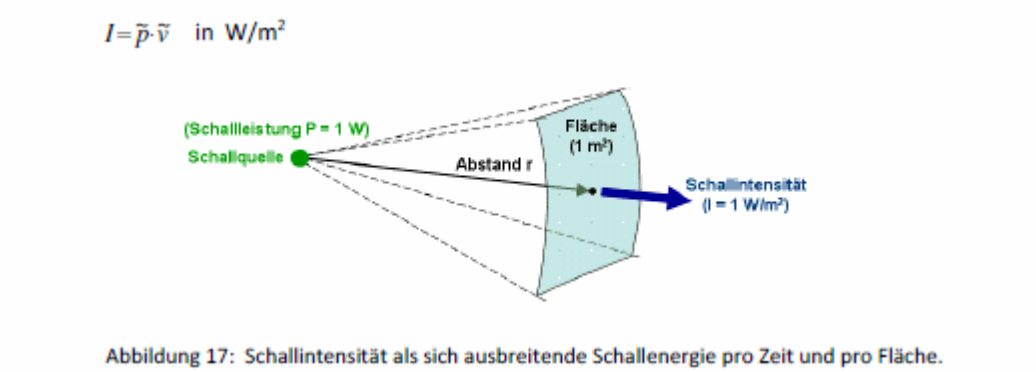

Abbildung 17: Schallintensität als sich ausbreitende Schallenergie pro Zeit und pro Fläche.

Fig. 17: Sound intensity as self-propagating sound energy per time and per surface area

(Schallleistung P = 1 W)	(Sound power P = 1 W)
Flaeche (1 m^2)	Surface (1 m^2)
Schallquelle	Sound source
Abstand r	Distance interval r
Schallintensitaet (I = W/m^2)	Sound intensity (I = W/m^2)

The sound intensity I is a vectoral value which is just as direction-dependent as the sound speed v, with its three direction components v_x v_y v_z.

In the near-field area (approximately at a distance r < 2 *lambda*), the properties of which are dependent both on the wavelength as well as on the propagation characteristic (spherical or cylindrical), the sound speed decreases perceptibly more sharply than in the far-field range r >> *lambda*, with the result that, in particular with tonal sound with additional local vibrations, a frequency-dependent complex and complicated relationship pertains between the sound speed and the sound pressure.

In the far-field area, by contrast, the simple, frequency-independent and constant relationship applies:

$$\tilde{p} = \rho c \cdot \tilde{v} = Z \cdot \tilde{v}$$

with the density p and sound propagation speed c. With hydro noise, the sound characteristic impedance Z amounts to:

Z = pc = 1.5 * 10^6 in Ns/m^3.

With the individual reference values for the sound pressure, the sound speed, and the sound intensity, there is now derived in the sector of acoustics the highly practical relationship that in the far-field area r >> a (and only in the far field!) the individual noise levels for the sound pressure, the sound speed, and the sound intensity are the same!

Hydro noise measurements of the sound pressure are usually only carried out in the far-field area, so that the sound pressure levels determined at the same time also represent the determinant sound intensity level. With the near-field measurements of the sound pressure and the determinations of the sound pressure levels within the framework of the ESRa tests, systematic measurement errors are therefore to be anticipated in relation to the determinant sound intensity levels.

The hydro noise irradiation of the pile-driving process at the Brodten Test Pile represents, according to Figs. 14-16, a transient rotation-symmetrical wave propagation process, with which the noise irradiating surface of the pile does indeed exhibit a cylindrical form, but is not to be described either by cylindrical or by spherical irradiation characteristics, since no tone content is present, the source of the sound migrates along the length of the pile, and the length of the pile wetted by the water, with direct hydro noise irradiation, amounts to only a fraction of the expansion wave length in the pile.

An analytical consideration of the hydro noise irradiation is therefore excluded. A more precise numerical analysis of the transient hydro noise irradiation is carried out with the special FDM program “TransDyn” (Elmer, 2004), which takes as the basis for the three-dimensional simulation exclusively the sound pressure and the three speed components, as phase-encumbered field values, which fully describes the transient wave propagation process in physical terms, and comes close to reality in the sense of sound intensity determination, even in the close vicinity area.

The three-dimensional numerical model comprises the water depth of 8.5 m with the hydro noise propagation in the area of the edge length of the model, of 12 m in each case, for a pile-driving impact according to Fig. 16, of 4 ms duration, whereby the noise excitation in the simulations from Figures 17 and 18 are derived in each case from the migrating expansion wave in the pile. The three-dimensional model contains approximately 10 million elements of 5 cm edge length.

The results of the comparative determination of the hydro noise levels in a water depth of 6 m and at different distances from the sound source, using the sound pressure, the sound speed, and the calculated maximum intensity, are represented in Figure 19. The maximum near-field error in the determination of the noise intensity level alone from the sound pressure amounts at the Test Pile, at a distance of 6 m, to a maximum of 1 dB.

For this reason, a systematic error of 1 dB can be assumed for the following measurement results in the close vicinity area.

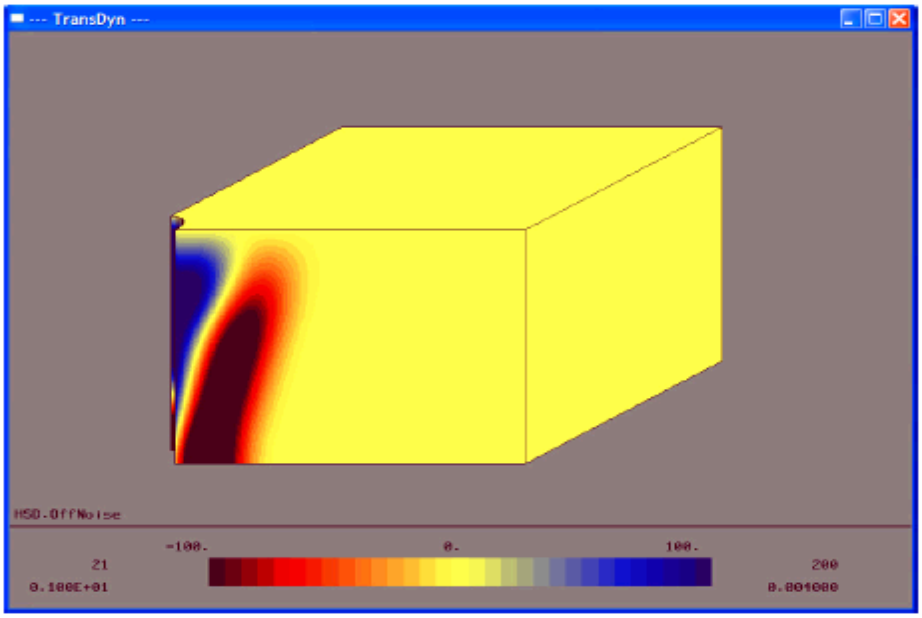

Abbildung 17: Hydroschalldruck-Verteilung im 3D-Modell nach 0,004 s in kPa.

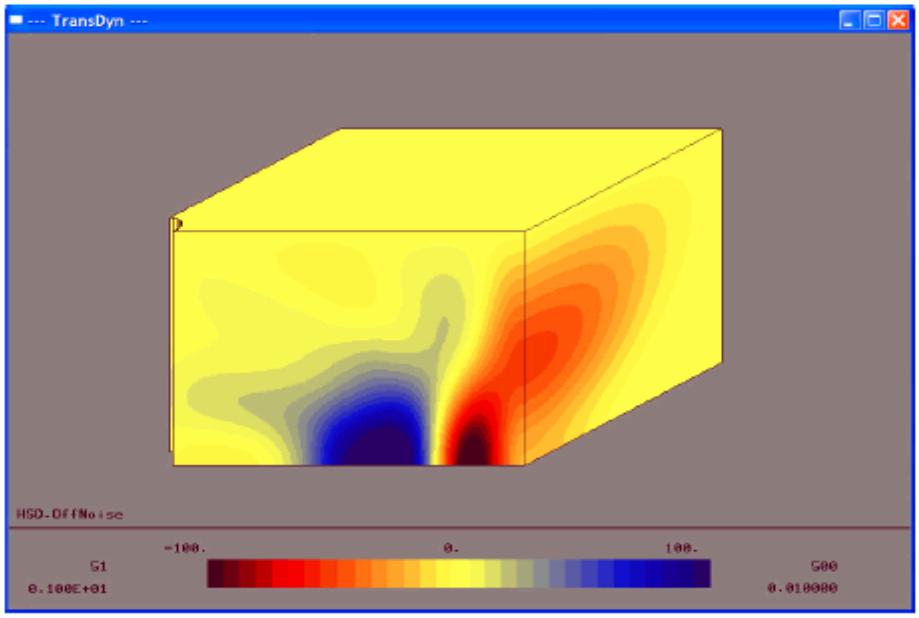

Abbildung 18: Hydroschalldruck-Verteilung im 3D-Modell nach 0,010 s in kPa.

Fig. 17: Hydro noise pressure distribution in the 3D model after 0.004 s in kPa
Fig. 18: Hydro noise pressure distribution in the 3D model after 0.010 s in kPa

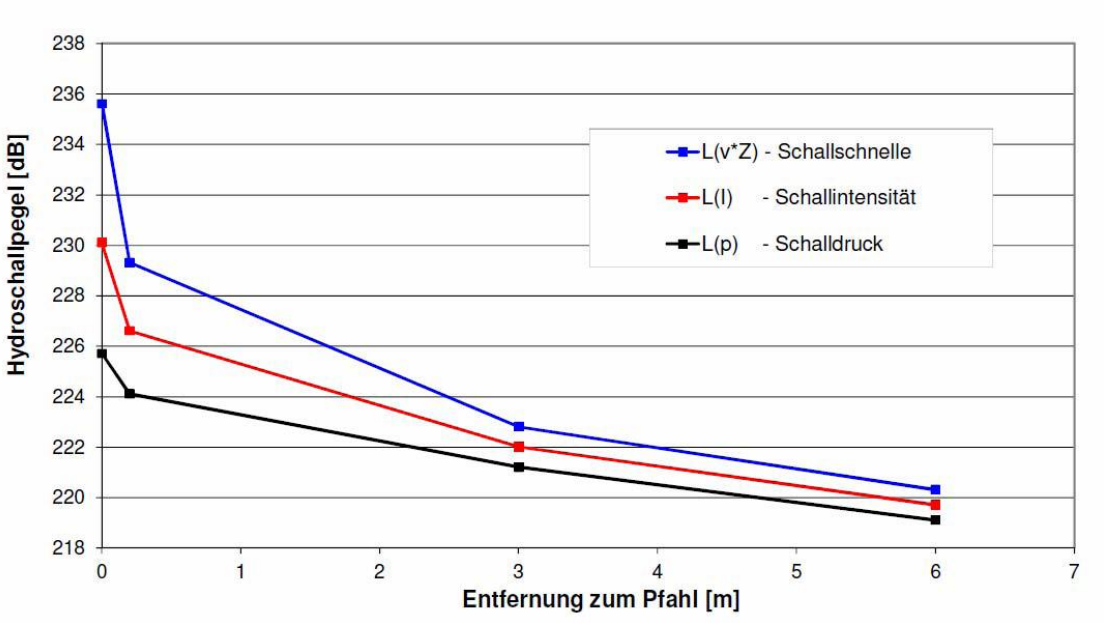

Fig. 19: Comparison of hydro noise level curves in the close vicinity area, from pressure, speed, and sound intensity, with maximum error of 1 dB at a distance of 6 m from the pile.

Hydroschallpegel [dB]	Hydro noise level [dB]
Entfernung zum Pfahl [m]	Distance to pile [m]
Schallschnelle	Sound speed
Schallintensitaet	Sound intensity
Schalldruck	Sound pressure

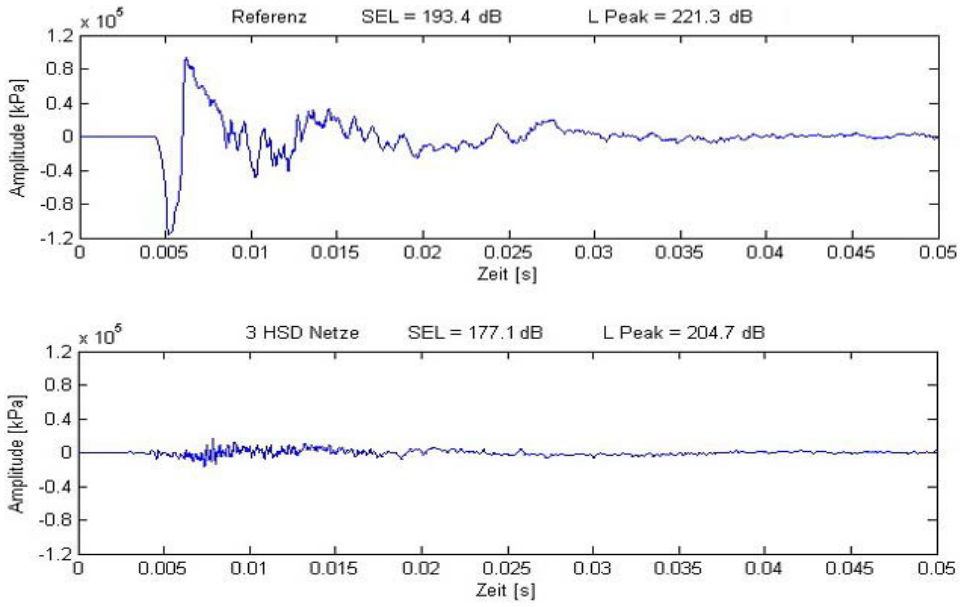

Fig. 20: Reduction of hydro noise pressure at 6 m due to hydro noise attenuators

Netze	Nets
Zeit [s]	Time [s]
Referenz	Reference

As a response to the shock process according to Fig. 16, represented in Fig. 20 is, by way of example, the hydro noise pressure measured at a distance of 6 m. There are still no noise reflections present here, or locally-induced indirect influences. As the close vicinity measurements show, with the hydro noise attenuators the direct noise energy of the ram shock is almost entirely reduced. The results of the close vicinity measurements can also be transferred, as system-inherent noise mitigations, to other situations as well.

Literature:

Elmer, K.-H.; Betke, K.; Neumann, T. (2007): Standard procedures for the determination and assessment of the burden on the marine environment due to noise emissions from OWEA, SCHALL 2; Federal Ministry of the Environment Research Report 0329947, March 2007.

Elmer, K.-H. (2004): Three-Dimensional Wave Propagation and Energy Flow; International Journal of Computational Engineering Science (IJCES), Imperial College Press, Vol.5, No.3, p. 481494, 2004.

Appendix: Summary of the third-octave analyses from all test variations

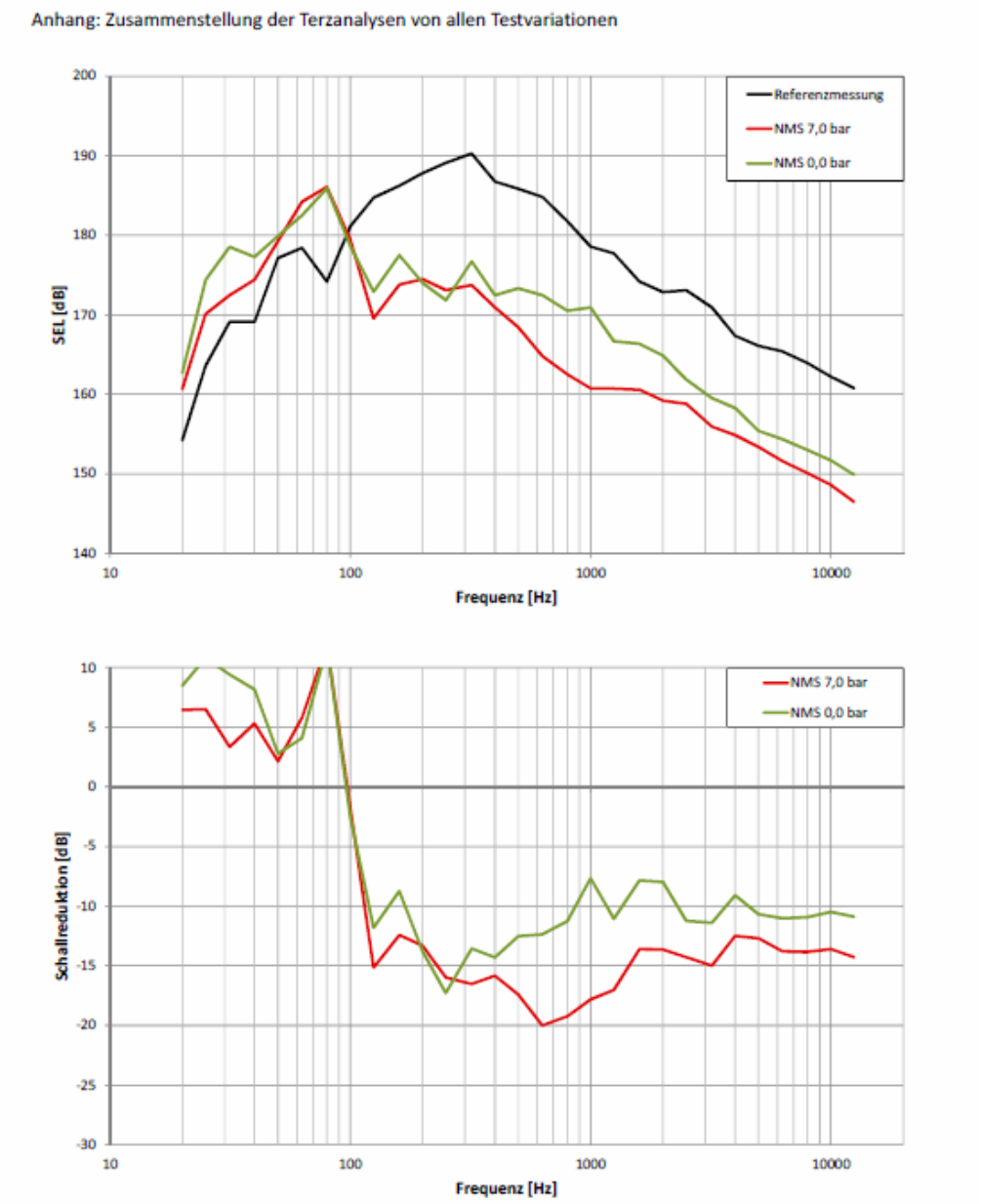

Terzanalysen bei Einsatz der IHC-Systeme und der Referenzmessung (oben) sowie die daraus resultierende Schallreduktion bei Einsatz der IHC-Systeme in Bezug auf die Referenzmessung (Messtag 1)

Frequenz [Hz]	Frequency [Hz]
Referenzmessung	Reference measurement
Schallreduktion [dB]	Noise reduction [dB]

Third-octave analysis with the use of the IHC systems and the reference measurement (top), and the noise reduction resulting from this, with the use of the IHC systems in relation to the references measurement (measurement day 1)

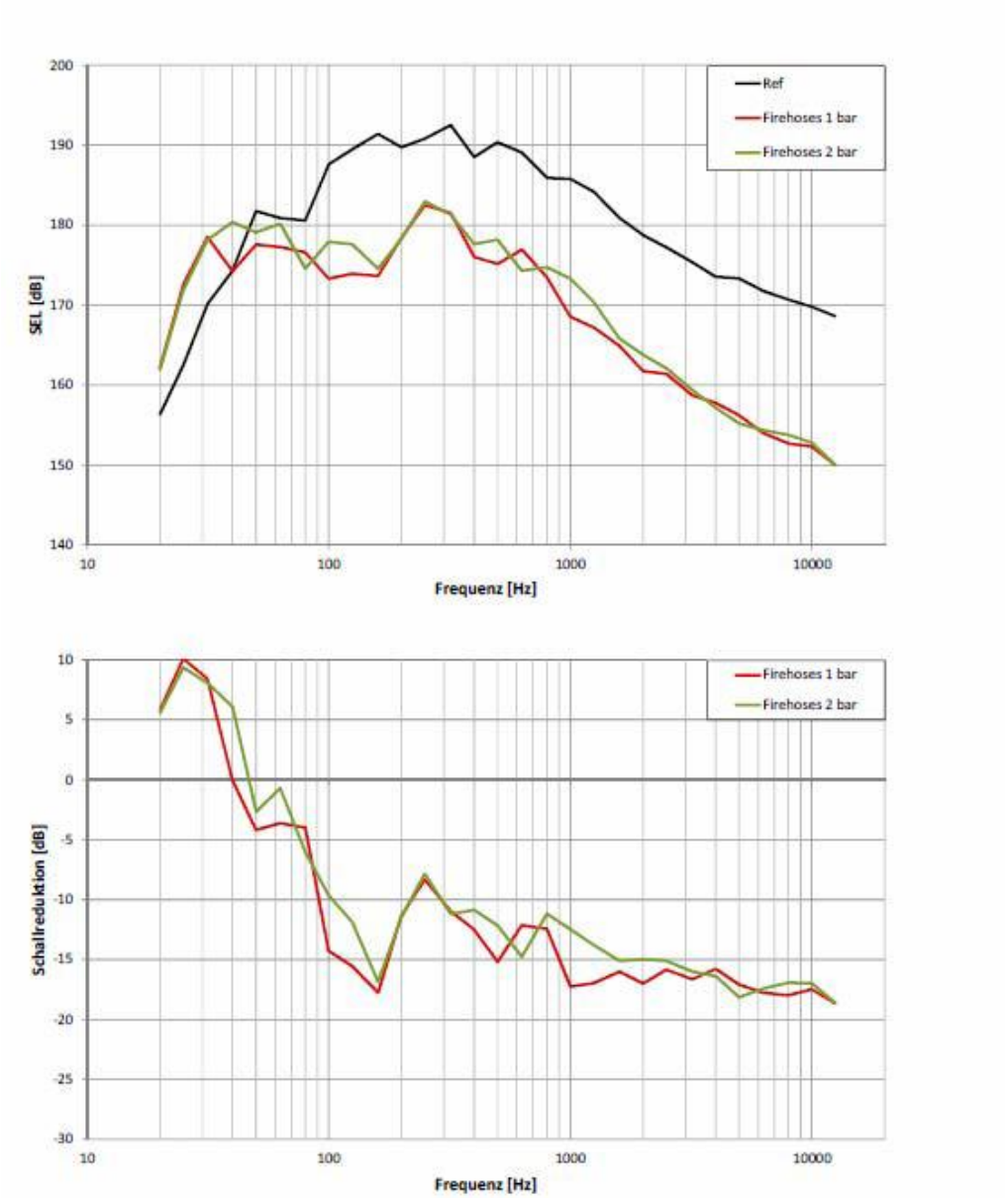

Terzanalysen bei Einsatz der Menck-Systeme und der Referenzmessung (oben) sowie die daraus resultierende Schallreduktion bei Einsatz der Menck-Systeme in Bezug auf die Referenzmessung (Messtag 2)

Frequenz [Hz]	Frequency [Hz]
Schallreduktion [dB]	Noise reduction [dB]
Firehoses 1 bar	Fire hoses 1 bar
Firehoses 2 bar	Fire hoses 2 bar

Third-octave analysis with the use of the Menck systems and the reference measurement (top), and the noise reduction resulting from this, with the use of the Menck systems in relation to the references measurement (measurement day 2)

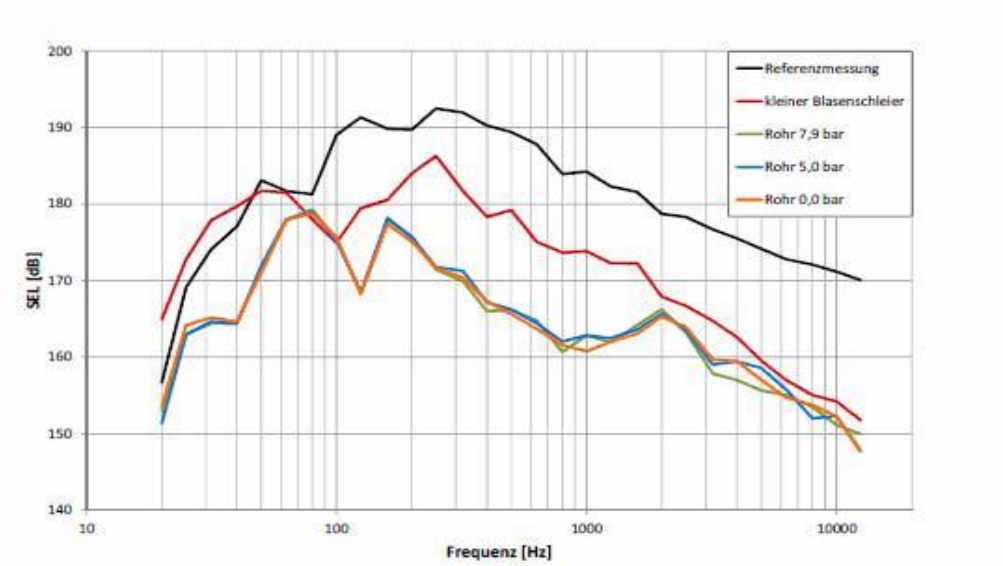

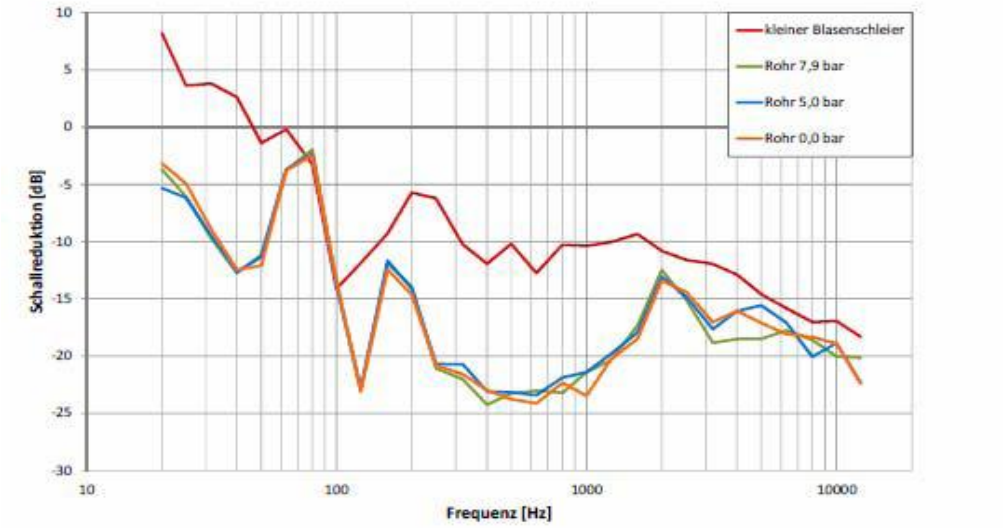

Terzanalysen bei Einsatz der Weyres-Systeme und der Referenzmessung (oben) sowie die daraus resultierende Schallreduktion bei Einsatz der Weyres-Systeme in Bezug auf die Referenzmessung (Messtag 3)

Third-octave analysis with the use of the Weyres systems and the reference measurement (top), and the noise reduction resulting from this, with the use of the Weyres systems in relation to the references measurement (measurement day 3)

Referenzmessung	Reference measurement
Kleiner Blasenschleier	Small bubble curtain
Rohr 7,9 bar	Tube 7.9 bar
Rohr 5,0 bar	Tube 5.0 bar
Rohr 0,0 bar	Tube 0.0 bar
Frequency [Hz]	Frequency [Hz]
Schallreduktion [dB]	Noise reduction [dB]

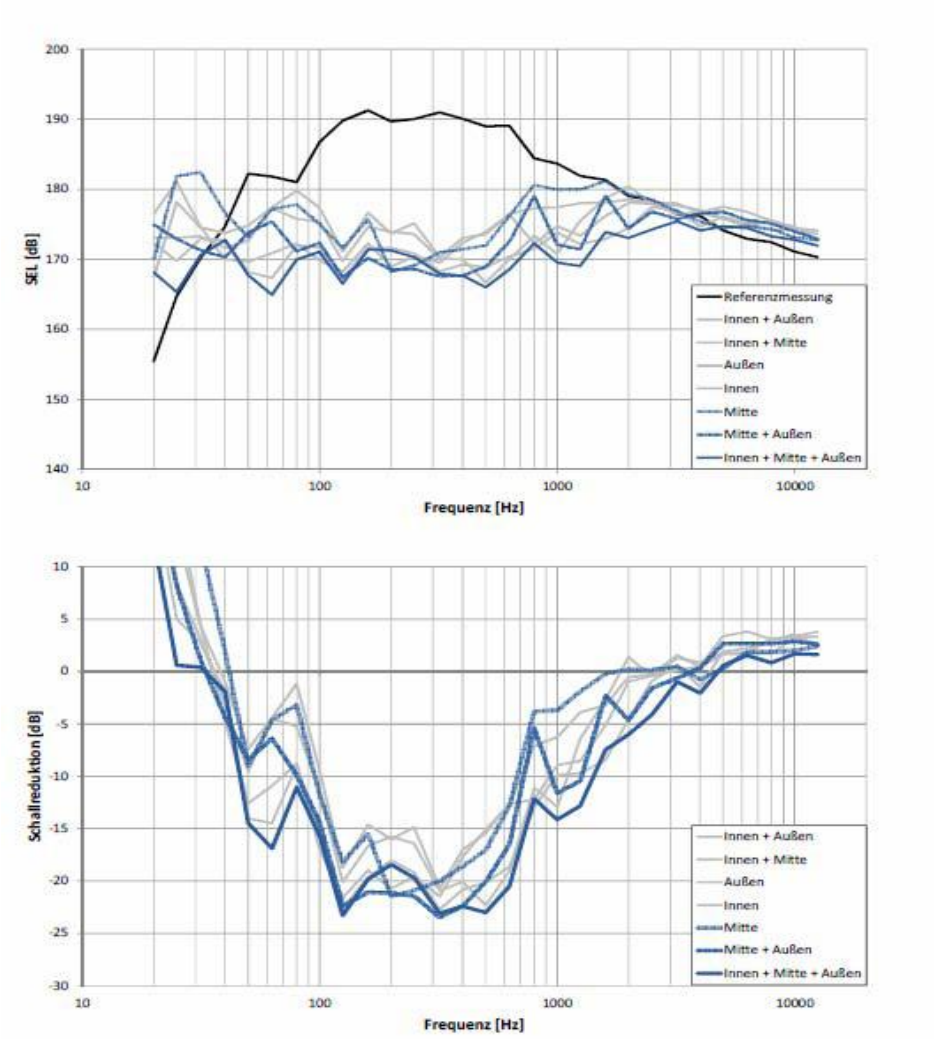

Terzanalysen bei Einsatz der HSD-Systeme und der Referenzmessung (oben) sowie die daraus resultierende Schallreduktion bei Einsatz der HSD-Systeme in Bezug auf die Referenzmessung (Messtag 4)

Third-octave analysis with the use of the HSD systems and the reference measurement (top), and the noise reduction resulting from this, with the use of the HSD systems in relation to the references measurement (measurement day 4)

Referenzmessung	Reference measurement
Frequenz [Hz]	Frequency [Hz]
Schallreduktion [dB]	Noise reduction [dB]
Innen + Aussen	Inner + outer
Innen + Mitte	Inner + middle
Aussen	Outer
Innen	Inner
Mitte	Middle
Mitte + Aussen	Middle + outer
Innen + Mitte + Aussen	Inner + middle + outer